

Exploring the use of Dye-Sensitisation by Visible Light and the Lotus Effect as new Approaches to Self-Cleaning Textiles

SHABANA AFZAL

Doctor of Philosophy (Chemistry)

School of Applied Sciences and Engineering
Monash University

October 2013



MONASH University

Addendum

No.	Examiner's comments	Responses
1	page v – correct “fee-base porphyrin”	“fee-base” has been replaced with “free-base”
2	page 2 – The paragraph on energy is not required. Photocatalysis is an area of its own that doesn't need to be linked to renewable energy, nor is this thesis focused on renewable energy.	This is examiner's opinion. We think it is relevant.
3	page 3 – “The higher photocatalytic efficiency of anatase is attributed to the fact that its conduction band potential is 0.2 eV more negative than that of rutile. Ref13” Is this statement correct? Please check this manuscript again and see if this statement can be referenced as such. Note that a comparison between photocatalytic activity of rutile and anatase of the same size and surface area has shown rutile to be more efficient than anatase.	The statement has been revised with more relevant reasoning. “The higher photocatalytic efficiency of anatase is attributed to the fact that anatase has higher oxygen exchange ability as compared to rutile”.
4	page 4 – “As mentioned above, photocatalysis involves continuous photoelectro-chemical and electro-chemical reactions which involve generation of electrons and holes” – it is no clear where this has been mentioned above.	The statement has been revised: “photocatalysis involves continuous photoelectro-chemical and electro-chemical reactions which involve generation of electrons and holes.”
5	page 6 – Figure 1.3 caption requires more detail, as do many of the captions in chapter 1. In all cases the caption should be all the reader needs to read to understand the figure, reading through the text should not be required. In regards to the figures – while a reference is given, shouldn't copyright have been obtained (and noted) to use these figures in the thesis?	This is examiner's opinion and we feel this is not necessary. Where needed, each diagram is referenced to the original work.
6	page 12 – There is discrepancy between the text and figure. The text states complete photo-decomposition was obtained after 4 hours, whereas the figure shows C/C ₀ to be > 0.4. Just because the graph/experiment ends at 4 hours does not mean that complete decomposition has occurred. (Note this is also an issue raised in the results and discussion chapters.)	The statement has been revised: “55% photodecomposition of Neolan Blue 2G was obtained after 4 hours of visible-light irradiation on 0.25% Fe-TiO ₂ coated cotton samples.”
7	page 13 – Figure 1.9 – the presence of the stain is not apparent on the pristine cellulosic fabrics, but the presence of TiO ₂ makes the stain more prominent. Why is this the case?	Presence of TiO ₂ makes the stain more prominent as compared to pristine because TiO ₂ -coated cotton is hydrophobic, so the stain occupies a small area on the surface and colour of the stain appears more intense. (<i>J. Mater. Chem.</i> , 2006, 16, 4567)
8	page 14 – Fig 1.10 Text associated with this figure - “The cotton fabric coated from N/TiO ₂ sol showed considerable photoactivity by degrading methyl orange under visible-light irradiation for 120 minutes” would suggest total degradation of the methyl orange at 120 minutes, not the ~0.3 C/C ₀ seen in the graph.	The statement has been revised: “The cotton fabric coated from N/TiO ₂ sol showed considerable photoactivity (70%) by degrading methyl orange under visible-light irradiation for 120 minutes.
9	page 30 – check reference to Figure 1.24 (which occurs before reference to Figure 1.23) as this doesn't correlate to the actual Figure 1.24.	Examiner missed the reference earlier in the section.
10	page 45 – C and C ₀ should be defined	C is the concentration of methylene blue after irradiation at different time intervals, whereas, C ₀ is the concentration of methylene blue before irradiation. The corresponding explanation is a part of already published work (chapter 2).
11	page 45 – it is claimed that complete degradation of MB occurs in 110 min, which is not what the graph indicates. Why is it that Figures 5 and 8 are plotted down to 0.1C/C ₀ and not 0? Please check the claim of “complete degradation” in all the results chapters.	The instrument is not sensitive enough to measure absorbance values below 0.1 accurately, therefore we have considered 0.1C/C ₀ as a complete degradation approximately, for all of the results in the chapters.
12	page 45 – it is not clear how the % degradation values are determined – “our results showed 38%, 67%,99% and 79% degradation...”	% degradation values are calculated from the graph curves for different concentrations given in figure 5.
13	page 56 – there are new peaks (apart from anatase) in the XRD patterns on the TiO ₂ coated cotton (Figure 2b). What is this due to?	We believe that these peaks stem from either impurities or background noise.
14	page 56 – why would there be strong association between FeTCCP molecules and TiO ₂ compared with CoTCCP and ZnTCCP. This should be explained.	The highest value of Stern-Volmer rate constant (K _{sv}), observed for FeTCCP could account for the strong association between FeTCCP molecules and TiO ₂ as compared to CoTCCP and ZnTCCP.

		This has already been explained in the section.
15	page 60 – why is there a shift in the XRD peak positions between d) and e)	We believe it could be due to a doping effect or some type of bonding with TiO ₂ .
16	page 65 – why would petroleum ether washing increase the absorbance of the FeTCPP sample?	For the normalized spectra, there is no increase in the absorbance of FeTCPP sample.
17	page 71 Figure 1 – the scale bars in this image are difficult to read, as are the a), b), c) etc. labelling within the image.	The scale bars values are; a, b & c = magnification (5000), thickness (1µm), WD (10 mm), 15.0 kv SEI, d, e & f = magnification (100,000), thickness (100 nm), WD (10 mm), 15.0 kv SEI
18	page 71 – “the degradation rate of MB for TCPP is twice as fast as that of CuTCPP” – this is not what the slope of the graphs would indicate.	We have calculated from the slope that degradation rate of MB for TCPP is faster than CuTCPP on the order of 2x.
19	page 71 Figure 5 – the caption should note half of each square was masked.	The caption cannot be amended in the already published work.
20	page 73 – when CuTCPP leached in petroleum ether this was claimed that it could be due to the weak interactions between carboxylate groups of dye and TiO ₂ , affected by the change in the polarity of medium. On page 58 when FeTCPP leached in detergent and water this was attributed to weak interactions between the dye carboxylate groups and TiO ₂ due to the change of pH and polarity of the medium. Why would the CuTCPP leach in petroleum ether while the FeTCPP leached in detergent and water and can the leaching in both cases be put down to the same reason?	The exact reason for leaching in different media is unknown at this stage. The statement cannot be modified further, as the section is a part of published work.
21	page 76 – labels are given in the spectrum but not explained in the caption.	Further explanation of the labels can be obtained from the reference cited in the section.
22	page 83 – how does small angle X-ray diffraction give crystallinity?	The word “small” has been replaced with “low” in the sentence.
23	page 85 – why does surface roughness introduce hydrophobicity – this needs to be explained.	The statement is referenced in the introduction of the chapter 5.
24	page 85 Figure 6 – why is the time required for photodegradation so much longer than the previous chapters?	In the solid phase, usually the reaction is slow as compared to that in the aqueous phase due to the nature of the radicals formed.
25	page 91 – the first phrase “In the field of renewable energy resources” is irrelevant as the photocatalytic degradation of organics is being studied, not, say, the photocatalytic production of H ₂ .	The statement has been modified.

Copyright Notices

Notice 1

Under the Copyright Act 1968, this thesis must be used only under the normal conditions of scholarly fair dealing. In particular no results or conclusions should be extracted from it, nor should it be copied or closely paraphrased in whole or in part without the written consent of the author. Proper written acknowledgement should be made for any assistance obtained from this thesis.

Notice 2

I certify that I have made all reasonable efforts to secure copyright permissions for third-party content included in this thesis and have not knowingly added copyright content to my work without the owner's permission

Declaration for thesis based on published/unpublished work

General declaration

In accordance with Monash University Doctorate Regulation 17/ Doctor of Philosophy and Master of Philosophy (MPhil) regulations, the following declarations are made:

I hereby declare that this thesis contains no material which has been accepted for the award of any other degree or diploma at any university or equivalent institution and that, to the best of my knowledge, this thesis contains no material previously published or written by another person, except where due reference is cited in the text of thesis.

This thesis consists of 3 original papers published in the peer reviewed journals and 1 submitted unpublished publication. The main theme of the thesis is to develop self-cleaning textiles based on visible-light activation of titania following dye-sensitisation approach, in conjunction with the lotus effect. The ideas, development and writing up of all the papers in the thesis were the responsibility of myself, working under the supervision of Dr. Walid A. Daoud, Prof. Steven J. Langford and Prof. Mark Sandeman at School of Applied Sciences and Engineering, Gippsland Campus and School of Chemistry, Clayton Campus, Monash University.

In the case of chapters 2-5, my contribution to the work involved the following:

Thesis chapter	Publication title	Publication status	Nature and extent of candidate's contribution
2	Self-cleaning cotton by porphyrin-sensitized visible-light photocatalysis	Published	Initiation, key ideas, experiments, data analysis and write up
3	Visible-light self-cleaning cotton by metalloporphyrin-sensitized photocatalysis	Published	Initiation, key ideas, experiments, data analysis and write up

4	Photostable self-cleaning cotton by a copper(II)porphyrin/TiO ₂ visible-light photocatalytic system	Published	Initiation, key ideas, experiments, data analysis and write up
5	Superhydrophobic and photocatalytic self-cleaning cotton	Submitted	Initiation, key ideas, experiments, data analysis and write up

I(have) / have not (circle that which applies) renumbered sections of submitted or published papers in order to generate a consistent presentation within the thesis.

Signed: ---



Shabana Afzal

Date: 11th Oct. 2013

Acknowledgements

All praises be to the Almighty Allah, the creator of all and the sustainer of all. Many thanks to Him, Who blessed me with the knowledge to differentiate between the right and wrong. All gratitude to Him as He blessed me with the guidance of the last Holy Prophet, Muhammad (PBUH).

I would like to express my sincere gratitude to my supervisors; Assist. Prof. Walid A. Daoud, Prof. Steven J. Langford and Prof. Mark Sandeman, for their continuous guidance, valuable suggestions, useful discussions and generous support throughout the course of my PhD program, including the planning and development of this thesis. I would especially like to thank Prof. Steven J. Langford for facilitating me to complete the experimental work in his laboratory, at Clayton campus.

My gratitude is also extended to the administrative staff and laboratory colleagues of Walid group and Langford group at Monash University for their technical assistance and cooperation in conducting my experimental work.

I would like to thank my parents whose countless prayers, support and patience gave me enough strength and courage to complete this task successfully. I thank to my husband for being supportive and helpful in my research work and amusing me in difficult times. Thanks to my brothers, who always encouraged my higher studies.

Thesis Abstract:

The primary motivation of the research work presented in this thesis is to develop dye-sensitised textiles capable of showing self-cleaning properties in daylight and indoor light environments. The photocatalytic degradation of organic contaminants by means of photoactive materials is one of the most effective and environmental-friendly methods for reducing the environmental pollution. Among the photoactive materials, anatase titanium dioxide is extensively investigated for a wide range of applications such as air purification, water treatment and self-cleaning surfaces. With high consumer demand for hygienic and contamination-free coatings, self-cleaning textiles based on anatase titanium dioxide photocatalysis have been of particular interest. However, the photocatalytic activity of anatase titanium dioxide is limited to ultraviolet region of the solar spectrum. To utilise the major portion of the solar spectrum, visible-light active photocatalytic systems are required in fabricating self-cleaning coatings.

Chapter 1 introduces the topic by giving an account on the chemistry behind the photocatalytic effect, dye-sensitisation, the use of porphyrins and examples of self-cleaning textiles that are state-of-the-art in the field. The chapter finishes by discussing the lotus effect and stating the thesis aims. By using *meso*-tetra(4-carboxyphenyl)porphyrin (TCPP) for sensitisation of TiO₂, visible-light driven self-cleaning cotton has successfully been developed, that exhibited superior photocatalytic self-cleaning properties to that of titanium dioxide or the dye in isolation (Chapter 2). A complete degradation of methylene blue was achieved under visible-light irradiation for 110 min. In addition, decolourisation of coffee and red wine stains was observed under visible-light irradiation for 16 h.

Chapter 3 and 4 investigate the use of metal complexes of TCPP (Fe, Co, Zn & Cu) as means of optimising the performance of our system on pristine cotton. In view of the practical applications of self-cleaning textiles, the stability of a photocatalyst is an important constraint. The results shown in this thesis indicate that *meso*-tetra(4-carboxyphenyl)-porphyrinato copper(II) (CuTCPP) showed enhanced photostability as compared to the high performing free-base porphyrin (TCPP).

To enhance the performance of these new materials further, the concept of lotus effect has been combined within the visible-light photocatalysis to prepare better self-cleaning textiles (Chapter 5). The dual functional textiles exhibited a superhydrophobic effect, in addition to the photodegradation of organic contaminants by visible-light photocatalysis. Superhydrophobic and photocatalytic self-cleaning textiles offer great potential for indoor and outdoor self-cleaning applications. Chapter 6 briefly summarises the thesis and adds future perspectives to this research.

Abbreviations and Acronyms

Abbreviations and Acronyms	Name
CB	Conduction band
CoTCPP	<i>meso</i> -tetra(4-carboxyphenyl)porphyrinato cobalt(II)
CuTCPP	<i>meso</i> -tetra(4-carboxyphenyl)porphyrinato copper(II)
DMF	Dimethylformamide
DSSC	Dye-sensitised solar cells
FeTCPP	<i>meso</i> -tetra(4-carboxyphenyl)porphyrinato iron(III)
HOMO	Highest occupied molecular orbital
IPCE	Incident photon to electron conversion efficiency
I_{sc}	Short-circuit photocurrent
LUMO	Lowest unoccupied molecular orbital
MB	Methylene blue
MTCPP	Metal complex of <i>meso</i> -tetra(4-carboxyphenyl)porphyrin
NHE	Normal hydrogen electrode
NMR	Nuclear magnetic resonance
NiTPP	5,10,15, 20-Tetraphenyl-21H,23H-porphine nickel(II)
4-NP	4-nitrophenol
OTMS	Trimethoxy(octadecyl)silane
Pp	Porphyrin
TCPP	<i>meso</i> -tetra(4-carboxyphenyl)porphyrin
TEA	Triethylamine
TPP	Tetraphenylporphyrin
TMeOPP	<i>meso</i> -tetra(4-methoxyphenyl)porphyrin
TSPP	<i>meso</i> -tetra(4-sulfonatophenyl)porphyrin
VB	Valence band
V_{oc}	Open-circuit photovoltage
WCA	Water contact angle
ZnTPP	5,10,15, 20-Tetraphenyl-21H,23H-porphine zinc(II)
ZnTCPP	<i>meso</i> -tetra(4-carboxyphenyl)porphyrinato zinc(II)
η	solar- to-electric energy conversion efficiency
η^c	Quantum efficiency
λ_{max}	Wavelength at maximum absorbance

Table of Contents

	Page No.
Title page	I
Addendum	II
Copyright notices	IV
General declaration	V
Acknowledgements	VII
Abstract	VIII
Abbreviations and Acronyms	X
Chapter 1: Introduction	1-39
1.1 Self-cleaning textiles	02
1.2 Photocatalytic effect of titanium dioxide	02
1.3 Practical applications of TiO ₂ photocatalysis	04
1.4 Mechanism of photocatalysis	04
1.5 TiO ₂ ; a semiconductor of choice	06
1.6 TiO ₂ -based self-cleaning textiles	07
1.7 Limitations and possible solutions	10
1.8 Visible-light induced photocatalysis	11
1.8.1 Band gap modification by transition metal doping	11
1.8.2 Band gap modification by non-metal doping	13
1.8.3 Semiconductor coupling	14
1.8.4 Dye sensitisation	15
1.9 Self-cleaning textiles based on dye-sensitised photocatalysis	16
1.10 Porphyrins	18
1.11 Photocatalytic efficiency of TiO ₂ based on porphyrin sensitisation	19

1.12	Lotus effect	25
1.13	Textiles with dual self-cleaning applications; superhydrophobic and photocatalytic properties	29
1.14	Research objectives	31
1.15	References	33

Chapter 2: Self-cleaning cotton by porphyrin-sensitised visible-light photocatalysis 40-50

	Declaration	40
	Abstract	42
2.1	Introduction	42
2.2	Experimental	42
2.2.1	Preparation of TiO ₂ /TCPP-coated cotton	42
2.2.2	Characterisation	43
2.2.3	Photocatalysis studies	43
2.2.4	Stability study	43
2.3	Results and discussion	43
2.3.1	SEM analysis	43
2.3.2	UV-Vis spectroscopy	44
2.3.3	XRD spectroscopy	44
2.3.4	Fluorescence spectroscopy	44
2.3.5	Self-cleaning performance	45
2.3.5.1	Photocatalytic degradation of methylene blue	45
2.3.5.2	Photocatalytic degradation of coffee and wine stains	45
2.3.6	Stability of TiO ₂ /TCPP coating	45
2.3.7	Photostability of TiO ₂ /TCPP coating	46
2.4	Conclusions	46
	Acknowledgements	47

Notes and references	47
Supporting information	48-50
Chapter 3: Visible-light self-cleaning cotton by metalloporphyrin-sensitised photocatalysis	51-66
Declaration	51
Abstract	53
3.1 Introduction	53
3.2 Experimental	53
3.2.1 Synthesis of MTCPP/TiO ₂ -coated cotton	54
3.2.2 Characterisation	54
3.2.3 Photocatalytic degradation	54
3.2.4 Stability of coating	54
3.3 Results and discussion	55
3.3.1 SEM analysis	55
3.3.2 XRD analysis	55
3.3.3 UV-Vis spectroscopy	55
3.3.4 Fluorescence spectroscopy	56
3.3.5 Self-cleaning properties: photocatalytic degradation of methylene blue	56
3.3.6 Stability of MTCPP/TiO ₂ -coating	57
3.4 Conclusions	59
Acknowledgements	59
References	59
Supplementary information	60-66

Chapter 4: Photostable self-cleaning cotton by a copper(II) porphyrin/TiO₂ photocatalytic system 67-79

Declaration	67
Abstract	69
4.1 Introduction	69
4.2 Experimental section	70
4.2.1 Synthesis of CuTCPP/TiO ₂ -coated cotton	70
4.2.2 Characterisation	70
4.2.3 Photocatalytic Studies	70
4.2.4 Stability of Coating	70
4.3 Results and discussion	70
4.3.1 SEM analysis	71
4.3.2 XRD analysis	71
4.3.3 UV-Vis spectroscopy	71
4.3.4 Photocatalytic degradation of methylene blue	72
4.3.5 Photocatalytic degradation of coffee and red wine stains	72
4.3.6 Photostability of CuTCPP/TiO ₂ catalyst	73
4.3.7 Stability of CuTCPP/TiO ₂ -coating	73
4.3.8 Mechanistic aspects	73
4.4 Conclusions	74
Acknowledgments	74
References	74
Supporting information	76-79

Chapter 5: Superhydrophobic and photocatalytic self-cleaning cotton 80-89

Declaration	80
Abstract	82
5.1 Introduction	82

5.2	Experimental	82
5.2.1	Fabrication of TCPP/TiO ₂ -coated cotton	82
5.2.2	Hydrophobisation of TCPP/TiO ₂ -coated cotton	83
5.2.3	Characterisation	83
5.2.4	Measurement of water contact angle	83
5.2.5	Photocatalytic studies	83
5.2.6	Durability of coating	83
5.3	Results and discussion	83
5.3.1	FESEM analysis	83
5.3.2	XRD analysis	84
5.3.3	UV-Vis spectroscopy	84
5.3.4	Solid state ²⁹ Si NMR spectroscopy	85
5.3.5	Superhydrophobic self-cleaning	85
5.3.6	Photocatalytic self-cleaning properties	85
5.3.7	Coating stability study	86
	Conclusions	86
	Acknowledgements	86
	References	86
	Table of content figure	88
	Supporting information	89

Chapter 6: Conclusion and perspectives 90-97

6.1	Summary	91
6.2	Limitations of visible-light driven self-cleaning textiles	93
6.3	Future of self-cleaning textiles	95
6.4	References	97

List of Figures

Chapter 1

1.1	Crystalline forms of TiO ₂	03
1.2	Applications of TiO ₂ photocatalysis	05
1.3	Mechanism of TiO ₂ photocatalysis	06
1.4	Band-gap energies of various semiconductors	07
1.5	Esterification of cellulose with the carboxylic group of the spacer leads to an attachment point to TiO ₂	08
1.6	Succinylation of keratin	09
1.7	The solar spectrum	11
1.8	Photocatalytic degradation of Neolan Blue 2G in an aqueous solution as a function of visible-light irradiation time for different substrates	12
1.9	Degradation of a red wine and coffee stains on control (pristine cellulosic fabrics), TiO ₂ and Au/TiO ₂ /SiO ₂ -coated fabrics before and after visible-light irradiation	13
1.10	Photocatalytic activities of cotton	14
1.11	A mechanism of photocatalysis through dye sensitisation	16
1.12	Potential dyes for sensitisation of TiO ₂	17
1.13	Structure of a porphine, the parent porphyrin structure	18
1.14	Classification of metalloporphyrin complexes	19
1.15	Structure of porphyrin with different functional groups	21
1.16	Energy level diagram describing the conduction and valence bands of TiO ₂ and energy levels of different porphyrins	22
1.17	Chemical structures of porphyrins with substituents at <i>ortho</i> and <i>para</i> -positions	24

1.18	Leaf of the lotus flower illustrating the superhydrophobic effect	26
1.19	Superhydrophobic films based on raspberry-like particles	27
1.20	Schematic presentation of the preparation of superhydrophobic surfaces on cotton substrate	28
1.21	Water repellent test on (a) pristine cotton fabric, (b) carbon nanotube-coated cotton fabric and (c) PBA-g-CNT coated cotton fabric	29
1.22	Fabrication of superhydrophobic surface on cotton substrate	29
1.23	(Left) SEM image of a polymer film with embedded anatase TiO ₂ nanoparticles (Right) UV-Vis spectra of superhydrophobic polymer films exposed to a resazurin dye under UV-irradiation	30
1.24	Discolouration of rhodamine b on the treated fabrics exposed to UV radiation for different periods of time	31
1.25	<i>Meso</i> -tetrakis(4-carboxyphenyl)porphyrin	32
1.26	Chemical structure of methylene blue	32
1.27	Chemical structure of trimethoxy(octadecyl)silane	32

Chapter 2

2.1	FESEM images of cotton samples	43
2.2	UV-Vis spectra of cotton samples	44
2.3	XRD spectra of cotton samples	44
2.4	Steady-state fluorescence spectra	45
2.5	Photocatalytic degradation of methylene blue	45
2.6	Degradation of coffee and red wine stains	46

2.7	TCPP retention in TiO ₂ /TCPP-coated cotton after washing with different solvents	46
2.8	Degradation of methylene blue for washed cotton samples	46
Chapter 3		
3.1	FESEM images of cotton samples	55
3.2	XRD spectra of cotton samples	56
3.3	UV-Vis spectra of cotton samples	56
3.4	UV-Vis and fluorescence spectra of MTCPP adsorbed on cotton in presence and absence of TiO ₂	57
3.5	Steady state fluorescence quenching of FeTCPP and Stern-Volmer plot	58
3.6	Photocatalytic degradation of methylene blue	58
Chapter 4		
4.1	FESEM images of cotton samples	71
4.2	XRD spectra of cotton samples	71
4.3	UV-Vis spectra of cotton samples	71
4.4	Photocatalytic degradation of methylene blue	72
4.5	Photocatalytic degradation of coffee and red wine stains	72
4.6	UV-Vis spectra of CuTCPP/TiO ₂ -coated cotton fabrics	73
4.7	Percentage retention of CuTCPP on cotton fabrics after washing with detergent, petroleum ether and water	73
4.8	Proposed photocatalytic mechanism	74

Chapter 5

5.1	FESEM images of cotton samples	84
5.2	XRD spectra of cotton samples	84
5.3	UV-Vis spectra of cotton samples	84
5.4	²⁹ Si NMR spectra	85
5.5	Images attained after 5 µL water droplets were placed on cotton samples	85
5.6	Degradation of methylene blue under visible-light irradiation	85
5.7	UV-Vis spectra of methylene blue adsorbed on cotton	86
5.8	Water contact angles of OTMS/TCP/PP/TiO ₂ -coated cotton fabrics as a function of the number of wash cycles	86

List of Tables

Chapter 1

1.1	Self-cleaning textiles based on TiO ₂ photocatalysis	10
1.2	Visible-light photocatalysis by porphyrin-sensitised TiO ₂	20
1.3	Comparison of UV-Vis and IV-characteristic properties of different porphyrins	21
1.4	Photocatalytic degradation of 4-nitrophenol	23
1.5	Photocatalytic degradation of 4-nitrophenol	25

Chapter 3

3.1	UV-Vis absorption of MTCPP in DMF and adsorbed on TiO ₂ -coated cotton	56
3.2	Retention of MTCPP on fabric and the corresponding photocatalytic efficiency after washing with different solvents	58

List of Schemes

Chapter 2

- 2.1 Formation of self-assembled monolayer of TCPP molecules
on TiO₂-coated cotton 43

Chapter 3

- 3.1 Formation of thin films of MTCPP on TiO₂-coated cotton 54

Chapter 4

- 4.1 Formation of thin films of CuTCPP on TiO₂-coated cotton 70

Chapter 5

- 5.1 Formation of hydrophobised OTMS/TCPP/TiO₂-coated
cotton 83

Chapter 1:

Introduction

CHAPTER 1: INTRODUCTION

1.1 Self-cleaning textiles

With high consumer demand for hygienic and contamination free materials, interest in developing self-cleaning coatings has grown rapidly in recent years.¹ Self-cleaning coatings have become an important labour-saving device because of the number of possible applications, such as self-cleaning paints,² glass-windows,³ cement,⁴ anti-fogging⁵ and anti-biofouling surfaces.⁶ In fact, the concept of self-cleaning surfaces has now been applied to textiles and is considered an important advance in smart clothing.⁷

Based on the nature of the self-cleaning mechanism, self-cleaning textiles are classified into two categories: hydrophobic and hydrophilic. In its extreme, the former is known as the 'lotus effect', and can be achieved by mimicking the natural features of lotus leaves.⁸ On these leaves, water attains the shape of spherical droplets, as the surface is superhydrophobic and readily rolls off thereby, carrying away any dirt particles. Hydrophilic self-cleaning, also known as the 'photocatalytic effect', is obtained by photoactive materials which chemically break down the adsorbed contaminants through photooxidation and photoreduction processes in the presence of light and moisture.⁹

1.2 Photocatalytic effect of titanium dioxide

Conventional methods of producing energy from fossil fuels have not only depleted fuel reserves but have also increased environmental pollution as a result of excessive fuel combustion. Keeping in view the high energy demand under these conditions, and making the environment safe at the same time, a field of alternate renewable energy resources is being developed. Amongst these resources, the use of solar light for electricity generation and environmental purification processes are of particular interest and extensive research has been carried out to fabricate photoactive materials to develop energy transducing systems.¹⁰

Titanium dioxide being a photoactive material, has gained much attention for its role in solar energy conversion. Moreover, it is being widely used in paints, cosmetics and food stuffs. In the simplest terms, TiO_2 is a photoactive semiconducting material. It exists in three allotropic forms: rutile, anatase and brookite (Figure 1.1).¹¹ Among these, rutile and anatase are commonly used in photocatalysis. However, anatase has always shown a much higher photocatalytic activity than rutile in all types of reaction media and in the presence of O_2 as an oxidising species.¹² For example, anatase exhibited three times faster rate of reaction for photocatalytic oxidation of cyclohexanone, as compared to that of rutile.¹² The higher photocatalytic efficiency of anatase is attributed to the fact that anatase has higher oxygen exchange ability as compared to rutile.¹³ In addition, anatase has a relatively lower electron-hole recombination rate as compared to rutile.¹²

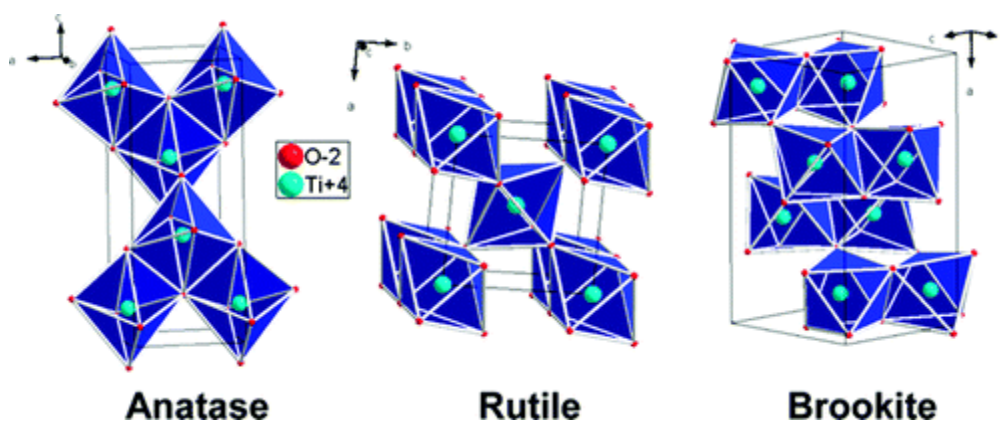


Figure 1.1: Crystalline forms of TiO_2 .¹¹

Heterogeneous photocatalysis is generally considered as a catalytic photochemical reaction that, in the case of TiO_2 , takes place on the surface of the semiconducting materials.¹⁴ Photocatalysis involves two reactions occurring simultaneously. The first is the oxidation from photogenerated holes and second is the reduction from photogenerated electrons. This can be seen by the photocatalytic reduction of gold chloride (AuCl_3) to metallic gold and silver nitrate (AgNO_3) to metallic silver on various oxides such as CeO_2 , Ta_2O_5 , Nb_2O_5 and TiO_2 upon illumination.¹⁵

1.3 Practical applications of TiO₂ photocatalysis

Goodever and Kitchner studied the photocatalytic decomposition of chlorazol sky blue on titania powder and proposed that titanium dioxide acts as a catalyst to accelerate the photochemical oxidation of the dye.¹⁶ Kato and Masho studied the photocatalytic activities of different TiO₂ powders to oxidise hydrocarbons and alcohols and found that anatase was more active than rutile.¹⁷ In 1972, Fujishima and Honda discovered the ability of TiO₂ to generate hydrogen and oxygen by water splitting.⁹ The first reported use of TiO₂ for the purification of water by photocatalytic decomposition of pollutants converted cyanide and sulphite to cyanate and sulphate, respectively, by photocatalytic oxidation.¹⁸

Since 1972, photocatalysis has continued to expand in both selective¹⁹ and unselective²⁰ oxidations of organic compounds for water and air purification. In such systems, powerful UV light is required. In water purification systems, removal of TiO₂ powders suspended in water proved to be difficult and cost ineffective. This criterion also limits application to situations where UV radiation is dominant. Furthermore, it became apparent in early 1990s that the amount of UV light present in natural sunlight or artificial light was insufficient to oxidise large quantities of organic contaminants. As a result, efforts turned to applications in which a relatively small number of UV photons could be used to carry out the reactions at TiO₂ surfaces. This initiated the development of self-cleaning, self-sterilising solid surfaces.²¹ Under such conditions, it was necessary to develop ways to coat various materials with TiO₂ films. These materials include self-cleaning glass, windows, ceramics, tiles, metals and textiles, as shown in Figure 1.2.

1.4 Mechanism of photocatalysis

In a heterogeneous photocatalytic system, semiconductor particles are in close contact with gaseous or liquid reaction media. Photocatalysis involves continuous photoelectrochemical and electrochemical reactions which involve generation of electrons and holes. Semiconductors like TiO₂ have a filled valence band and an empty conduction band.



Figure 1.2: Applications of TiO_2 photocatalysis.

The energy difference between the lowest energy level of the conduction band and the highest energy level of the valence band is called the band gap energy (E_g). For TiO_2 (anatase), E_g is 3.2 eV. When TiO_2 is irradiated with photons of energy; UV light ($\lambda < 385$ nm), greater than its band gap energy, then an electron (e^-) promotes from valence band to the conduction band, leaving a hole (h^+) behind (Figure 1.3). These photo-excited electron hole pairs diffuse to the surface of the catalyst and take part in a series of oxidation-reduction reactions at the interface.

On TiO_2 , oxidation reactions might involve oxygen evolution, hydroxyl radical production or organic oxidation, whereas reduction reactions might involve reduction of oxygen to superoxide radical anion, hydrogen peroxide or water.¹⁰ The radicals formed are usually reactive, reacting instantaneously with organic contaminants present in the vicinity. This reaction leads to degradation of the contaminants into relatively simple compounds e.g. CO_2 and H_2O (Figure 1.3).

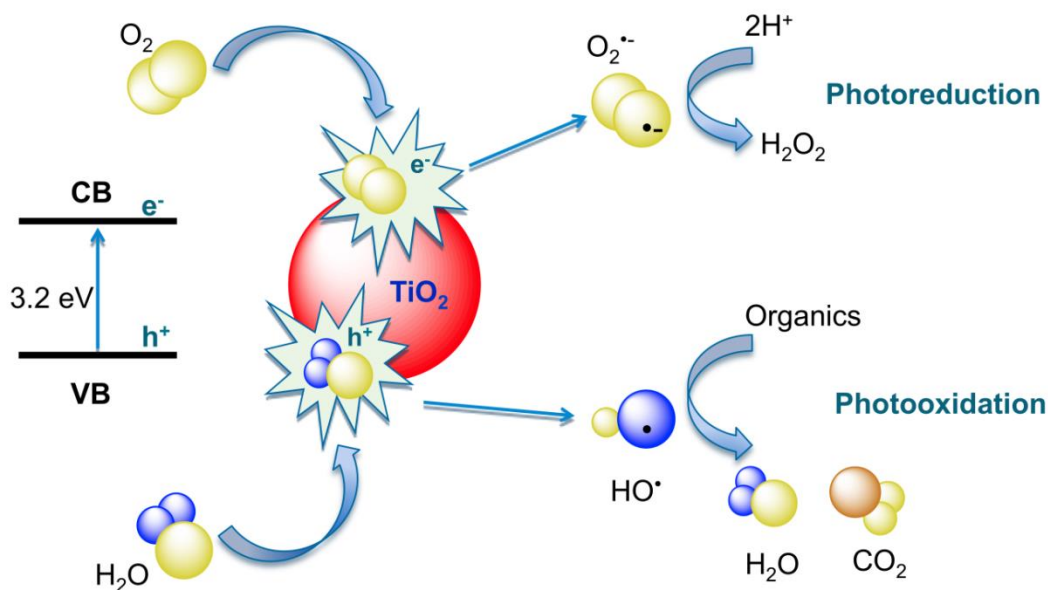


Figure 1.3: Mechanism of TiO_2 photocatalysis.

1.5 TiO_2 ; a semiconductor of choice

The conduction band potential of the semiconductor and redox potentials of the adsorbing species on the surface of the semiconductor are key parameters which determine the ability of a semiconductor to undergo photo-induced electron transfer. For an efficient photocatalysis, the redox potential should lie within the band gap of the semiconductor photocatalyst to allow evolution of hydrogen and oxygen from water and for the formation of radicals such as $\cdot\text{OH}$, $\text{O}_2^{\cdot-}$ and H_2O_2 .²² An energy band diagram for some common semiconductors is given in Figure 1.4.

In addition, the catalysts should remain stable in air and water-rich environments to increase versatility and pragmatic applications. Semiconductors with narrow band gaps such as Fe_2O_3 (2.3 eV), GaP (2.23 eV) and GaAs (1.4 eV) are unstable in aqueous media and therefore not suitable for most photocatalytic applications.²³ An efficient photocatalyst for degradation of organic pollutants is ZnO (3.2 eV) but unfortunately it undergoes photocorrosion in acidic aqueous conditions.²⁴ Titanium dioxide having the same band gap of 3.2 eV, has been preferred to other semiconductors because of its high oxidising ability, high chemical stability, low cost and non-toxic nature.²⁵

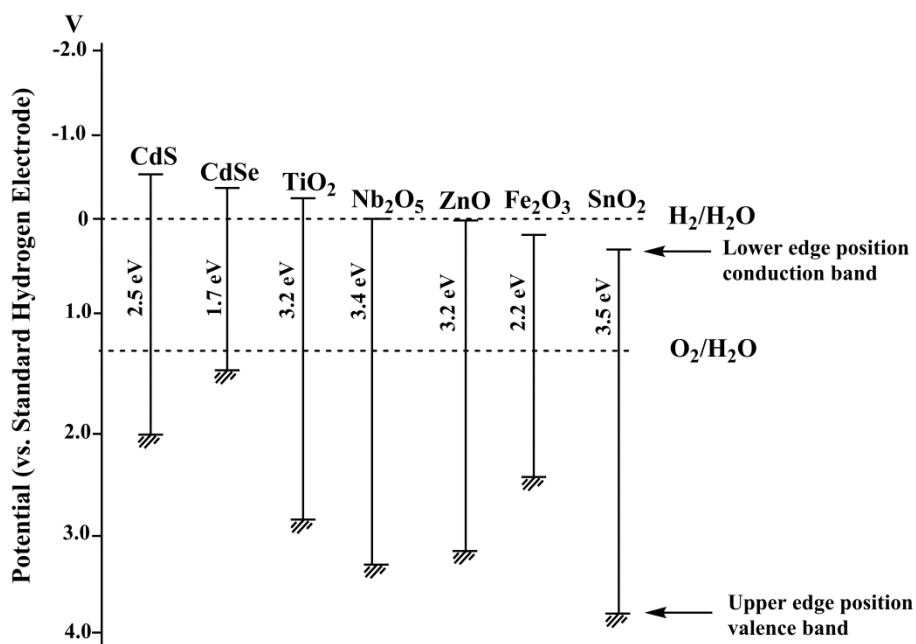


Figure 1.4: Band gap energies of various semiconductors.²⁶

1.6 TiO₂-based self-cleaning textiles

The discovery of the photocatalytic properties of titania has brought with it new opportunities towards the concept of self-cleaning.⁷ From the development of self-cleaning glass, ceramics and metals, research has now been extended to fabrication of self-cleaning textiles.²⁷ Clothes that can clean themselves, without the use of laundry detergent, can no longer be regarded as unrealistic.

Based on nano-crystalline TiO₂, a number of self-cleaning textiles have successfully been developed using cotton,²⁸ wool²⁹ and polyester.³⁰ However, most of these materials work only under exposure to UV irradiation or sunlight. In view of commercial applications based on a low temperature sol-gel process (~60°C), members of our group have developed a self-cleaning cotton.²⁸ In this process, a thin coating of anatase titania has been applied to cotton fabric using a conventional dip-pad-dry-cure method. Titania-coated cotton fabric has shown significant self-cleaning properties such as degradation of coffee and wine stains under UV irradiation, as well as good anti-bacterial activity.²⁸ In another example, aqueous

dispersions of Degussa P-25 TiO_2 (70% anatase, 30% rutile) and silicone softeners have also been applied to cotton fabrics and their photocatalytic activity has been evaluated for decomposition of gaseous ammonia under UV irradiation.³¹ Others have successfully developed UV-active cellulose fibres by using a low temperature sol-gel method ($\sim 100^\circ\text{C}$). The photocatalytic activity of fibres has been found to be retained even after 20 washing cycles.³²

As photocatalytic efficiency also depends upon the amount of catalyst present, research efforts have also been focused on strategies to increase the quantity of titania on textile surfaces. These include modification of textiles by physical or chemical surface pre-treatments prior to coating with TiO_2 .^{33, 34} For example, cotton fabrics have been activated physically by RF, MW and UV plasma,³³ inducing negatively charged functional groups such as carboxylates ($-\text{COO}^-$) and peroxyanions ($-\text{OO}^-$) on the textile surface. These functional groups have strong affinity to bind with TiO_2 particles. Cotton fibres have shown to exhibit significant photocatalytic efficiency for mineralisation of coffee, red wine, make up and grease stains under daylight irradiation.³³ Chemical spacers such as poly-carboxylic acids have also been used on cotton textiles.³⁴ These spacers attach to the hydroxyl groups of cellulose by forming esters. In such a system, TiO_2 particles bind to the cotton surface by chemical means through spacers (Figure 1.5).

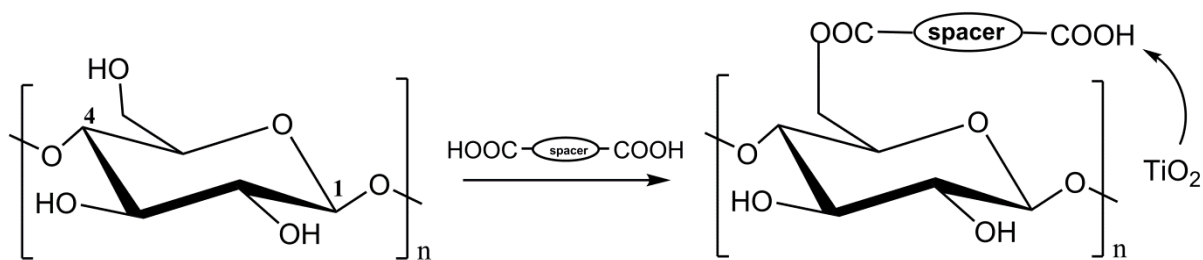
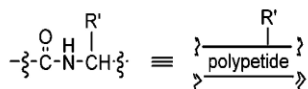
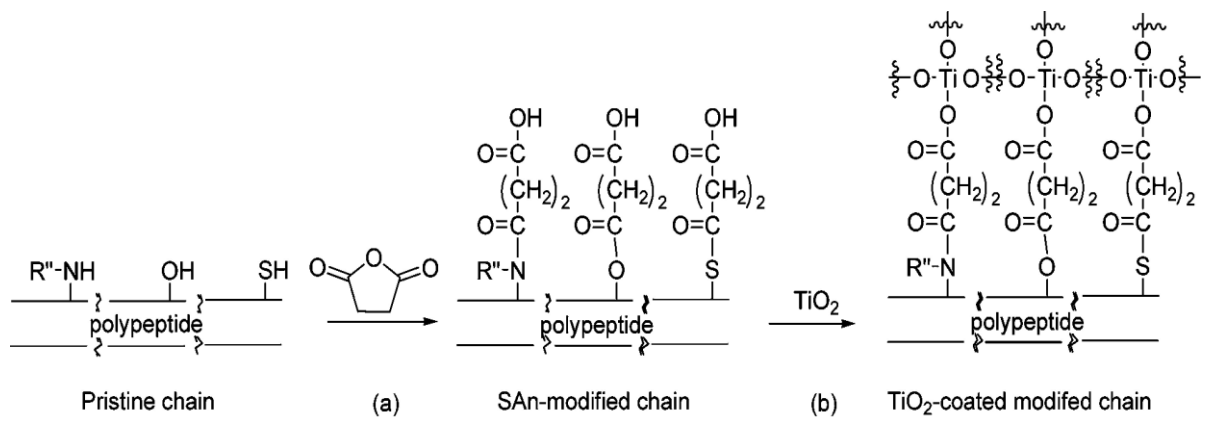


Figure 1.5: Esterification of cellulose with the carboxylic group of the spacer leads to an attachment point to TiO_2 .³⁴

The self-cleaning performance of polyester fibres³⁰ and wool-polyamide textiles³⁵ obtained by plasma treatment under UV and daylight, respectively, have also been studied. The layer by layer deposition of TiO₂ nanoparticles on cationically modified woven cotton fabrics, followed by treatment with anionic TiO₂ colloid and cationic TiO₂ colloid solution has been found to degrade red wine stains under UV irradiation.³⁶

A self-cleaning wool capable of degrading organic pollutants under UV irradiation has also been developed.²⁹ In this case, surface modification of wool fabric was carried out before treatment with a titania nanosol to enable strong bonding with the anatase nanocrystals, since wool is a keratinous fibrous protein with sulphur containing cysteine amino acid constituents. According to this work, and unlike cotton, wool fibres contain less than 50% the amount of hydroxyl and carboxylic acid groups. Therefore, surface modification was required in order to introduce surface functional groups capable of having a strong affinity with titanium dioxide. In this regard, acylation of fibres allowed enrichment of carboxylic acid groups in their backbone chains (Figure 1.6).



R' = reactive functional group; e.g. -R''NH, -OH, -SH

Figure 1.6: Succinylation of keratin.²⁹

Table 1.1 summarises the literature regarding self-cleaning textiles based on TiO₂ photocatalysis.

Table 1.1: Self-cleaning textiles based on TiO₂ photocatalysis.

Source of irradiation	Textiles	Photocatalyst	Stain used/ irradiation time	Irradiance (mW/cm ²)
UV (365 nm)	Cotton ²⁸	Anatase TiO ₂	Neolan blue 2G (8 h), Wine, coffee (20 h)	1.3 95
	Polyester fibres ³⁰	Anatase TiO ₂	Neolan blue 2G (3 h), Coffee (12 h), Wine (5 h)	1.3 95
	Wool ²⁹	Anatase TiO ₂	Methylene blue (15 h), Wine (20 h)	45 45
	Cotton ³¹	Degussa P-25	Gaseous Ammonia (50 min)	
Solar simulated light (290-3000 nm)	Cellulose fibre ³²	Anatase TiO ₂	Methylene blue (20 h)	50
	Polyester, wool ³⁷	Rutile/Anatase/ SiO ₂	Coffee, make up, grease (24 h)	50
	Cotton ³⁸	Ag/SiO ₂ /TiO ₂	Wine (24 h)	50
Visible-light ($\lambda >$ 400 nm)	Cotton ³⁹	Au/SiO ₂ /TiO ₂	Wine, Coffee (20 h)	95
	Cotton ⁴⁰	Fe/ TiO ₂	Neolan Blue 2 G (4 h)	50
	Cotton ⁴¹	TEA/Ag/TiO ₂	Methyl orange (120 min)	

1.7 Limitations and possible solutions

Titanium dioxide is a benchmark for UV photocatalysis only. Anatase TiO₂, which is the most photoactive phase of TiO₂, only absorbs UV light at wavelengths shorter than 380 nm.⁴² As a result of its wide band gap (3.2 eV), TiO₂ is inactive under visible-light, being unable to utilise the major portion of the solar spectrum as sunlight consists of 5% of UV light, 46% of visible light and 47% of infrared light

(Figure 1.7).⁴³ Therefore, visible-light active titanium dioxide photocatalytic systems are needed for outdoor applications in daylight and indoor applications as well.⁴⁴

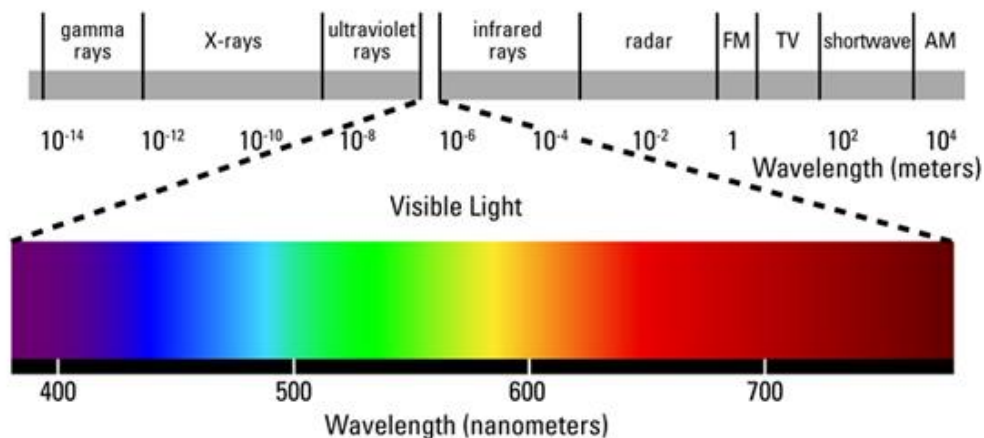


Figure 1.7: The solar spectrum.⁴³

1.8 Visible-light induced photocatalysis

To utilise visible-light for photocatalysis, several different approaches have been reported in literature, such as band gap modification by doping with metals⁴⁵ or non-metals,⁴⁶ coupling TiO₂ with other semiconductors of a narrow band gap⁴⁷ and dye-sensitisation.²²

1.8.1 Band gap modification by transition metal doping

Transition metal ion doping such as Fe³⁺, Cr³⁺, Co²⁺, V⁴⁺ and Mo⁵⁺ can enhance the photocatalytic activity of TiO₂ towards visible light.^{45, 48} Transition metal doping can improve the visible-light photocatalytic efficiency of TiO₂ through different mechanisms, which includes the introduction of new impurity states within the band gap of TiO₂, overlapping of the conduction band of TiO₂ with *d* orbitals of transition metals and reduction in recombination rate by separation of electron hole pairs.²² However, a specific concentration range of metal is effective (~ 0.5 % w/w), as it improves the trapping efficiency of electrons by prohibiting the electron-hole

recombination during illumination.⁴⁵ At higher concentrations, these ions act as recombination centres leading to lower visible-light activity.

Among various transition metals used, Fe-doping is the most widely studied.⁴⁹ Doping of Fe through an ion-implantation technique has produced more pronounced effect into the band edge of TiO₂ to visible light than Fe doping by the sol-gel method.⁵⁰ Vanadium-doping by means of the sol-gel method has also shown better photocatalytic rates under visible-light irradiation along with increased hydrophilicity.⁵¹ Visible-light activities have been demonstrated for Pt-doped TiO₂ against oxidative and reductive degradation of chlorinated organic compounds. In such a system, the platinum introduces intra-gap impurity states, enabling valence band electrons of TiO₂ to absorb visible-light.⁵² The photocatalytic degradation of rhodamine 6G has also been investigated using Ag-doped TiO₂.⁵³ The silver ions suppress the recombination by quick scavenging of the photogenerated electrons.

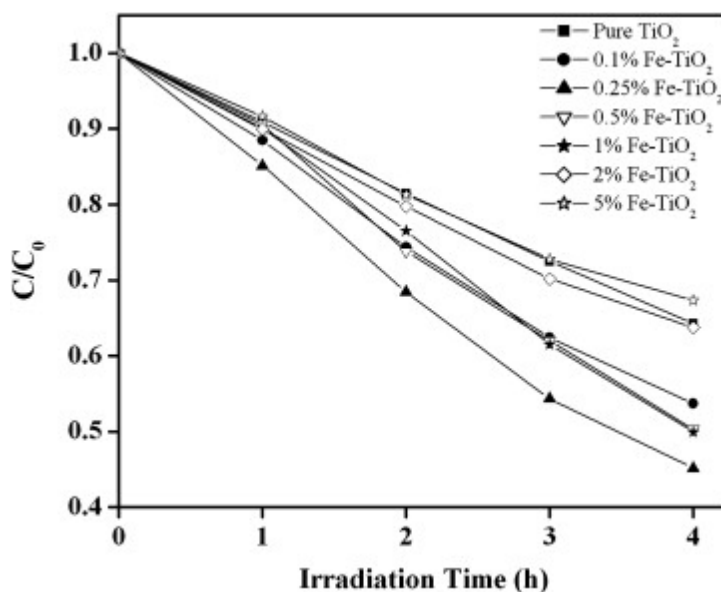


Figure 1.8: Photocatalytic degradation of Neolan Blue 2G in an aqueous solution as a function of visible-light irradiation time for different substrates.⁴⁰

55% photodecomposition of Neolan Blue 2G was obtained after 4 hours of visible-light irradiation on 0.25% Fe-TiO₂ coated cotton samples (Figure1.8).⁴⁰ In the case of Au/SiO₂/TiO₂ coated cotton, significant discolouration of coffee and red wine stains was achieved after 24 hours of visible-light irradiation (Figure1.9).³⁹

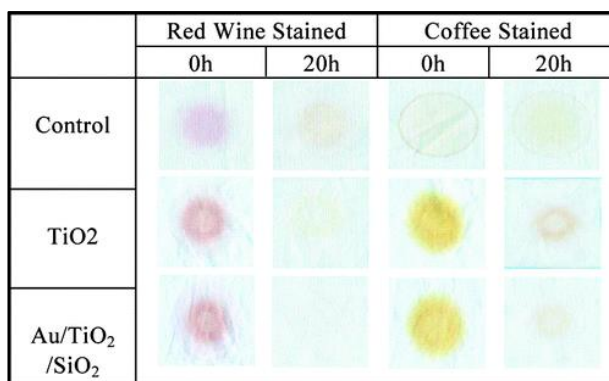


Figure 1.9: Degradation of red wine and coffee stains on control (pristine cellulosic fabrics), TiO₂ and Au/TiO₂/SiO₂-coated fabrics before and after visible-light irradiation.³⁹

1.8.2 Band gap modification by non-metal doping

Another promising approach to achieve visible-light activation is interstitial doping of non-metal elements such as N, C, S, B and F into a TiO₂ matrix.^{46, 54} Among them, *N*-doping has been extensively investigated. *N*-doped TiO₂ has been prepared by variety of methods which include physical methods such as magnetron sputtering,⁵⁵ implantation,⁵⁶ high temperature sintering of TiO₂ under nitrogen atmosphere,⁵⁷ chemical methods such as sol-gel,⁵⁸ hydrothermal treatment in the presence of a precursor containing ammonia or organic amines.⁵⁹ However, preparation routes play an important role in determining the characteristics of the visible-light absorption band of doped TiO₂. For example, dopants can act as recombination centres, thus decreasing the photocatalytic efficiency of TiO₂ under visible-light.⁶⁰

Different mechanisms have been reported in the literature regarding visible-light activity of TiO₂ by *N*-doping. There are suggestions that nitrogen doping results in band gap narrowing by mixing O 2*p* states with N 2*p* states of substituted N atoms in newly formed valence band.⁴⁶ Contrary to this, others suggest the isolated N 2*p* states are formed above the valence band maximum of TiO₂, responsible for band gap narrowing in *N*-doped TiO₂.⁶¹ It has also been proposed that in doped TiO₂, nitrogen produces oxygen-deficient localised states, which induces visible-light absorption.⁶² As compared to single non-metal atoms doping, co-doping with two non-metal atoms such as N and S,⁶³ N and C,⁶⁴ N and B,⁶⁵ and N and F,⁶⁶ have shown more beneficial effects. Improvement in visible-light efficiency can be due to synergistic effect of the two non-metals.²²

Long and co-workers have used triethylamine (TEA) in combination with AgI to synthesise *N*-doped TiO₂ sols.⁴¹ The cotton fabric coated from N/TiO₂ sol showed considerable photoactivity (70 %) by degrading methyl orange under visible-light irradiation for 120 minutes (Figure 1.10).

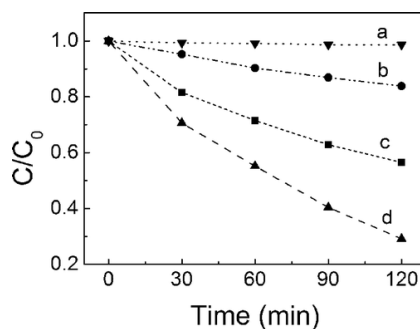


Figure 1.10: Photocatalytic activities of (a) cotton, (b) TiO₂/ cotton, (c) N/TiO₂ cotton and (d) Ag/N/TiO₂ cotton.⁴¹

1.8.3 Semiconductor coupling

Coupling semiconductors with narrow band gaps to TiO₂ represents another promising approach that can be utilised to extend the photocatalytic response of TiO₂ in the visible region of the electromagnetic spectrum.²² In a coupled semiconductor system, a small band gap semiconductor absorbs visible-light and thus acts as a photosensitiser for TiO₂. The sensitised semiconductor injects electrons into the conduction band of TiO₂, which can move to the surface of TiO₂ and produce reactive oxidative species.

Semiconductors like Bi₂S₃,⁴⁷ CdS,⁶⁷ CdSe,⁶⁸ V₂O₅⁶⁹ and CdO⁷⁰ have been reported to sensitise TiO₂ in the visible spectrum. Efficient electron transfer between sensitiser and TiO₂ depends on the potential difference of their conduction bands.⁶⁸ To work, the conduction and valence band potential of titania should be more negative than that of sensitiser semiconductor. Conduction band potentials of some semiconductors such as Bi₂S₃ (-0.76 V), CdS (-0.95 V) and CdSe (-1.0 V) are more negative than that of TiO₂ (-0.5 V) versus a normal hydrogen electrode (NHE). Amongst the various semiconductors, CdSe quantum dots are particularly of interest and have extensively been studied.⁶⁸ For example, significant degradation of 4-

chlorophenol has been observed by using CdSe quantum dots coupled with TiO₂ under visible-light illumination.⁶⁸

Similar to the activation of TiO₂ by metal/non-metal doping, the amount of semiconductor also affects the efficiency of a coupled system, since higher concentrations of the sensitizer semiconductor can block the surface of the catalyst and inhibit ensuing redox reactions. Furthermore, accumulation of charge carriers may increase the probability of electron-hole recombination, which in turn reduces photocatalytic efficiency of the coupled system. If holes are not engaged in furthering redox reactions, they can photocorrode the sensitizer semiconductor.²²

1.8.4 Dye-sensitisation

Photosensitisation of TiO₂ can also be achieved by visible-light absorbing dyes. Specifically in the field of dye-sensitised solar cells (DSSC), research related to the fabrication of suitable organic dyes is of great interest.⁷¹ However, because of its diverse applications, research regarding dye-sensitised applications in photocatalysis has also been growing over the past decades.⁷²

In this form of sensitisation, the dye is usually adsorbed on the TiO₂ surface through electrostatic, hydrophobic or chemical interactions.²² Sensitisation usually occurs by excitation of dye molecules under visible-light illumination and then subsequent electron injection into the conduction band (CB) of TiO₂. When visible-light falls on the catalyst surface in the presence of dye, it is the dye molecule that first gets excited promoting an electron from the ground state (HOMO) of dye molecule to the excited state (LUMO). The energy level of the excited state (LUMO) lies higher than the CB of TiO₂, as shown in Figure 1.11. As the LUMO of the dye molecules has more negative potential compared, to the CB potential of TiO₂, electrons can be easily injected into the CB of TiO₂ in a relaxation process.

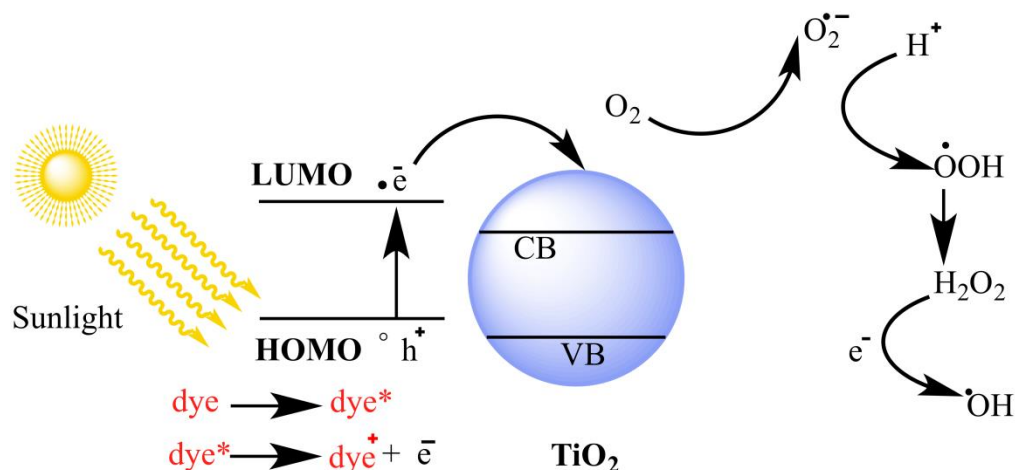


Figure 1.11: A mechanism of photocatalysis through dye-sensitisation.

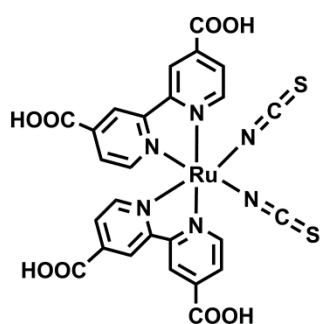
1.9 Self-cleaning textiles based on dye-sensitised photocatalysis

Despite the aforementioned strategies for TiO_2 activation in the visible-region, very few visible-light driven self-cleaning textiles have been developed (Table 1.1). Visible-light self-cleaning textiles may be developed following a dye-sensitisation approach. In this regard, there is a need to select particular dyes with specific characteristics for success. These include:

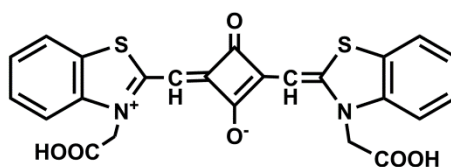
- The dye should be photochemically stable. It should not be degraded by the catalyst itself;
- The absorption properties of the dye should cover a broad spectral range (390-800 nm);
- The dye should have a low chance for recombination (less photoluminescence);
- The dye should allow a high rate of electron injection to TiO_2 *i.e.* the dye possesses functional groups capable of strong binding with TiO_2 to enhance charge transfer;
- The dye should possess a high quantum yield;

- The excited-state lifetime of the dye should be long enough lived to allow efficient charge transfer to TiO_2 .

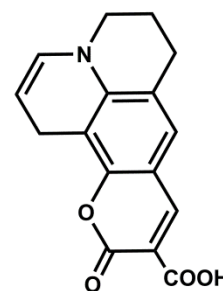
Various dyes have potential to be used for the photosensitisation of TiO_2 such as ruthenium bipyridyl complexes, coumarins, squarines, perylenes, porphyrins and phthalocyanines (Figure 1.12).⁷³ The dyes mentioned here are being used mainly for dye-sensitised solar cells (DSSC). Ruthenium dyes have been found to give maximum efficiency for sensitising TiO_2 in dye sensitised solar cells.⁷⁴ However, due to their limited availability and harmful impacts on the environment, cheaper and safer alternate dyes are being investigated such as porphyrins⁷⁵ and phthalocyanines.⁷⁶ Other dyes such as erthrosine B,⁷⁷ rose bengal,⁷⁸ eosin,⁷⁹ and acid red,⁸⁰ have been found to be efficient but unstable.



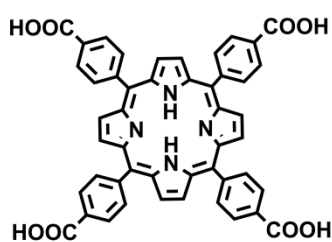
Ruthenium bipyridyl complex



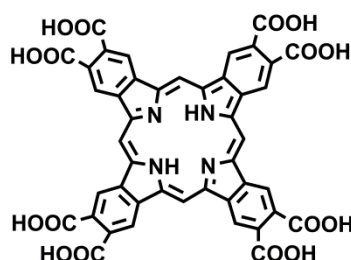
Squaraine



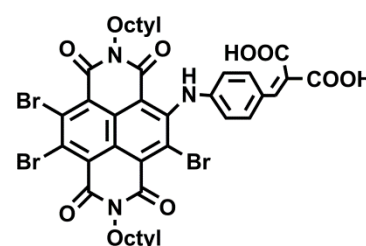
Coumarin



Porphyrin



Phthalocyanine



Naphthalene Diimide

Figure 1.12: Dyes potentially useful for the sensitisation of TiO_2 .

Despite having lower photosensitising efficiencies than ruthenium bipyridyl complexes,⁸¹ porphyrins or their metal complexes can be better substitutes for ruthenium dyes because of their strong absorption coefficient in the visible spectrum, good chemical photostability,⁸² low cost of production and lower toxicity.⁷⁵ Moreover, they can be easily modified by addition of peripheral substituents and by metal complexation.

1.10 Porphyrins

Plants collect solar energy by enhanced light absorption through porphyrin-based chromophores (chlorophyll) (Figure 1.13). These chlorophyll chromophores act as a light-harvesting antenna.⁸³ They absorb incident light and then channel the excitation energy to reaction centres, where light-induced charge separation takes place. Inspired by their primary role in photosynthesis, these chlorophyll chromophores are being mimicked by functionalised porphyrin-derivatives.⁸⁴

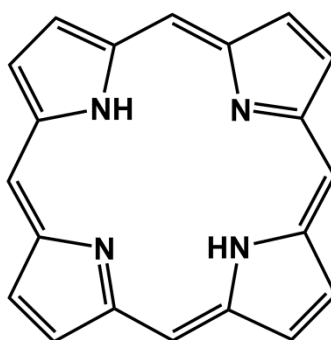
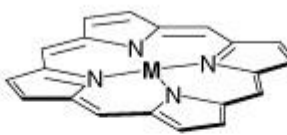


Figure 1.13: Structure of a porphine, the parent porphyrin structure.

Porphyrins are macrocycles exhibiting high conjugation and extensive delocalisation. Owing to their delocalised structure and very strong absorption at 400–450 nm (Soret band) as well as absorption in the 500–700 nm (Q-bands),⁸⁵ porphyrins have been studied as promising candidates for their applications in molecular electronic and photonic devices,⁸⁶ dye-sensitised solar cells^{73b} and for photocatalytic degradation of organic compounds, when coupled with TiO_2 .⁸²

Porphyrins are able to complex with many of the metal ions listed in the periodic table, resulting in four to six co-ordination metal complexes (Figure 1.14). Metal complexes of porphyrins can absorb visible light with high absorptivity and thus can

act as better photosensitisers in catalytic electron transfer reactions than metal free porphyrins.⁸⁷

	2	3	4	5	6	7	8	9	10	11	12	13	14	15	16	
1																
2																Be
3	Mg												Al	Si	P	S
4	Ca	Sc	Ti	V	Cr	Mn	Fe	Co	Ni	Cu	Zn	Ga	Ge	As	Se	
5	Sr	Y	Zr	Nb	Mo	Tc	Ru	Rh	Pd	Ag	Cd	In	Sn	Sb	Te	
6	Ba	La	Hf	Ta	W	Re	Os	Ir	Pt	Au	Hg	Tl	Pb	Bi	Po	
7	Ra	Ac														

M	Six coordinated high valent complexes
M	Other types of complexes
M	Absence of complexes

Figure 1.14: Classification of metalloporphyrin complexes.⁸⁸

Studies have been carried out in the past few years to investigate the effect of porphyrins and metal porphyrins on visible-light sensitisation of TiO₂ powder. These efforts include photodegradation of acid chrome blue K,⁸⁹ rhodamine b,⁹⁰ atrazine,⁹¹ 4-nitrophenol,⁹² methylene blue,⁹³ 2,4-dichlorophenol⁹⁴ and acid orange.⁹⁵ More recently, self-cleaning glasses based on mesoporous TiO₂ films impregnated with *meso*-tetrakis(4-sulfonatophenyl)porphyrin have been developed for visible-light indoor air oxidation.⁹⁶

Table 1.2 gives a summary of different porphyrin derivatives reported in the literature, used for photocatalytic degradation of different organic dyes under visible-light irradiation.

1.11 Photocatalytic efficiency of TiO₂ based on porphyrin sensitisation

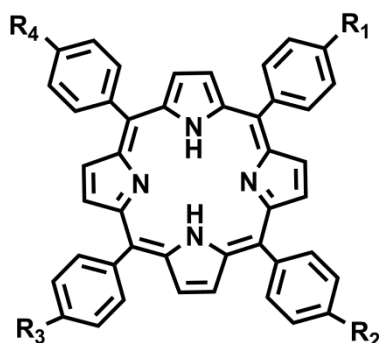
Apart from the influence of a particular dye on the photocatalytic efficiency of TiO₂, there are many other factors that can alter the photocatalytic efficiency of TiO₂. Details of these factors are elaborated as following;

a. Nature of functional groups

Research has been carried out to study the effect of different substituents within porphyrin derivatives.⁹⁹ Comparison of the photochemical properties and photosensitisation phenomenon for three free-base porphyrins with different functional groups has also been reported.^{99a} These functional groups include carboxylic acid, sulphonic acid and simple phenyl groups as shown in the Figure 1.15.

Table 1.2: Visible-light photocatalysis by porphyrin-sensitised TiO₂.

Catalyst	Porphyrin	Stain used/ Irradiation time	% age degrad.	Irradiance
Composite	TPP ⁹⁰	Rhodamine B (30 min)	51 %	200 (W) Incand. Lamp
	NiTPP, ZnTPP ⁹³	Methylene blue (6 h)	95%, 90%	3 (mW/cm ²)
	NiTPP ⁹⁴	2,4-dichlorophenol (4 h)	81%	0.16 (mW/cm ²)
	T CPP ⁸⁹	Acidchrome blue K (30 min)	95%	200 (W) Incand. Lamp
	CuT CPP ⁹¹	Atrazine (60 min)	82%	
	CuT CPP ⁹⁷	Methylene blue (45 min)	59%	200 (W) Incand. Lamp
Coating (glass wool)	T CPP ⁹⁸	Acetone (30 min)	25%	1 (mW/cm ²)
Coating (glass)	T SPP ⁹⁶	Acetaldehyde (120 min)	19%	0.02 (mW/cm ²)



$R_1 = R_2 = R_3 = R_4 = \text{COOH}$, TCPP;
 $R_1 = R_2 = R_3 = R_4 = \text{SO}_3^-$, TSPP;
 $R_1 = R_2 = R_3 = R_4 = \text{H}$, TPP

Figure 1.15: Structure of a porphyrin with different functional groups.^{99a}

Results comparing spectral measurements and photochemical properties imply that the binding state between the dye and semiconductor is an important factor for photosensitisation of the semiconductor. Tetra-carboxylic acid porphyrins such as TCPP have shown the highest incident photon-to-electron conversion efficiency (IPCE) among different substituted porphyrin derivatives (Table 1.3).^{99a} Strong binding of a carboxylic acid group to titanium dioxide enhances the electron injection efficiency.

Table 1.3: Comparison of UV-Vis and IV-characteristic properties of different porphyrins.^{99a}

Dye	λ_{max} (nm) (in presence of TiO_2)	IPCE (%)	V_{oc} (mV)	I_{sc} (μA)	η (%)
TCPP	422 (S), 523, 559, 596, 653 (Q)	40	360	2700	0.36
TSPP	422 (S), 521, 555, 596, 654 (Q)	10	290	630	0.04
TPP	418 (S), 518, 551, 592, 649 (Q)	2	340	320	0.006

S = Soret band of porphyrins, Q = four Q bands of porphyrins

The ability of porphyrins with varying functional groups to inject electrons into the conduction band of TiO_2 can be evaluated by comparing the energy difference between the conduction band of TiO_2 and the oxidation potential values of the porphyrins in their excited state. It can be clearly observed from Figure 1.16 that TCPP exhibits more negative oxidation potential (-1.36 V) in the excited state as compared to TSPP and TMeOPP. As a result, more efficient electron injection into conduction band of TiO_2 is expected by TCPP.^{99b}

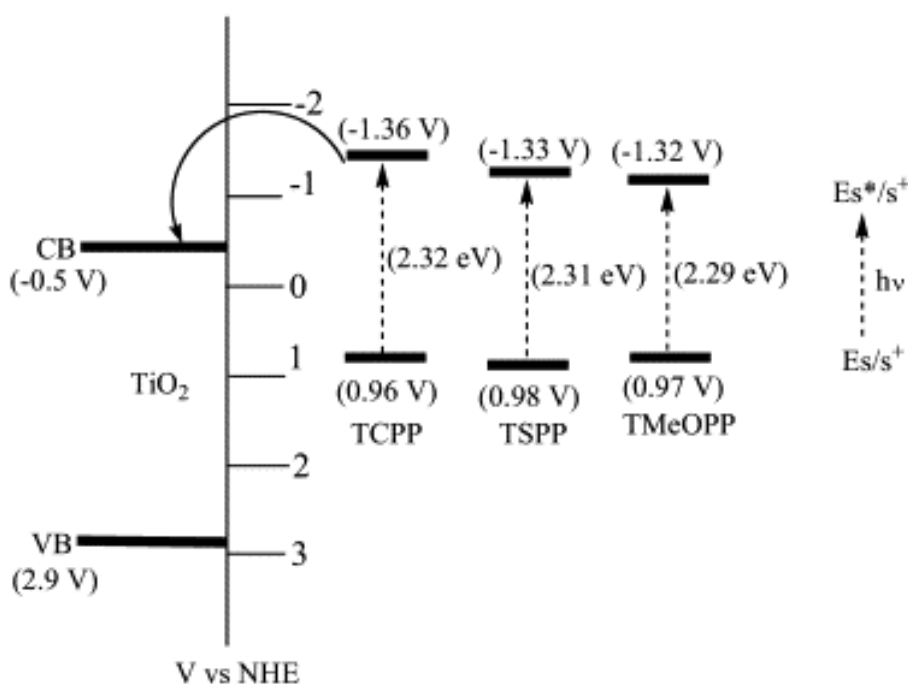


Figure 1.16: Energy level diagram describing the conduction and valence bands of TiO_2 and energy levels of different porphyrins.^{99b}

b. Nature of metal centre

The type of metal coordinated in the macrocyclic ring of the porphyrin is another important factor in determining the photocatalytic efficiency of titanium dioxide. In this regard, Mele and his co-workers have investigated the role of metal in the macrocycle on the photocatalytic performance of TiO_2 .⁸² Porphyrin complexes with three different metals: iron, manganese and copper were synthesised and then impregnated with TiO_2 . These TiO_2 /metal complexes samples were tested for the photocatalytic degradation of 4-nitrophenol in aqueous solutions. TiO_2 impregnated

with copper(II) porphyrin showed the highest photoreactivity as shown in Table 1.4. Only a slight beneficial effect was observed with iron(III) porphyrin, while the presence of manganese(III) porphyrin appeared to be detrimental.

Table 1.4: Photocatalytic degradation of 4-nitrophenol (4-NP).⁸²

Sample	Amount of sensitiser (μM)	Initial reaction rate ($\text{mol L}^{-1} \text{s}^{-1}$)	Quantum efficiency (η^c)
TiO₂		501	0.79
H₂Pp	6.65	606	0.95
CuPp	5.55	1225	1.93
	6.65	1162	1.83
	8.35	1087	1.71
FePp	3.49	617	0.97
	7.44	544	0.86
	13.64	535	0.84
MnPp	3.30	385	0.61
	6.65	399	0.63
	13.30	367	0.58

η^c = The ratio of the number of moles of the reacted 4-NP to the number of moles of the photons emitted by the UV lamp

c. Concentration of porphyrin dye

For titanium dioxide to have maximum rate of photocatalytic reaction, there has to be an optimum concentration of the dye, impregnated into TiO₂. Too high or too low concentration is not suitable for achieving maximum photocatalysis. In this case a copper(II) porphyrin with a concentration of 5.55 $\mu\text{M g}^{-1}$ of TiO₂ has been reported to show the highest rate of reaction (Table 1.4) in the degradation of 4-nitrophenol.

Table 1.5: Photocatalytic degradation of 4-nitrophenol (4-NP).¹⁰⁰

Samples	<i>meso</i> -phenyl substituent	Initial reaction rate (mol L ⁻¹ s ⁻¹)	% age degrd. of 4- NP
TiO ₂		0.16	5.1
H ₂ Pp	Para	0.16	4.5
	Ortho	0.25	7.1
ZnPp	Para	0.40	7.6
	Ortho	0.55	10.2
CoPp	Para	0.57	10.2
	Ortho	0.87	18.0
CuPp	Para	9.67	91.9
	Ortho	10.80	95.1

1.12 Lotus-effect

The story of self-cleaning materials begins in nature with the Lotus flower, which is considered sacred in India, China and Japan.¹⁰¹ It is venerated because of its exceptional purity. Lotus plants grow in muddy water, but its leaves stand meters above the water and are considered never dirty. Rain water washes dirt from the leaf more readily than any other plant. This property of the lotus leaf (Figure 1.18) was first recorded by Wilhelmm Barthlott in 1970.¹⁰¹

The lotus leaf exhibits excellent properties of self-cleaning because of two features on its surface; waxiness (due to the presence of water-repelling agents) and microscopic bumps; which impart roughness to the surface (Figure 1.18).¹⁰² As a result, the contact angle of a water droplet with the surface increases to such an extent (>150°) that water attains the shape of a spherical droplet.⁸ In doing so, it rolls off the surface and can take away any soluble dirt particles with it. The result is that the leaf surface stays neat and clean. This extreme water repellence is known as superhydrophobicity and such behaviour is known as the “lotus effect” or “superhydrophobic effect”.



Figure 1.18: Leaf of the lotus flower illustrating the superhydrophobic effect.¹⁰²

Based on the self-cleaning properties of the lotus leaf, scientists have fabricated artificial superhydrophobic surfaces.⁸ In designing such surfaces, two important factors are considered, surface energy and surface roughness.¹⁰³ Hydrophobicity is usually obtained with low surface energy materials such as organic silanes, fluorinated silanes, alkyl amines and silicates.¹⁰⁴ Despite this, a material of the lowest surface energy gives a water contact angle (WCA) of 120° . To obtain a superhydrophobic surface with WCA greater than 150° , surface roughness is also required. The techniques being used to create superhydrophobic surfaces include wet chemical reactions,¹⁰⁵ self-assembly,¹⁰⁶ sol-gel methods,¹⁰⁷ layer-by-layer deposition,¹⁰⁸ polymerisation reactions,¹⁰⁹ electrochemical deposition,¹¹⁰ chemical vapour deposition,¹¹¹ electro-spinning,¹¹² plasma-etching¹¹³ and laser treatment.¹¹⁴

The concept of superhydrophobic textiles was introduced in 1945, when alkyl silanes were used as low surface energy materials to hydrophobise fabrics.¹¹⁵ The silane reacts with moisture in the fibrous material, allowing hydrolysis and condensation to form a hydrophobic layer. This method has also been applied to polyester fabric to impart superhydrophobic properties.¹¹⁶ Moreover, fluorinated organic compounds have been used to induce superhydrophobic character as a result of their extremely low surface energies. Plasma coating of a perfluorocarbon has also been applied to cotton to impart hydrophobic properties to the fabric.¹¹⁷ Thin films of teflon were deposited onto cellulose fabrics by pulsed laser deposition that conveyed additional roughness to cellulose fabrics at nano-meter scale.¹¹⁴

Though useful in demonstrating hydrophobicity, fluorinated compounds have toxic effects on the environment and health when in contact with skin for prolonged times.¹¹⁸ Hence, research efforts have been aimed at fabricating superhydrophobic textiles based on non-fluorinated organic compounds. To this end, a transparent superhydrophobic silica coating film on cotton has been prepared at low temperature.¹¹⁸ The coating was produced by co-hydrolysis and polycondensation of a hexadecyltrimethoxysilane, tetraethoxyorthosilicate and 3-glycidyl oxypropyltrimethoxysilane mixtures. The presence of glycidyl groups allowed the formation of a strong bond between the coating and the surface of the cotton fibres. This gave the surface an increased durability.

To increase the surface roughness extra-substrate nanostructures have also been applied such as nanoparticles,¹¹⁹ nanorods,¹²⁰ and nanowires.¹²¹ A simple and robust method for preparing superhydrophobic films with a dual-size hierarchical structure from raspberry shaped particles has been reported and summarised in Figure 1.19.^{119b} Amine-functionalised silica particles were deposited on epoxy films, followed by hydrophobisation with mono-epoxy-functionalised polydimethylsiloxane. The advancing WCA on these superhydrophobic hybrid films was about 165° and the roll-off angle of a 10 μ L droplet was 3°.

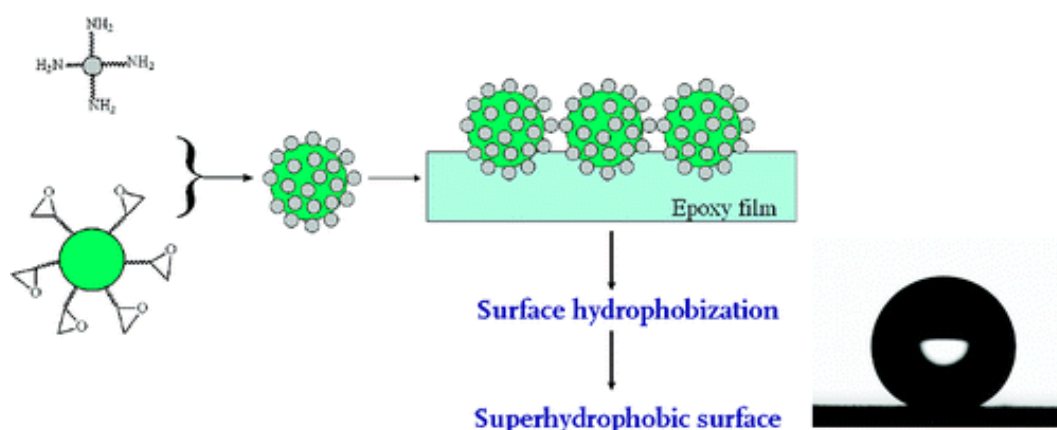


Figure 1.19: Superhydrophobic films based on raspberry-like particles.^{119b}

Durable superhydrophobic textiles with a WCA of 170° have also been fabricated.¹²² Amino-functionalised silica nanoparticles were attached to cotton fibres modified with epoxy groups, followed by hydrophobisation with 1H,1H,2H,2H-perfluorodecyltrichlorosilane (PFTDS) and stearic acid (Figure 1.20).

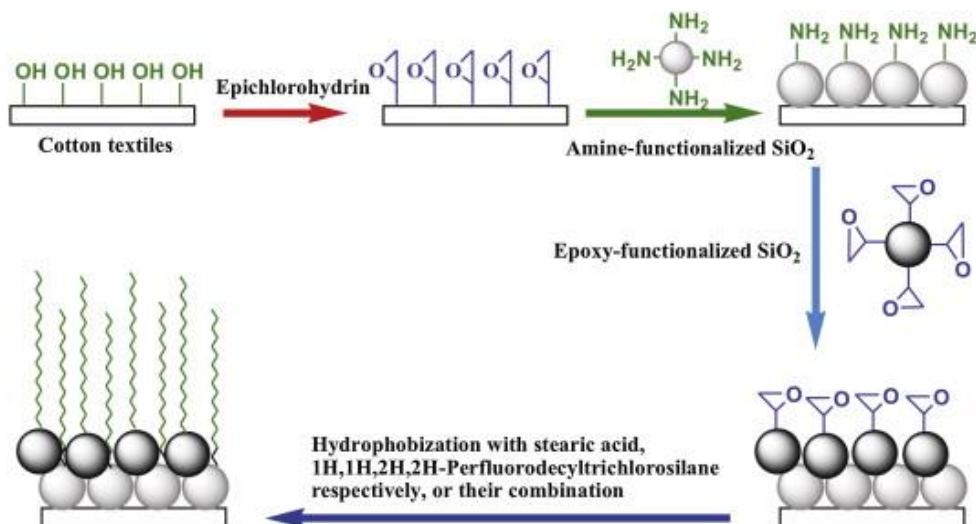


Figure 1.20: Schematic presentation of the preparation of superhydrophobic surfaces on cotton substrate.¹²²

In this process, strong covalent bonds were formed between amino groups of the SiO₂ particles and the epoxy groups on cotton substrate. More layers of silica were deposited on the cotton by the same mechanism. Liu *et al.* reported the fabrication of “artificial lotus leaf structures” on cotton textiles using carbon nanotubes (CNT).¹⁰³ Polybutylacrylate (PBA) grafted carbon-nanotubes were used as building blocks to biomimic the surface microstructures of lotus leaves at the nanoscale level. Cotton fibres covered with poly(butylacrylate)-modified CNTs showed a high level of roughness inducing superhydrophobic character to fibres (Figure 1.21).

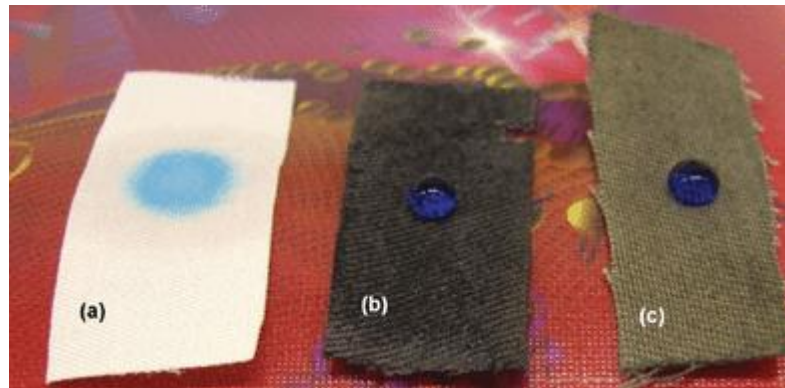


Figure 1.21: Water repellent test on (a) pristine cotton fabric, (b) carbon nanotube-coated cotton fabric and (c) PBA-g-CNT coated cotton fabric.¹⁰³

In addition to using silica, other nanocrystalline oxides have also been used to create rough surface textiles such as TiO_2 ,¹²³ ZnO ,^{123b} and CeO_2 .¹²⁴ By adopting a simple sol-gel method, bi-functional cotton textiles exhibiting superhydrophobicity and UV-shielding properties have been fabricated using CeO_2 sol coating, followed by modification with dodecafluoroheptyl-propyl-trimethoxysilane (DFTMS) (Figure 1.22).¹²⁴

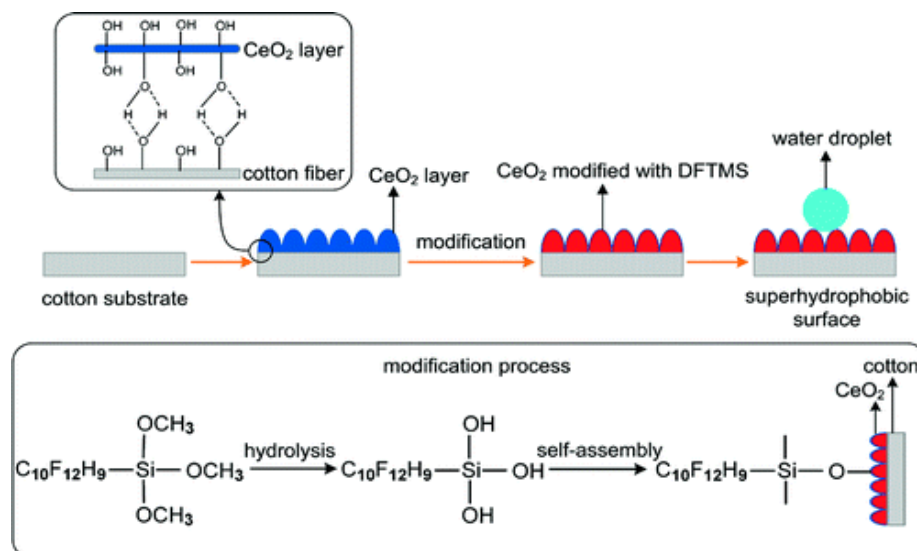


Figure 1.22: Fabrication of superhydrophobic surface on cotton substrate.¹²⁴

1.13 Textiles with dual self-cleaning applications; superhydrophobic and photocatalytic properties

There are limited examples of self-cleaning materials in the literature that work on both principles; superhydrophobic and photocatalytic self-cleaning mechanisms.¹²⁵ An Indium hydroxide [In(OH)₃] nanocube film using a simple amino acid-assisted hydrothermal process has been fabricated that showed a WCA of 150°.^{125e} At the same time, these films displayed photocatalytic properties showing 93 % degradation of rhodamine b under UV irradiation for 16 hours.

Superhydrophobic photocatalytic surfaces have been developed by incorporating titania nanoparticles into a polydimethylsiloxane (PDMS) polymer matrix by aerosol assisted chemical vapour deposition method (AACVD) (Figure 1.24).^{125f} The films exhibiting a WCA of 162°, showed complete degradation of resazurin dye under UV light (Figure 1.23).

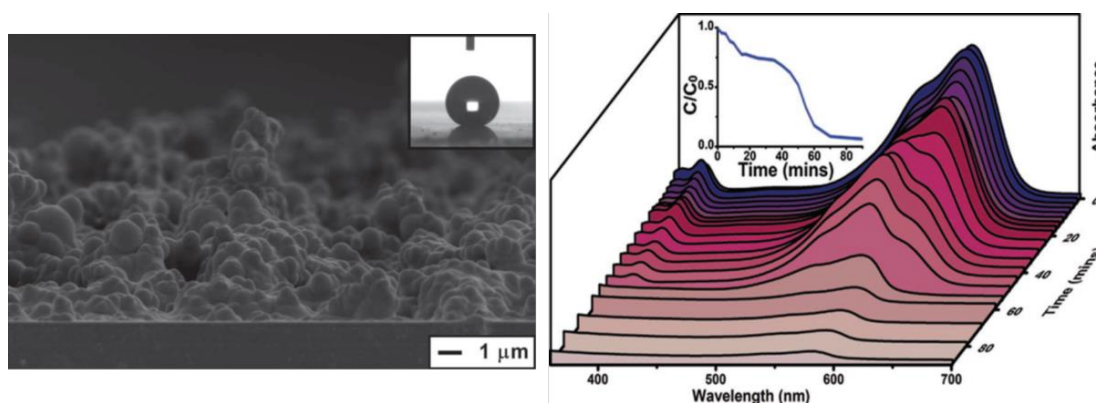


Figure 1.23: (Left) SEM image of a polymer film with embedded anatase TiO₂ nanoparticles, (Right) UV-Vis spectra of superhydrophobic polymer films exposed to a resazurin dye under UV-irradiation.^{125f}

The development of dual function self-cleaning textiles can have many advantages. Extreme water repellence can keep away water soluble impurities on one hand, while the accumulation of organic impurities can be prevented by photocatalysis on the other hand. So far, only one paper in the literature has reported on bi-functional self-cleaning textiles. Zhang *et al.* have functionalised cotton fabrics with titania nanoparticles and dodecafluoroheptyl-propyl-trimethoxy silane (DFTMS).^{125g} The

cotton fabrics showed excellent water repellent properties with a WCA of 162° and photocatalytic degradation of rhodamine b, as well under UV light (Figure 1.24).

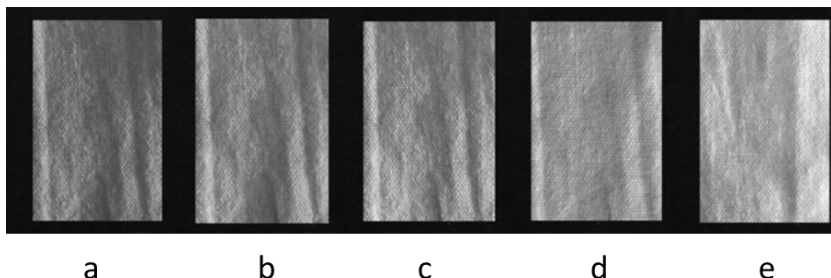


Figure 1.24: Discolouration of rhodamine b on the treated fabrics exposed to UV radiation for different periods of time: (a) 0; (b) 5; (c) 10; (d)15 min, in reference to blank cotton fabric (e).^{125g}

1.14 Research objectives

The main aim of this research is to develop “visible-light activated superhydrophobic self-cleaning textiles”, exhibiting efficient self-cleaning properties based on visible-light TiO_2 photocatalysis and the lotus-effect cleaning phenomena. The specific objectives of this research project are given below:

Objective I

To study the visible-light activation of titanium dioxide by a dye-sensitisation approach using porphyrins and its application to fabrics in order to develop self-cleaning fabrics, capable of self-cleaning in daylight and indoor light environments. The dye explored for visible-light activation of TiO_2 will be *meso*-tetra(4-carboxyphenyl)porphyrin (TCPP) (Figure 1.25). The synthesis and application of metal complexes of *meso*-tetra(4-carboxyphenyl)porphyrin to TiO_2 -coated cotton will also be explored focusing on Fe, Co, Zn and Cu.

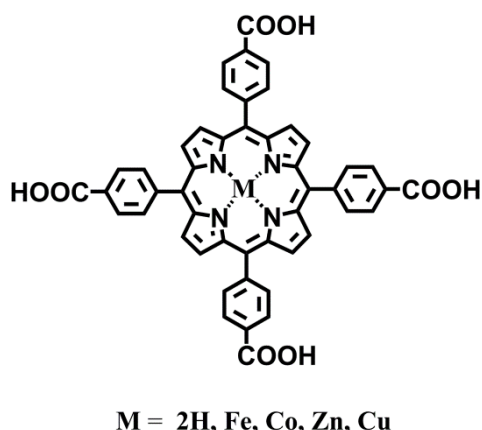


Figure 1.25: *meso*-tetrakis(4-carboxyphenyl) porphyrin (TCPP).

Our research will explore methylene blue as the stain dye for quantitative evaluation of self-cleaning properties in the experiments (Figure 1.26). This is so as to be able to compare our results with known literature results for improvement.

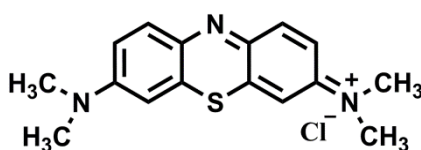


Figure 1.26: Chemical structure of methylene blue.

Objective II

To develop self-cleaning fabrics by combining two self-cleaning phenomena *i.e.* the lotus-effect utilising a superhydrophobic approach and titanium dioxide based self-cleaning process making use of the hydrophilic approach.

For hydrophobisation, we will explore the use of trimethoxy(octadecyl)silane (OTMS) (Figure 1.27) in concert to our porphyrin systems.

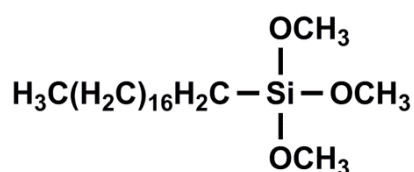


Figure 1.27: Chemical structure of trimethoxy(octadecyl) silane (OTMS).

1.15 References

1. Parkin, I. P.; Palgrave, R. G. *J. Mater. Chem.* **2005**, *15*, 1689-1695.
2. Reisch, M. S. "Essential Minerals" *Chem. Eng. News Archive* **2003**, *81* (13), p13.
3. Reisch, M. "Cleaning Glass: A Thing Of The Past?" *Chem. Eng. News Archive* **2001**, *79* (27), p 8.
4. Chen, H.; Nanayakkara, C. E.; Grassian, V. H. *Chem. Rev.* **2012**, *112*, 5919-5948.
5. Gao, X.; Yan, X.; Yao, X.; Xu, L.; Zhang, K.; Zhang, J.; Yang, B.; Jiang, L. *Adv. Mat.* **2007**, *19*, 2213-2217.
6. Genzer, J.; Efimenko, K. *Biofouling* **2006**, *22*, 339-360.
7. Tung, W. S.; Daoud, W. A. *J. Mater. Chem.* **2011**, *21*, 7858-7869.
8. Bhushan, B. *Langmuir* **2012**, *28*, 1698-1714.
9. Fujishima, A.; Honda, K. *Nature* **1972**, *238*, 37-38.
10. Fujishima, A.; Zhang, X.; Tryk, D. A. *Surf. Sci. Rep.* **2008**, *63*, 515-582.
11. Dambournet, D.; Belharouak, I.; Amine, K. *Chem. Mater.* **2009**, *22*, 1173-1179.
12. Sclafani, A.; Herrmann, J. M. *J. Phys. Chem.* **1996**, *100*, 13655-13661.
13. Li, G.; Richter, C. P.; Milot, R. L.; Cai, L.; Schmuttenmaer, C. A.; Crabtree, R. H.; Brudvig, G. W.; Batista, V. S. *Dalton Trans.* **2009**, *45*, 10078-10085. DOI: 10.1039/b908686b.
14. Hoffmann, M. R.; Martin, S. T.; Choi, W.; Bahnemann, D. W. *Chem. Rev.* **1995**, *95*, 69-96.
15. Renz, C. *Helve. Chim. Acta* **1932**, *15*, 1077-1084.
16. (a) Goodeve, C. F.; Kitchener, J. A. *Trans. Faraday Soc.* **1938**, *34*, 902-908. (b) Goodeve, C. F.; Kitchener, J. A. *Trans. Faraday Soc.* **1938**, *34*, 570-579.
17. Kato, S.; Mashio, F.; Zasshi, K. K. *J. Chem. Soc. Japan, Indust. Chem. Sect.* **1964**, *67*, 1136-1140.
18. Frank, S. N.; Bard, A. J. *J. Phys. Chem.* **1977**, *81*, 1484-1488.
19. Fox, M. A.; Dulay, M. T. *Chem. Rev.* **1993**, *93*, 341-357.
20. Mills, A.; Davies, R. H.; Worsley, D. *Chem. Soc. Rev.* **1993**, *22*, 417-425.
21. (a) Matsubara, H.; Takada, M.; Koyoma, S.; Hashimoto, K.; Fujishima, A. *Chem. Lett.* **1995**, *24*, 767-768. (b) Linsebigler, A. L.; Lu, G.; Yates, J. T. *Chem. Rev.* **1995**, *95*, 735-758.
22. Rehman, S.; Ullah, R.; Butt, A. M.; Gohar, N. D. *J. Hazard. Mater.* **2009**, *170*, 560-569.
23. Bak, T.; Nowotny, J.; Rekas, M.; Sorrell, C. C. *Int. J. Hydrogen Energ.* **2002**, *27*, 991-1022.
24. Fouad, O. A.; Ismail, A. A.; Zaki, Z. I.; Mohamed, R. M. *Appl. Catal. B: Environ.* **2006**, *62*, 144-149.

25. Fujishima, A.; Rao, T. N.; Tryk, D. A. *J. Photochem. Photobiol. C: Photochem. Rev.* **2000**, *1*, 1-21.
26. Benedix, R.; Dehn, F.; Quaas, J.; Orgass, M. *Leipzig Annual Civil Engineering Report, University of Leipzig, Lacer No. 5.* **2000**, p 157-168.
27. Roach, P.; Shirtcliffe, N. J.; Newton, M. I. *Soft Matter* **2008**, *4*, 224-240.
28. Qi, K.; Daoud, W. A.; Xin, J. H.; Mak, C. L.; Tang, W.; Cheung, W. P. *J. Mater. Chem.* **2006**, *16*, 4567-4574.
29. Daoud, W. A.; Leung, S. K.; Tung, W. S.; Xin, J. H.; Cheuk, K.; Qi, K. *Chem. Mater.* **2008**, *20*, 1242-1244.
30. Qi, K.; Xin, J. H.; Daoud, W. A.; Mak, C. L. *Int. J. Appl. Ceram. Technol.* **2007**, *4*, 554-563.
31. Dong, Y. C.; Zhang, L. W.; Liu, R. H.; Zhu, T. F. *J. Appl. Polym. Sci* **2006**, *99*, 286-291.
32. Uddin, M. J.; Cesano, F.; Bonino, F.; Bordiga, S.; Spoto, G.; Scarano, D.; Zecchina, A. *J. Photochem. Photobiol. A: Chem.* **2007**, *189*, 286-294.
33. Bozzi, A.; Yuranova, T.; Guasaquillo, I.; Laub, D.; Kiwi, J. *J. Photochem. Photobiol. A: Chem.* **2005**, *174*, 156-164.
34. Meilert, K. T.; Laub, D.; Kiwi, J. *J. Mol. Catal. A: Chem.* **2005**, *237*, 101-108.
35. Yuranova, T.; Laub, D.; Kiwi, J. *Catal. Today* **2007**, *122*, 109-117.
36. Ugur, S. S.; Sariisik, M.; Aktas, A. H. *Nanotechnology* **2010**, *21*, 325603 (8p).
37. Bozzi, A.; Yuranova, T.; Kiwi, J. *J. Photochem. Photobiol. A: Chem.* **2005**, *172*, 27-34.
38. Kiwi, J.; Pulgarin, C. *Catal. Today* **2010**, *151*, 2-7.
39. Wang, R.; Wang, X.; Xin, J. H. *ACS Appl. Mater. Interfaces* **2009**, *2*, 82-85.
40. Qi, K.; Fei, B.; Xin, J. H. *Thin Solid Films* **2011**, *519*, 2438-2444.
41. Wu, D.; Long, M. *ACS Appl. Mater. Interfaces* **2011**, *3*, 4770-4774.
42. Miyauchi, M.; Nakajima, A.; Watanabe, T.; Hashimoto, K. *Chem. Mater.* **2002**, *14*, 2812-2816.
43. <http://www.ewellnessglobal.com/apps/blog/entries/show/26752124-light-are-we-suffering-from-malillumination>.
44. Fujishima, A.; Zhang, X. *C. R. Chimie*, **2006**, *9*, 750-760.
45. Choi, W.; Termin, A.; Hoffmann, M. R. *J. Phys. Chem.* **1994**, *98*, 13669-13679.
46. Asahi, R.; Morikawa, T.; Ohwaki, T.; Aoki, K.; Taga, Y. *Science* **2001**, *293*, 269-271.
47. Bessekhoud, Y.; Robert, D.; Weber, J. V. *J. Photochem. Photobiol. A: Chem.* **2004**, *163*, 569-580.
48. (a) Nagaveni, K.; Hegde, M. S.; Madras, G. *J. Phys. Chem. B* **2004**, *108*, 20204-20212. (b) Zhu, J.; Deng, Z.; Chen, F.; Zhang, J.; Chen, H.; Anpo, M.; Huang, J.; Zhang, L. *Appl. Catal. B: Environ.* **2006**, *62*, 329-335. (c) Di Paola, A.; Marci, G.;

- Palmisano, L.; Schiavello, M.; Uosaki, K.; Ikeda, S.; Ohtani, B. *J. Phys. Chem. B* **2001**, *106*, 637-645.
49. (a) Vijayan, P.; Mahendiran, C.; Suresh, C.; Shanthi, K. *Catal. Today* **2009**, *141*, 220-224. (b) Khan, R.; Kim, S. W.; Kim, T.-J.; Nam, C.-M. *Mater. Chem. Phys.* **2008**, *112*, 167-172. (c) Adán, C.; Bahamonde, A.; Fernández-García, M.; Martínez-Arias, A. *Appl. Catal. B: Environ.* **2007**, *72*, 11-17. (d) Hung, W.-C.; Fu, S.-H.; Tseng, J.-J.; Chu, H.; Ko, T.-H. *Chemosphere* **2007**, *66*, 2142-2151.
50. (a) Bouras, P.; Stathatos, E.; Lianos, P. *Appl. Catal. B: Environ.* **2007**, *73*, 51-59. (b) Ambrus, Z.; Balázs, N.; Alapi, T.; Wittmann, G.; Sipos, P.; Dombi, A.; Mogyorósi, K. *Appl. Catal. B: Environ.* **2008**, *81*, 27-37. (c) Yamashita, H.; Harada, M.; Misaka, J.; Takeuchi, M.; Neppolian, B.; Anpo, M. *Catal. Today* **2003**, *84*, 191-196. (d) Yen, C.-C.; Wang, D.-Y.; Shih, M.-H.; Chang, L.-S.; Shih, H. C. *Appl. Surf. Sci.* **2010**, *256*, 6865-6870.
51. Li, H.; Zhao, G.; Han, G.; Song, B. *Surf. Coat. Technol.* **2007**, *201*, 7615-7618.
52. Kim, S.; Hwang, S.-J.; Choi, W. *J. Phys. Chem. B* **2005**, *109*, 24260-24267.
53. Seery, M. K.; George, R.; Floris, P.; Pillai, S. C. *J. Photochem. Photobiol. A: Chem.* **2007**, *189*, 258-263.
54. (a) Sakthivel, S.; Kisch, H. *Angew. Chem. Int. Ed.* **2003**, *42*, 4908-4911. (b) Ohno, T.; Akiyoshi, M.; Umebayashi, T.; Asai, K.; Mitsui, T.; Matsumura, M. *Appl. Catal. A: General* **2004**, *265*, 115-121. (c) Zhao, W.; Ma, W.; Chen, C.; Zhao, J.; Shuai, Z. *J. Am. Chem. Soc.* **2004**, *126*, 4782-4783. (d) Yu, J. C.; Yu, J.; Ho, W.; Jiang, Z.; Zhang, L. *Chem. Mater.* **2002**, *14*, 3808-3816.
55. Kitano, M.; Funatsu, K.; Matsuoka, M.; Ueshima, M.; Anpo, M. *J. Phys. Chem. B* **2006**, *110*, 25266-25272.
56. Irie, H.; Washizuka, S.; Yoshino, N.; Hashimoto, K. *Chem. Comm.* **2003**, *9*, 1298-1299.
57. Nakamura, R.; Tanaka, T.; Nakato, Y. *J. Phys. Chem. B* **2004**, *108*, 10617-10620.
58. Qiao, M.; Chen, Q.; Wu, S.; Shen, J. *J. Sol-Gel Sci. Technol.* **2010**, *55*, 377-384.
59. (a) Wu, D.; Long, M.; Cai, W.; Chen, C.; Wu, Y. *J. Alloys Compd.* **2010**, *502*, 289-294. (b) Sakthivel, S.; Janczarek, M.; Kisch, H. *J. Phys. Chem. B* **2004**, *108*, 19384-19387.
60. Liu, G.; Wang, L.; Yang, H. G.; Cheng, H.-M.; Lu, G. Q. *J. Mat. Chem.* **2010**, *20*, 831-843.
61. Irie, H.; Watanabe, Y.; Hashimoto, K. *J. Phys. Chem. B* **2003**, *107*, 5483-5486.
62. Ihara, T.; Miyoshi, M.; Iriyama, Y.; Matsumoto, O.; Sugihara, S. *Appl. Catal. B: Environ.* **2003**, *42*, 403-409.
63. Sakai, Y. W.; Obata, K.; Hashimoto, K.; Irie, H. *Vacuum* **2008**, *83*, 683-687.
64. Zhang, S.; Song, L. *Catal. Comm.* **2009**, *10*, 1725-1729.
65. In, S.; Orlov, A.; Berg, R.; García, F.; Pedrosa-Jimenez, S.; Tikhov, M. S.; Wright, D. S.; Lambert, R. M. *J. Am. Chem. Soc.* **2007**, *129*, 13790-13791.

66. Wu, Y.; Xing, M.; Tian, B.; Zhang, J.; Chen, F. *Chem. Eng. J.* **2010**, *162*, 710-717.
67. Wu, L.; Yu, J. C.; Fu, X. *J. Mol. Catal. A: Chem.* **2006**, *244*, 25-32.
68. Ho, W.; Yu, J. C. *J. Mol. Catal. A: Chem.* **2006**, *247*, 268-274.
69. Liu, J.; Yang, R.; Li, S. *Rare Metals* **2006**, *25*, 636-642.
70. Kanjwal, M.; Barakat, N.; Sheikh, F.; Kim, H. *J. Mater. Sci.* **2010**, *45*, 1272-1279.
71. Wang, Q.; Campbell, W. M.; Bonfantani, E. E.; Jolley, K. W.; Officer, D. L.; Walsh, P. J.; Gordon, K.; Humphry-Baker, R.; Nazeeruddin, M. K.; Grätzel, M. *J. Phys. Chem. B* **2005**, *109*, 15397-15409.
72. Kim, W.; Tachikawa, T.; Majima, T.; Choi, W. *J. Phys. Chem. C* **2009**, *113*, 10603-10609.
73. (a) Mishra, A.; Fischer, M. K. R.; Bäuerle, P. *Angew. Chem. Int. Ed.* **2009**, *48*, 2474-2499. (b) Li, L.-L.; Diau, E. W.-G. *Chem. Soc. Rev.* **2013**, *42*, 291-304.
74. Grätzel, M. *J. Photochem. Photobiol. A: Chem.* **2004**, *164*, 3-14.
75. Campbell, W. M.; Jolley, K. W.; Wagner, P.; Wagner, K.; Walsh, P. J.; Gordon, K. C.; Schmidt-Mende, L.; Nazeeruddin, M. K.; Wang, Q.; Grätzel, M.; Officer, D. L. *J. Phys. Chem. C* **2007**, *111*, 11760-11762.
76. Liu, M. O.; Tai, C.-h.; Sain, M.-z.; Hu, A. T.; Chou, F.-i. *J. Photochem. Photobiol. A: Chem.* **2004**, *165*, 131-136.
77. Kamat, P. V.; Fox, M. A. *Chem. Phys. Lett.* **1983**, *102*, 379-384.
78. Ross, H.; Bendig, J.; Hecht, S. *Sol. Energ. Mat. Sol. Cells* **1994**, *33*, 475-481.
79. Abe, R.; Hara, K.; Sayama, K.; Domen, K.; Arakawa, H. *J. Photochem. Photobiol. A: Chem.* **2000**, *137*, 63-69.
80. Moon, J.; Yun, C. Y.; Chung, K.-W.; Kang, M.-S.; Yi, J. *Catal. Today* **2003**, *87*, 77-86.
81. Tachibana, Y.; Haque, S. A.; Mercer, I. P.; Durrant, J. R.; Klug, D. R. *J. Phys. Chem. B* **2000**, *104*, 1198-1205.
82. Mele, G.; Del Sole, R.; Vasapollo, G.; Garcia-Lopez, E.; Palmisano, L.; Jun, L.; Slota, R.; Dyrda, G. *Res. Chem. Intermed.* **2007**, *33*, 433-448.
83. Anderson, J. M. *Aust. J. Plant Physiol.* **1999**, *26*.
84. Balaban, T. S. *Acc. Chem. Res.* **2005**, *38*, 612-623.
85. Anderson, H. L. *Inorg. Chem.* **1994**, *33*, 972-981.
86. (a) Lammi, R. K.; Wagner, R. W.; Ambroise, A.; Diers, J. R.; Bocian, D. F.; Holten, D.; Lindsey, J. S. *J. Phys. Chem. B* **2001**, *105*, 5341-5352. (b) Liu, Z. M.; Yasserli, A. A.; Lindsey, J. S.; Bocian, D. F. *Science* **2003**, *302*, 1543-1545.
87. (a) Anderson, S.; Anderson, H. L.; Sanders, J. K. M. *Acc. Chem. Res.* **1993**, *26*, 469-475. (b) Mele, G.; Del Sole, R.; Vasapollo, G.; García-López, E.; Palmisano, L.; Schiavello, M. *J. Catal.* **2003**, *217*, 334-342.
88. Shiragami, T.; Matsumoto, J.; Inoue, H.; Yasuda, M. *J. Photochem. Photobiol. C: Photochem. Rev.* **2005**, *6*, 227-248.

89. Li, D.; Dong, W.; Sun, S.; Shi, Z.; Feng, S. *J. Phys. Chem. C* **2008**, *112*, 14878-14882.
90. Huang, H.; Gu, X.; Zhou, J.; Ji, K.; Liu, H.; Feng, Y. *Catal. Comm.* **2009**, *11*, 58-61.
91. Granados-Oliveros, G.; Páez-Mozo, E. A.; Ortega, F. M.; Ferronato, C.; Chovelon, J.-M. *Appl. Catal. B: Environ.* **2009**, *89*, 448-454.
92. Duan, M.-y.; Li, J.; Mele, G.; Wang, C.; Lü, X.-f.; Vasapollo, G.; Zhang, F.-x. *J. Phys. Chem. C* **2010**, *114*, 7857-7862.
93. Chang, M. Y.; Chang, C. Y.; Hsieh, Y. H.; Yao, K. S.; Cheng, T. C.; Ho, C. T. *Multi-Functional Materials and Structures, Pts 1 and 2*, **2008**, 47-50, 471-474.
94. Chang, M.-Y.; Hsieh, Y.-H.; Cheng, T.-C.; Yao, K.-S.; Wei, M.-C.; Chang, C.-Y. *Thin Solid Films* **2009**, *517*, 3888-3891.
95. Kim, W.; Park, J.; Jo, H. J.; Kim, H.-J.; Choi, W. *J. Phys. Chem. C* **2007**, *112*, 491-499.
96. Ismail, A. A.; Bahnemann, D. W. *ChemSusChem* **2010**, *3*, 1057-1062.
97. Wan, J.; Wu, Z.; Wang, H.; Zheng, X. *In Eco-Dyeing, Finishing and Green Chemistry*, **2012**, *441*, p 544-548.
98. Lin, C. H.; Chang, C. Y.; Chang, Y. J.; Lee, Y. C.; Hwa, M. Y.; Chang, Y. S. *Trans Tech Publications, Switzerland* **2010**, *123-125*, 923-926.
99. (a) Ma, T.; Inoue, K.; Noma, H.; Yao, K.; Abe, E. *J. Photochem. Photobiol. A: Chem.* **2002**, *152*, 207-212. (b) Kathiravan, A.; Renganathan, R. *J. Colloid Interface Sci.* **2009**, *331*, 401-407.
100. Wang, C.; Yang, G.-m.; Li, J.; Mele, G.; Słota, R.; Broda, M. A.; Duan, M.-y.; Vasapollo, G.; Zhang, X.; Zhang, F.-X. *Dyes Pigm.* **2009**, *80*, 321-328.
101. (a) Barthlott, W.; Neinhuis, C. *Planta* **1997**, *202*, 1-8. (b) Neinhuis, C.; Barthlott, W. *Ann. Bot.* **1997**, *79*, 667-677.
102. <http://www.adamrachwal.com/self-coating-super-hydrophobic-nano-surface/>
103. Liu, Y.; Tang, J.; Wang, R.; Lu, H.; Li, L.; Kong, Y.; Qi, K.; Xin, J. H. *J. Mater. Chem.* **2007**, *17*, 1071-1078.
104. Ma, M.; Hill, R. M. *Curr. Opin. Colloid Interface Sci.* **2006**, *11*, 193-202.
105. (a) Wang, S.; Feng, L.; Jiang, L. *Adv. Mater.* **2006**, *18*, 767-770. (b) Zimmermann, J.; Reifler, F. A.; Fortunato, G.; Gerhardt, L.-C.; Seeger, S. *Adv. Funct. Mater.* **2008**, *18*, 3662-3669.
106. Yin, S.; Wu, D.; Yang, J.; Lei, S.; Kuang, T.; Zhu, B. *Appl. Surf. Sci.* **2011**, *257*, 8481-8485.
107. (a) Tadanaga, K.; Kitamuro, K.; Matsuda, A.; Minami, T. *J. Sol-Gel Sci. Technol.* **2003**, *26*, 705-708. (b) Nakajima, A.; Fujishima, A.; Hashimoto, K.; Watanabe, T. *Adv. Mater.* **1999**, *11*, 1365-1368. (c) Lakshmi, R. V.; Bharathidasan, T.; Basu, B. J. *Appl. Surf. Sci.* **2011**, *257*, 10421-10426.
108. (a) Zhang, L.; Chen, H.; Sun, J.; Shen, J. *Chem. Mater.* **2007**, *19*, 948-953. (b) Zhao, Y.; Xu, Z.; Wang, X.; Lin, T. *Langmuir* **2012**, *28*, 6328-6335.

109. Ramirez, S. M.; Diaz, Y. J.; Sahagun, C. M.; Duff, M. W.; Lawal, O. B.; Iacono, S. T.; Mabry, J. M. *Polym. Chem.* **2013**, *4*, 2230-2234.
110. (a) Zhang, X.; Shi, F.; Yu, X.; Liu, H.; Fu, Y.; Wang, Z.; Jiang, L.; Li, X. *J. Am. Chem. Soc.* **2004**, *126*, 3064-3065. (b) Jafari, R.; Menini, R.; Farzaneh, M. *Appl. Surf. Sci.* **2010**, *257*, 1540-1543.
111. (a) Huang, L.; Lau, S. P.; Yang, H. Y.; Leong, E. S. P.; Yu, S. F.; Prawer, S. *J. Phys. Chem. B* **2005**, *109*, 7746-7748. (b) Ishizaki, T.; Hieda, J.; Saito, N.; Takai, O. *Electrochim. Acta* **2010**, *55*, 7094-7101.
112. (a) Acatay, K.; Simsek, E.; Ow-Yang, C.; Menciloglu, Y. Z. *Angew. Chem., Int. Ed.* **2004**, *43*, 5210-5213. (b) Ma, M.; Hill, R. M.; Lowery, J. L.; Fridrikh, S. V.; Rutledge, G. C. *Langmuir* **2005**, *21*, 5549-5554.
113. Takke, V.; Behary, N.; Perwuelz, A.; Campagne, C. *J. Appl. Polym. Sci.* **2011**, *122*, 2621-2629.
114. Daoud, W. A.; Xin, J. H.; Zhang, Y. H.; Mak, C. L. *Thin Solid Films* **2006**, *515*, 835-837.
115. Parker, D. *US pat.* **1945**, 2 386 259.
116. Gao, L.; McCarthy, T. J. *Langmuir* **2006**, *22*, 5998-6000.
117. Zhang, J.; France, P.; Radomyselskiy, A.; Datta, S.; Zhao, J.; van Ooij, W. *J. Appl. Polym. Sci.* **2003**, *88*, 1473-1481.
118. Daoud, W. A.; Xin, J. H.; Tao, X. M. *J. Am. Ceram. Soc.* **2004**, *87*, 1782-1784.
119. (a) Ebert, D.; Bhushan, B. *Langmuir* **2012**, *28*, 11391-11399. (b) Ming, W.; Wu, D.; van Benthem, R.; de With, G. *Nano Lett.* **2005**, *5*, 2298-2301. (c) Ling, X. Y.; Phang, I. Y.; Vancso, G. J.; Huskens, J.; Reinhoudt, D. N. *Langmuir* **2009**, *25*, 3260-3263. (d) Deng, X.; Mammen, L.; Zhao, Y.; Lellig, P.; Müllen, K.; Li, C.; Butt, H.-J.; Vollmer, D. *Adv. Mater.* **2011**, *23*, 2962-2965. (e) Amigoni, S.; Taffin de Givenchy, E.; Dufay, M.; Guittard, F. *Langmuir* **2009**, *25*, 11073-11077. (f) Xu, Q. F.; Wang, J. N.; Sanderson, K. D. *ACS Nano* **2010**, *4*, 2201-2209.
120. (a) Guo, P.; Zheng, Y.; Wen, M.; Song, C.; Lin, Y.; Jiang, L. *Adv. Mater.* **2012**, *24*, 2642-2648. (b) Feng, X.; Feng, L.; Jin, M.; Zhai, J.; Jiang, L.; Zhu, D. *J. Am. Chem. Soc.* **2003**, *126*, 62-63. (c) Feng, X.; Zhai, J.; Jiang, L. *Angew. Chem. Int. Ed.* **2005**, *44*, 5115-5118.
121. (a) Verplanck, N.; Galopin, E.; Camart, J.-C.; Thomy, V.; Coffinier, Y.; Boukherroub, R. *Nano Lett.* **2007**, *7*, 813-817. (b) Coffinier, Y.; Janel, S.; Addad, A.; Blossey, R.; Gengembre, L.; Payen, E.; Boukherroub, R. *Langmuir* **2007**, *23*, 1608-1611.
122. Xue, C.-H.; Jia, S.-T.; Zhang, J.; Tian, L.-Q. *Thin Solid Films* **2009**, *517*, 4593-4598.
123. (a) Xue, C.-H.; Jia, S.-T.; Chen, H.-Z.; Wang, M. *Sci. Technol. Adv. Mater.* **2008**, *9* (035001), pp 5. (b) Shi, Y.; Wang, Y.; Feng, X.; Yue, G.; Yang, W. *Appl. Surf. Sci.* **2012**, *258*, 8134-8138.
124. Duan, W.; Xie, A.; Shen, Y.; Wang, X.; Wang, F.; Zhang, Y.; Li, J. *Ind. Eng. Chem. Res.* **2011**, *50*, 4441-4445.

125. (a) Macias-Montero, M.; Borrás, A.; Saghi, Z.; Romero-Gomez, P.; Sanchez-Valencia, J. R.; Gonzalez, J. C.; Barranco, A.; Midgley, P.; Cotrino, J.; Gonzalez-Elipé, A. R. *J. Mater. Chem.* **2012**, *22*, 1341-1346. (b) Watanabe, T.; Yoshida, N. *Chem. Rec.* **2008**, *8*, 279-290. (c) Yoshida, N.; Takeuchi, M.; Okura, T.; Monma, H.; Wakamura, M.; Ohsaki, H.; Watanabe, T. *Thin Solid Films* **2006**, *502*, 108-111. (d) Nakajima, A.; Hashimoto, K.; Watanabe, T.; Takai, K.; Yamauchi, G.; Fujishima, A. *Langmuir* **2000**, *16*, 7044-7047. (e) Cao, H.; Zheng, H.; Liu, K.; Fu, R. *Cryst. Growth Des.* **2009**, *10*, 597-601. (f) Crick, C. R.; Bear, J. C.; Kafizas, A.; Parkin, I. P. *Adv. Mater.* **2012**, *24*, 3505-3508. (g) Zhang, Y.; Li, S.; Huang, F.; Wang, F.; Duan, W.; Li, J.; Shen, Y.; Xie, A. *Russ. J. Phys. Chem. A* **2012**, *86*, 413-417.



Declaration for Thesis Chapter 2

Declaration by candidate

In the case of Chapter 2, the nature and extent of my contribution to the work was the following:

Nature of contribution	Extent of contribution
Initiation, interpretation, experiments, data analysis and writing up	65 %

The following co-authors contributed to the work. If co-authors are students at Monash University, the extent of their contribution in percentage terms must be stated:

Name	Nature of contribution	Extent of contribution (%) for student co-authors only
Walid A. Daoud	Supervision, interpretation, suggestion, discussion and revision	N/A
Steven J. Langford	Supervision, interpretation, suggestion, discussion and revision	N/A

The undersigned hereby certify that the above declaration correctly reflects the nature and extent of the candidate's and co-authors' contributions to this work.

Candidate's
Signature

	Date 4/10/2013
--	-------------------

Main
Supervisor's
Signature

	Date 4/10/2013
--	-------------------

Chapter 2:

Self-cleaning cotton by porphyrin-sensitised visible-light photocatalysis

Self-cleaning cotton by porphyrin-sensitized visible-light photocatalysis†

Shabana Afzal,^a Walid A. Daoud^{*a} and Steven J. Langford^b

Received 11th October 2011, Accepted 10th January 2012

DOI: 10.1039/c2jm15146d

Self-assembled monolayers of *meso*-tetra(4-carboxyphenyl) porphyrin (TCPP) were formed on anatase coated-cotton fabric to confer visible-light sensitized self-cleaning properties. A complete degradation of methylene blue in 110 min and removal of coffee and red wine stains in 16 h indicate that TiO₂/TCPP-coated cotton fabrics exhibit superior visible-light self-cleaning performance as compared to bare TiO₂-coated cotton. The fabrics were characterized by UV-Vis, FESEM, XRD and fluorescence spectroscopy. Visible-light induced self-cleaning cotton offers a great potential for indoor self-cleaning applications.

1. Introduction

Nano-crystalline anatase titanium dioxide (TiO₂) has received considerable attention as a photo- and redox-active material in many applications, such as dye-sensitized solar cells, air purification, sterilization, organic pollutants degradation and self-cleaning glass.¹ Due to its non-toxicity, low cost, chemical stability and high oxidizing ability, anatase TiO₂ has been regarded as the most promising environment-friendly photocatalyst.² In fact, the application of TiO₂ in self-cleaning textiles has received increasing attention in recent years.^{2a} In this regard, extensive research has been carried out to grow TiO₂ nanocrystals on natural and synthetic fibres,³ leading to the successful development of a number of UV-active self-cleaning textiles. These textiles include cotton, surface-modified cotton, surface-modified polyester and wool.⁴ However, pure TiO₂ can only absorb UV light of wavelength equal or below 385 nm due to its wide band gap (3.2 eV).⁵ In order to extend the light absorption of TiO₂ toward the visible region, various strategies have been implemented including doping TiO₂ with metals, such as Ag, Au, Fe and Gd,⁶ and non-metals, such as C, N and S.⁷

Dye-sensitization has been considered as an alternative approach to induce visible-light photocatalysis.⁸ Application of various dyes, such as Erythrosine-B, Rose Bengal, Eosin Y and Acid Red 44, has been found efficient but endurable due to the instability of the dye.⁹ Enhanced light absorption through porphyrin-based chlorophyll chromophores to collect solar energy is accomplished naturally by plants. Inspired by their primary role in photosynthesis, application of porphyrins in visible-light sensitization of TiO₂ is particularly interesting

because of their high light absorption coefficient and high photostability as compared to other dyes.¹⁰ Porphyrins have strong absorption in the 400–450 nm region (Soret band) and weak absorption in the 500–700 nm region (Q bands).¹¹ Many research efforts have recently been devoted to investigate the effect of porphyrins and metal porphyrins on visible-light sensitization of TiO₂ powder. These efforts include photodegradation of acid chrome blue K, rhodamine B, atrazine, 4-nitrophenol, methylene blue, 2,4-dichlorophenol and acetaldehyde.¹²

To the best of our knowledge, no literature has been reported on visible-light-active self-cleaning fabrics based on dye-sensitization. Here, we present the first application of *meso*-tetra(4-carboxyphenyl)porphyrin (TCPP)-sensitized TiO₂ in self-cleaning cotton showing significant photocatalytic activity under visible-light as compared to bare TiO₂. Transparent thin layers of nanocrystalline anatase TiO₂ were formed on cotton fabric by a dip-pad-dry-cure process,^{4b} whereas self-assembled monolayers of TCPP dye were formed on TiO₂-coated cotton by a post-adsorption method,^{12c} as shown in Scheme 1. Based on the target application, porphyrins were particularly selected in our study, as they are less hazardous in the case of skin contact as compared to the conventional highly efficient photosensitizing dyes such as ruthenium complexes.

2. Experimental

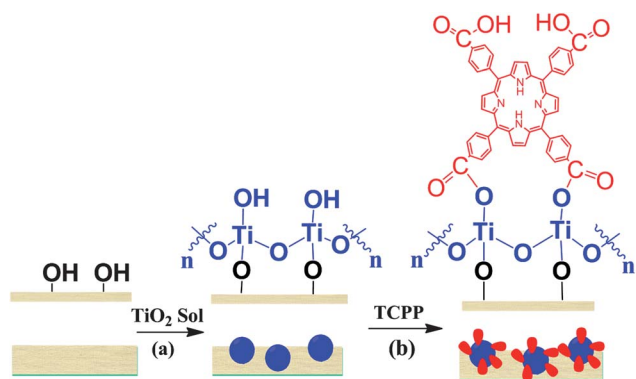
2.1. Preparation of TiO₂/TCPP-coated cotton

For the preparation of anatase TiO₂ colloid, a solution of titanium tetraisopropoxide and acetic acid was added dropwise to acidified water (HNO₃ = 1.4%). The mixture was vigorously stirred at 60 °C for 16 h. The as-prepared sol was used to prepare TiO₂ thin coatings on scoured cotton fabric by a dip-pad-dry-cure method. Cotton was scoured by a non-ionic detergent (Kieralon® F-OLB Conc.) in order to remove impurities such as wax and grease. The scouring of cotton fabric was carried at 80 °C for 30 min. The scoured fabric pieces were dipped in the

^aSchool of Applied Sciences and Engineering, Monash University, Churchill, Victoria, 3842, Australia. E-mail: [redacted]

^bSchool of Chemistry, Monash University, Clayton, Victoria, 3800, Australia

† Electronic Supplementary Information (ESI) available: UV-Vis spectroscopy results for TCPP and for evaluation of coating stability. See DOI: 10.1039/c2jm15146d



Pristine cotton **TiO₂-coated cotton** **TiO₂/TCPP-coated cotton**

Scheme 1 Formation of self-assembled monolayer of TCPP molecules on TiO₂-coated cotton. (a) Treatment of pristine cotton with TiO₂ colloid (dip-pad-dry-cure method) to form TiO₂ coatings on cotton. (b) Treatment of TiO₂-coated cotton with TCPP solution in DMF to form TCPP/TiO₂-coated cotton.

TiO₂ sol for 1 min and then pressed in automatic horizontal press at a nip pressure of 2.75 kg cm⁻² with a roller rotation speed of 7.5 rpm. After 5 min, pressed samples were exposed to ammonia fumes until surface pH 7 was reached. The samples were dried at 80 °C in an oven and then cured at 120 °C for 3 min. For deposition of TCPP, TiO₂-coated fabrics were dipped in TCPP solution of different concentrations (200, 100, 20, 5 and 1 μM) in dimethylformamide (DMF) and heated at 100 °C for 5 h approximately. Samples were then washed with DMF and water in order to remove excess TCPP.

2.2. Characterization

Morphological studies of the samples were conducted using field emission electron microscopy (JEOL 7001F FEGSEM). The crystallinity of TiO₂ coatings formed on the cotton samples was evaluated by low angle X-ray diffraction (XRD, Philip 1140 diffractometer). The UV-Vis absorption spectrum of TCPP in DMF was recorded on Lambda 950 Perkin Elmer spectrophotometer. The UV-Vis absorption spectra of pristine and TiO₂/TCPP-coated cotton samples were recorded on Lambda 950 Perkin Elmer spectrophotometer with 150 mm integrating sphere setup. All the samples were masked allowing only 2 × 2 mm area exposed to illumination by the light source. The steady-state fluorescence quenching study was conducted using fluorescence spectrophotometer (Fluoromax 4, Horiba Scientific).

2.3. Photocatalysis studies

For experiments of photocatalytic degradation of methylene blue (MB), TiO₂/TCPP-coated cotton pieces (1 g, 1 × 1 cm) were immersed in beakers containing acidified MB (20 ml, 15.6 μM, pH = 1). The beakers were irradiated by visible-light for 110 min using fluorescent lamp, (30 W, 5.02 mW cm⁻² irradiance) containing small UV content (0.01 mW cm⁻² irradiance), while vigorously shaken. Prior to irradiation, beakers were kept in dark for at least 1 h in order to attain adsorption-desorption equilibrium. The change in concentration of MB was monitored

by recording the UV-Vis absorption spectra at different time intervals, during the course of photocatalytic reaction.

For the degradation of coffee and red wine stains experiments, cotton pieces (5 × 5 cm) coated with TiO₂, TCPP and TiO₂/TCPP were stained with coffee (20 μl, 1.8 g of coffee/150 ml of hot water) and red wine (20 μl). After air-drying, the samples were irradiated by visible-light for 16 h using fluorescent lamp (30W, 5.02 mW cm⁻² irradiance).

2.4. Stability study

The stability of TiO₂/TCPP coating on cotton was tested against detergent, water and petroleum ether, using a modified AATCC Test Method 190-2003. Samples were washed with each solvent for 45 min at room temperature at a constant stirring of 400 rpm. The samples were then rinsed with water and dried at room temperature. UV-Vis spectra of the samples were recorded before and after washing. For the evaluation of photostability of TCPP, TiO₂/TCPP-coated samples were irradiated under visible-light for 30 h. UV-Vis spectra of the samples were recorded before and after irradiation.

3. Results and discussion

3.1. SEM analysis

In order to investigate the surface morphology of coated and pristine cotton samples, a comparison between FESEM images at 5000 and 1000 magnification is illustrated in Fig. 1. Lower magnification images (Fig. 1a, c and e) reveal the integrity of the cotton fibres after coating with TiO₂ and TCPP, whereas in the

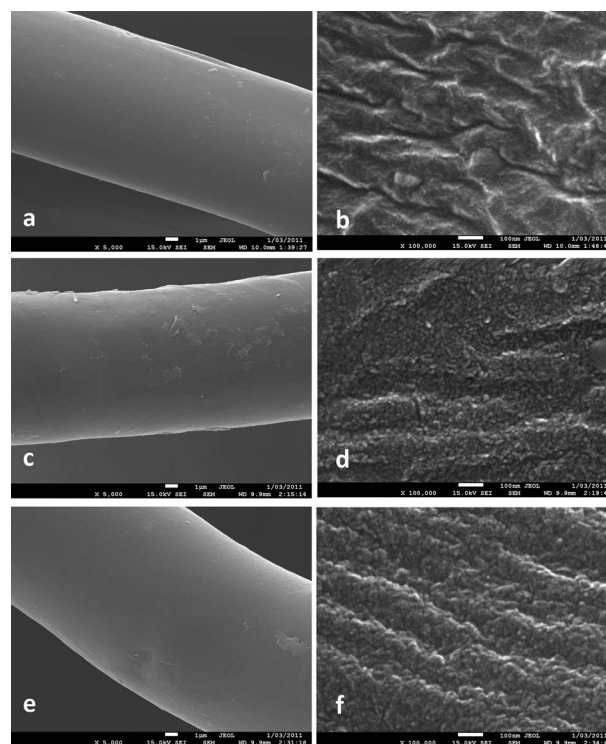


Fig. 1 FESEM images of pristine cotton (a and b), TiO₂-coated cotton (c and d), TiO₂/TCPP-coated cotton (e and f).

high magnification images, voids can be seen in pristine cotton (Fig. 1b). These voids seem to be filled completely and homogeneously with TiO₂ nanoparticles of about 10 nm in diameter (Fig. 1d). However, surface aggregates with diameter greater than 10 nm can also be observed. In the case of TiO₂/TCPP-coated samples, the TiO₂ nanoparticles are covered by a monolayer of TCPP (Fig. 1f).

3.2. UV-Vis spectroscopy

In order to study the binding of the porphyrin dye with TiO₂, UV-Vis spectra of TCPP in DMF and TCPP adsorbed on cotton were recorded in the absence and presence of TiO₂ (Fig. 2). UV-Vis spectrum of pristine cotton was also recorded for comparison. The study shows visible-light absorption between 400 to 700 nm in all samples except for pristine cotton, where no dye is present (Fig. 2). The absorption spectrum of TCPP in DMF shows a strong peak at 418 nm for Soret band (Fig. 2d), whereas in TiO₂-coated cotton the absorption is shifted by 9 nm to 427 nm (Fig. 2c). This red shift can be attributed to the strong interaction between the carboxylate groups of TCPP and the cationic TiO₂ surface. For TCPP adsorbed on TiO₂ particles, a red shift of ~ 8 nm has been reported in literature.¹³ For TCPP adsorbed on cotton in absence of TiO₂, a red shift of ~ 6 nm can be observed in the Soret band (Fig. 2b & Supporting information Fig. S1). This could be due to the interaction of TCPP with the hydroxyl groups of cotton.

The absorption peaks in the 500–690 nm region correspond to the Q bands of porphyrin. These peaks can also be easily observed in TCPP-coated cotton and TCPP/TiO₂-coated cotton (Fig. 2b, c). However, in the presence of DMF (Fig. 2d) these peaks are quenched due to the interaction of TCPP with the polar solvent.^{13c}

3.3. XRD spectroscopy

The crystallinity of titania particles coated on the cotton fabric was studied by XRD. In the diffraction patterns of TiO₂-coated

cotton and TiO₂/TCPP-coated cotton, the three peaks at $2\theta = 25.4^\circ$, 38.0° and 48.0° indicate the presence of the anatase phase of TiO₂ (Fig. 3). The observed characteristic peaks of anatase TiO₂ in TCPP/TiO₂-coated cotton indicate that TiO₂ has retained its crystallinity in the presence of porphyrin. However, the intensity of anatase peaks is very small in TiO₂-coated cotton as the bulk of the X-ray signal comes from the underlying cotton substrate, where the cotton-associated signals are more dominant and those of anatase are suppressed. Furthermore, the peaks are also broad due to the small size of anatase crystallites.^{4b}

3.4. Fluorescence spectroscopy

Steady-state fluorescence quenching experiments were conducted to measure the efficiency of electron injection from the dye molecules into TiO₂ (Fig. 4). The fluorescence spectrum of 20 μ M TCPP adsorbed on pristine cotton displays two emission peaks at 653 and 718 nm. For TCPP adsorbed on TiO₂-coated cotton, there was a considerable decrease in the intensity of the emission

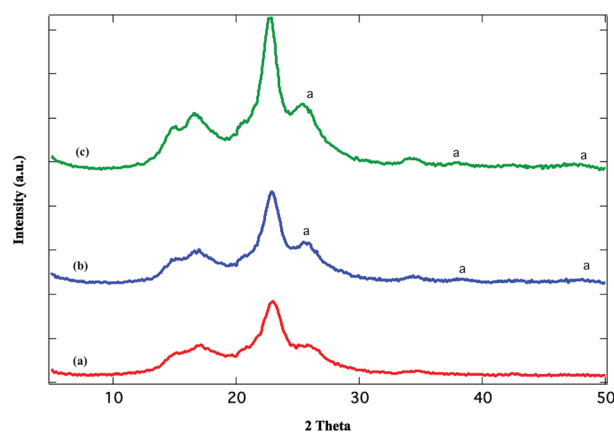


Fig. 3 XRD spectra of cotton (a) pristine, (b) TiO₂-coated, (c) TiO₂/TCPP-coated (a, anatase).

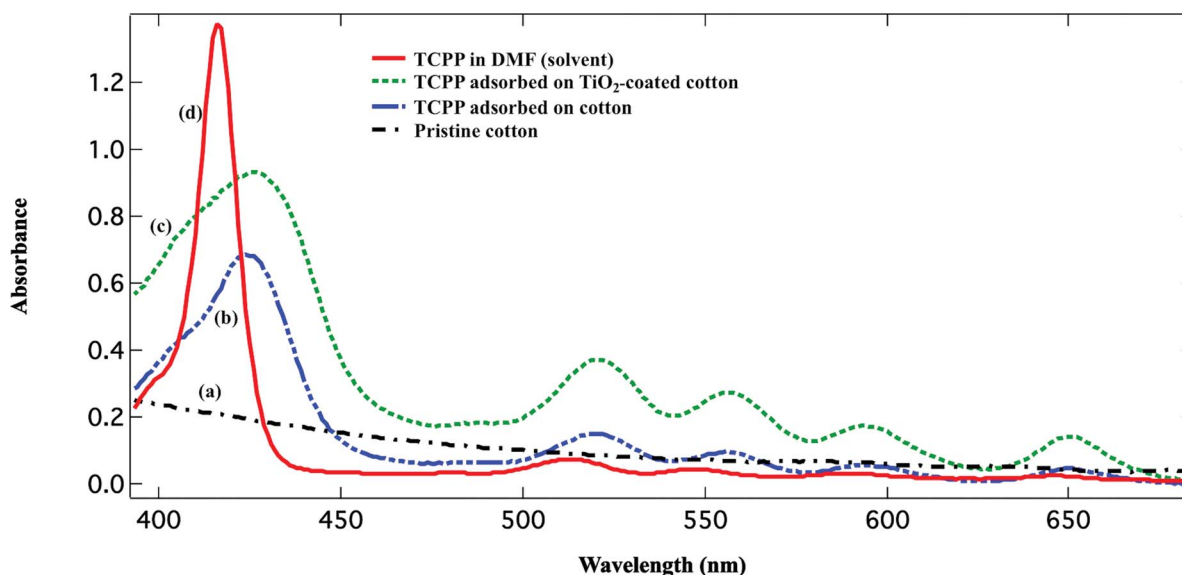


Fig. 2 UV-Vis spectra of pristine cotton (a), TCPP adsorbed on cotton (b), TCPP adsorbed on TiO₂-coated cotton (c), TCPP in DMF (d).

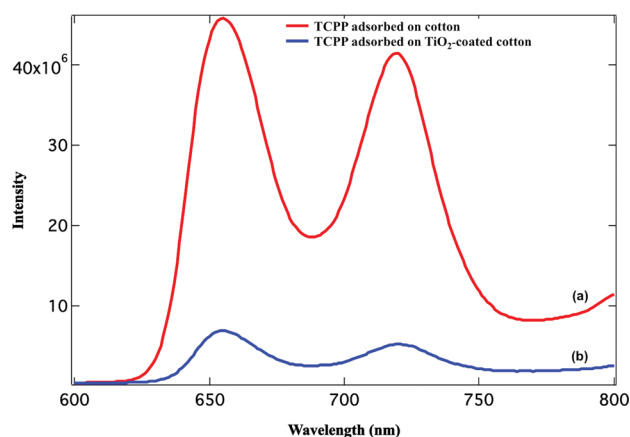


Fig. 4 Steady-state fluorescence spectra of TCPP (a) adsorbed on cotton, (b) TiO_2 -coated cotton.

peaks, as compared to TCPP adsorbed on pristine cotton. The decrease in emission intensity can be attributed to quenching by TiO_2 , suggesting an efficient photoinduced process from TCPP to TiO_2 nanoparticles.

3.5. Self-cleaning performance

3.5.1. Photocatalytic degradation of methylene blue. The self-cleaning properties of TiO_2 /TCPP-coated fabrics were evaluated quantitatively by monitoring the photocatalytic degradation of methylene blue (MB). The photocatalytic efficiency of different cotton samples is compared in Fig. 5. MB was found to be stable in absence of TiO_2 and TCPP under visible light. However, in presence of TiO_2 , TCPP, and TiO_2 /TCPP-coated samples under visible-light, MB undergoes degradation, as monitored by the UV-Vis spectra recorded at different time intervals. Pristine, TiO_2 -coated, and TCPP-coated samples were used for comparison. The straight line obtained for pristine sample indicates the

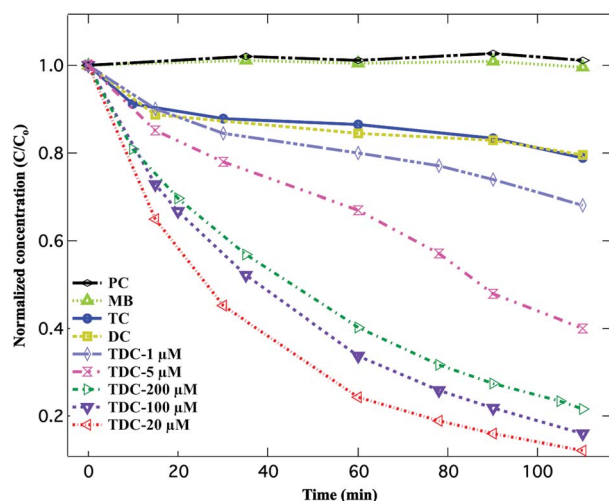


Fig. 5 Degradation of MB (20 ml, 15.6 μM , $\text{pH} = 1$) by 1 g of: pristine cotton (PC), TiO_2 -coated cotton (TC), TCPP-coated cotton (DC) and TiO_2 /TCPP-coated cotton (TDC) samples obtained from 1, 5, 20, 100 and 200 μM TCPP solutions, under visible-light irradiation (5.02 mWcm^{-2} irradiance) for 110 min.

absence of any photocatalytic activity by cotton itself. It is remarkable to note here that in addition to TiO_2 -coated sample, TCPP-coated sample has also shown some photocatalytic activity towards degradation of MB. Porphyrins have already been reported to show photocatalytic activity on their own.¹⁴ TiO_2 /TCPP-coated samples were found to be significantly more photoactive than TiO_2 -coated samples, however an optimum amount of the photosensitizer is required to efficiently sensitize TiO_2 . It is therefore sufficient to form a monolayer on the surface of a catalyst for minimum aggregation and thus maximum light absorption.¹⁵ Hence, five different concentrations (1, 5, 20, 100 and 200 μM) of TCPP dye were used in order to find out the optimum concentration toward photocatalytic dye degradation.

Our results showed 38%, 67%, 99%, 83% and 79% degradation of MB, respectively, with increasing concentrations of 1–200 μM . Among these, the TiO_2 /TCPP-coated sample with TCPP concentration of 20 μM showed the highest photocatalytic efficiency leading to a complete degradation of MB in 110 min of irradiation under visible-light.

3.5.2. Photocatalytic degradation of coffee and wine stains.

To further investigate the self-cleaning performance of TCPP/ TiO_2 -coated cotton in visible-light, qualitative tests for the removal of coffee and red wine stains were conducted (Fig. 6). A significant discolouration of coffee and wine stains was observed for TCPP/ TiO_2 -coated sample after 8 h of irradiation, as compared to TiO_2 -coated sample, whereas the maximum discolouration of stains was achieved after 16 h of irradiation.

The mechanism for degradation of MB, coffee and wine stains under visible-light is based on photosensitization of TiO_2 by porphyrin. This sensitization usually occurs by excitation of dye molecules under visible-light illumination and subsequent electron injection into the conduction band of TiO_2 leading to formation of O_2^- radicals in presence of oxygen. These radicals cause oxidation of organic impurities adsorbed on the surface of the catalyst.^{12d}

3.6. Stability of TiO_2 /TCPP coating

Textiles are subject to frequent washing; therefore the stability of the catalyst coating on textiles is an important requirement in view of its practical application. In our case, the catalyst is a composite of TiO_2 and TCPP, therefore good adhesion of TiO_2 particles to both cotton and TCPP molecules is required. It has been reported that TiO_2 shows strong affinity toward cotton with high level of stability against washing which may be attributed to covalent bonds formed due to dehydration reaction between the hydroxyl groups of cotton and hydroxyl groups of titania.³ The stability of TCPP was tested by subjecting the TiO_2 /TCPP-coated samples to three different media; detergent, petroleum ether and water (Fig. 7). The change in TCPP concentration was monitored by recording UV-Vis spectra before and after washing (Supporting information, Fig. S2).

Samples washed with petroleum ether and water showed the highest TCPP retention (98%) which can be attributed to strong interaction between the carboxylate groups of TCPP and TiO_2 nanoparticles in neutral environment ($\text{pH} = 7$). However, this interaction had been affected when the samples were washed with a detergent solution ($\text{pH} > 8$), showing a reduced TCPP retention

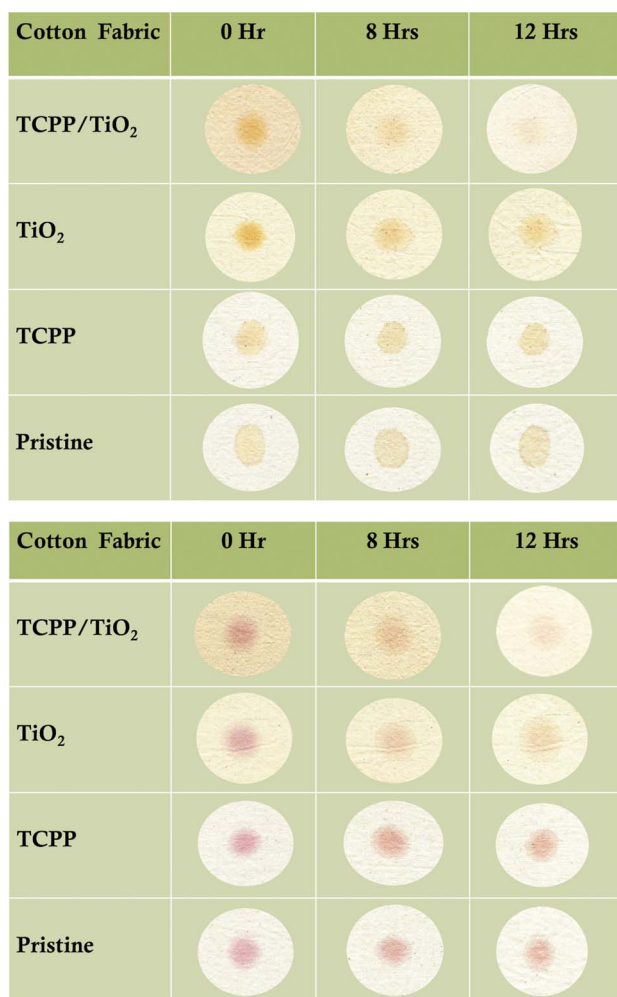


Fig. 6 (a) Degradation of coffee stains on pristine cotton, TCPP-coated cotton, TiO₂-coated cotton and TiO₂/TCPP-coated cotton samples after 0, 8 and 16 h of visible-light irradiation (5.02 mWcm⁻² irradiance). (b) Degradation of red wine stains on pristine cotton, TCPP-coated cotton, TiO₂-coated cotton and TiO₂/TCPP-coated cotton samples after 0, 8 and 16 h of visible-light irradiation (5.02 mW cm⁻² irradiance).

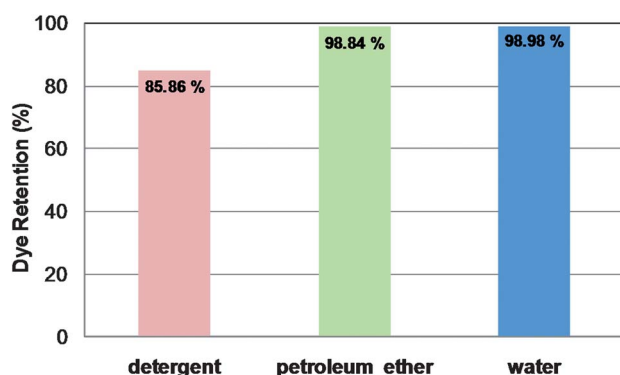


Fig. 7 TCPP retention in TiO₂/TCPP-coated cotton after washing with different solvents.

of 85%. Thus, the binding of TCPP with TiO₂ particles is pH dependent.¹⁶ When the detergent-washed TiO₂/TCPP-coated sample was tested for its photocatalytic activity under

visible-light, it showed 55% degradation of MB in 110 min as compared to 99% of unwashed sample (Fig. 8).

3.7. Photostability of TiO₂/TCPP-coated cotton

This study was conducted in order to determine the stability of TCPP under visible-light. The optimized TiO₂/TCPP-coated sample using 20 μM TCPP with the highest photocatalytic efficiency, was subjected to visible-light irradiation for 30 h. The change in concentration of TCPP was monitored by recording UV-Vis spectra before and after irradiation at different time intervals. Within the first 10 h of irradiation, a significant degradation of 78% occurred. However, in the following 10 h, no further degradation of TCPP was observed. This was confirmed by the reproducibility of the absorption peak intensity in the UV-Vis spectrum, even after 30 h of irradiation (Supporting information, Fig.S3).

The 22% retention of TCPP could be attributed to the strong binding of TCPP to cellulose matrix of cotton, leading to a high level of light stability. Sensitizing dyes incorporated into polymer matrices are known to be photostable.¹⁷ A sample irradiated for 12 h with 22% TCPP retention was further analyzed for self-cleaning performance. Even with such a small amount of TCPP retained, the sample achieved 38% degradation of MB in 110 min, outperforming the TiO₂-coated sample (Fig. 8).

4. Conclusions

Visible-light active self-cleaning cotton has successfully been developed using a dye-sensitization approach, toward indoor self-cleaning applications. Self-assembled monolayers of TCPP have been formed on TiO₂-coated cotton by a simple post-adsorption method. TiO₂/TCPP-coated cotton has shown significant photocatalytic activity in the degradation of methylene blue, coffee and red wine stains as compared to TiO₂-coated cotton. Although, in this study we have achieved the proof of

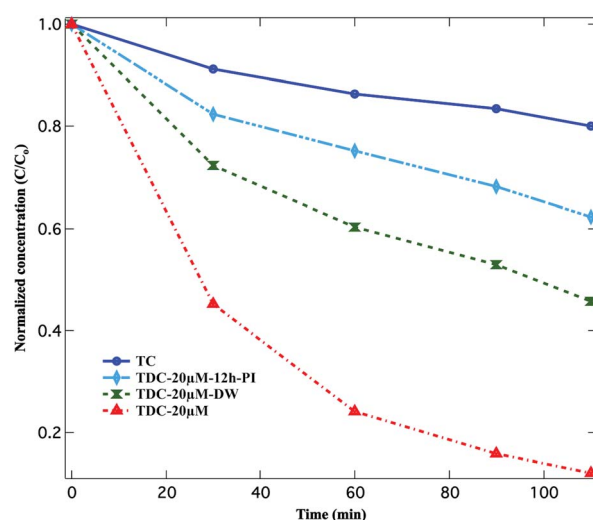


Fig. 8 Degradation of MB (20 ml, 15.6 μM, pH = 1) by 1 g of; TC: TiO₂-coated cotton, TDC-20 μM: TiO₂/TCPP-coated cotton sample obtained from 20 μM TCPP solution, under visible-light irradiation (5.02 mW cm⁻² irradiance) for 110 min. DW: detergent washed, 12h-PI: photo-irradiated for 12 h.

concept of dye-sensitized textiles for visible-light self-cleaning, TCPP has not shown significant photostability. Since, the stability of a photocatalyst is one of the important parameters in determining its practical application; further research toward the development of TCPP-coated textiles with enhanced dye-stabilization as well as the use of more stable and efficient dyes is currently in progress.

Acknowledgements

We thank the Monash Centre for Electron Microscopy (MCEM), Australia for providing assistance in FESEM measurement and Dr S. V. Bhosale, School of Chemistry, Monash University, Clayton Campus, Australia for providing TCPP. Mr. M. K. Kashif (Monash University, Clayton) is also acknowledged for providing assistance in XRD and fluorescence spectroscopy measurements.

Notes and references

- (a) D. Chen, Y.-B. F. Huang, Cheng and R. A. Caruso, *Adv. Mater.*, 2009, **21**, 2206; (b) J. Peral and D. F. Ollis, *J. Catal.*, 1992, **136**, 554; (c) Y. Kikuchi, K. Sunada, T. Iyoda, K. Hashimoto and A. Fujishima, *J. Photochem. Photobiol., A*, 1997, **106**, 51; (d) X. Fu, W. A. Zeltner and M. A. Anderson, *Appl. Catal., B*, 1995, **6**, 209; (e) T. Noguchi, A. Fujishima, P. Sawunyama and K. Hashimoto, *Environ. Sci. Technol.*, 1998, **32**, 3831.
- (a) M. Peplow, *Nature*, 2004, **429**, 620; (b) M. R. Hoffmann, S. T. Martin, W. Choi and D. W. Bahnemann, *Chem. Rev.*, 1995, **95**, 69; (c) A. Fujishima, T. N. Rao and D. K. Tryk, *J. Photochem. Photobiol., C*, 2000, **1**, 1.
- (a) J. H. Xin, W. A. Daoud and Y. Y. Kong, *Text. Res. J.*, 2004, **74**, 97; (b) W. A. Daoud and J. H. Xin, *J. Am. Ceram. Soc.*, 2004, **87**, 953; (c) W. A. Daoud, J. H. Xin and Y.-H. Zhang, *Surf. Sci.*, 2005, **599**, 69; (d) W. A. Daoud, J. H. Xin, Y.-H. Zhang and K. Qi, *J. Non-Cryst. Solids*, 2005, **351**, 1486; (e) W. S. Tung and W. A. Daoud, *J. Mater. Chem.*, 2011, **21**, 7858.
- (a) W. A. Daoud, S. K. Leung, W. S. Tung, J. H. Xin, K. Cheuk and K. Qi, *Chem. Mater.*, 2008, **20**, 1242; (b) K. Qi, W. A. Daoud, J. H. Xin, C. L. Mak, W. Tang and W. P. Cheung, *J. Mater. Chem.*, 2006, **16**, 4567; (c) A. Bozzi, T. Yuranova, I. Guasaquillo, D. Laub and J. Kiwi, *J. Photochem. Photobiol., A*, 2005, **174**, 156; (d) K. Qi, J. H. Xin, W. A. Daoud and C. L. Mak, *Int. J. Appl. Ceram. Technol.*, 2007, **4**, 554.
- M. Miyauchi, A. Nakajima, T. Watanabe and K. Hashimoto, *Chem. Mater.*, 2002, **14**, 2812.
- (a) T. Yuranova, A. G. Rincon, C. Pulgarin, D. Laub, N. Xantopoulos, H. J. Mathieu and J. Kiwi, *J. Photochem. Photobiol., A*, 2006, **181**, 363; (b) J. Kiwi and C. Pulgarin, *Catal. Today*, 2010, **151**, 2; (c) M. J. Uddin, F. Cesano, D. Scarano, F. Bonino, G. Agostini, G. Spoto, S. Bordiga and A. Zecchina, *J. Photochem. Photobiol., A*, 2008, **199**, 64; (d) R. Wang, X. Wang and J. H. Xin, *ACS Appl. Mater. Interfaces*, 2009, **2**, 82; (e) W. S. Tung and W. A. Daoud, *ACS Appl. Mater. Interfaces*, 2009, **1**, 2453; (f) S. Bingham and W. A. Daoud, *J. Mater. Chem.*, 2011, **21**, 2041.
- (a) L. Zhao, X. Chen, X. Wang, Y. Zhang, W. Wei, Y. Sun, M. Antonietti and M.-M. Titirici, *Adv. Mater.*, 2010, **22**, 3317; (b) S. S. Soni, M. J. Henderson, J.-F. Bardeau and A. Gibaud, *Adv. Mater.*, 2008, **20**, 1493; (c) R. Bacsa, J. Kiwi, T. Ohno, P. Albers and V. J. Nadtochenko, *J. Phys. Chem. B*, 2005, **109**, 5994.
- S. Rehman, R. Ullah, A. M. Butt and N. D. Gohar, *J. Hazard. Mater.*, 2009, **170**, 560.
- (a) J. C. Zhao, C. C. Chen and W. H. Ma, *Top. Catal.*, 2005, **35**, 269; (b) P. V. Kamat and M. A. Fox, *Chem. Phys. Lett.*, 1983, **102**, 379; (c) H. Ross, J. Bendig and S. Hecht, *Sol. Energy Mater. Sol. Cells*, 1994, **33**, 475; (d) R. Abe, K. Hara, K. Sayama, K. Domen and H. Arakawa, *J. Photochem. Photobiol., A*, 2000, **137**, 63; (e) J. Moon, C. Y. Yun, K.-W. Chung, M.-S. Kang and J. Yi, *Catal. Today*, 2003, **87**, 77.
- G. Mele, R. Del Sole, G. Vasapollo, E. Garcia-Lopez, L. Palmisano, L. Jun, R. Slota and G. Dyrda, *Res. Chem. Intermed.*, 2007, **33**, 433.
- H. L. Anderson, *Inorg. Chem.*, 1994, **33**, 972.
- (a) S. Rodrigues, K. T. Ranjit, S. Uma, I. N. Martyanov and K. J. Klabunde, *Adv. Mater.*, 2005, **17**, 2467; (b) A. A. Ismail and D. W. Bahnemann, *ChemSusChem*, 2010, **3**, 1057; (c) D. Li, W. Dong, S. Sun, Z. Shi and S. Feng, *J. Phys. Chem. C*, 2008, **112**, 14878; (d) H. Huang, X. Gu, J. Zhou, K. Ji, H. Liu and Y. Feng, *Catal. Commun.*, 2009, **11**, 58; (e) G. Granados-Oliveros, E. A. Páez-Mozo, F. M. Ortega, C. Ferronato and J.-M. Chovelon, *Appl. Catal., B*, 2009, **89**, 448; (f) M.-y. Duan, J. Li, G. Mele, C. Wang, X.-f. Lü, G. Vasapollo and F.-x. Zhang, *J. Phys. Chem. C*, 2010, **114**, 7857; (g) M. Y. Chang, C. Y. Chang, Y. H. Hsieh, K. S. Yao, T. C. Cheng and C. T. Ho, *Multi-Functional Materials and Structures, Pts 1 and 2*, 2008, **47-50**, 471; (h) M. Y. Chang, Y. H. Hsieh, T. C. Cheng, K. S. Yao, M. C. Wei and C. Y. Chang, *Thin Solid Films*, 2009, **517**, 3888.
- (a) C. E. Diaz-Urbe, M. C. Daza, F. Martinez, E. A. Páez-Mozo, C. L. B. Guedes and E. D. Mauro, *J. Photochem. Photobiol., A*, 2010, **215**, 172; (b) T. Ma, K. Inoue, H. Noma, K. Yao and E. Abe, *J. Photochem. Photobiol., A*, 2002, **152**, 207; (c) M. Makarska, St. Radzki and J. Legendziewicz, *J. Alloys Compd.*, 2002, **341**, 233.
- T. Shiragami, J. Matsumoto, H. Inoue and M. Yasuda, *J. Photochem. Photobiol., C*, 2005, **6**, 227.
- C. Wang, J. Li, G. Mele, M.-y. Duan, X.-f. Lü, L. Palmisano, G. Vasapollo and F.-x. Zhang, *Dyes Pigm.*, 2010, **84**, 183.
- W. Li, N. Gandra, E. D. Ellis, S. Courtney, S. Li, E. Butler and R. Gao, *ACS Appl. Mater. Interfaces*, 2009, **1**, 1778.
- Y. Li, H. Zhang, X. Hu, X. Zhao and Min Han, *J. Phys. Chem. C*, 2008, **112**, 14973.

Supporting Information

Self-Cleaning Cotton by Porphyrin-sensitized Visible-Light Photocatalysis

Shabana Afzal,^a Walid A. Daoud,^a and Steven J. Langford^b

^aSchool of Applied Sciences and Engineering, Monash University, Churchill, Victoria 3842, Australia

^bSchool of Chemistry, Monash University, Clayton, Victoria 3800, Australia

1. UV-Vis absorption spectroscopy of TCPP

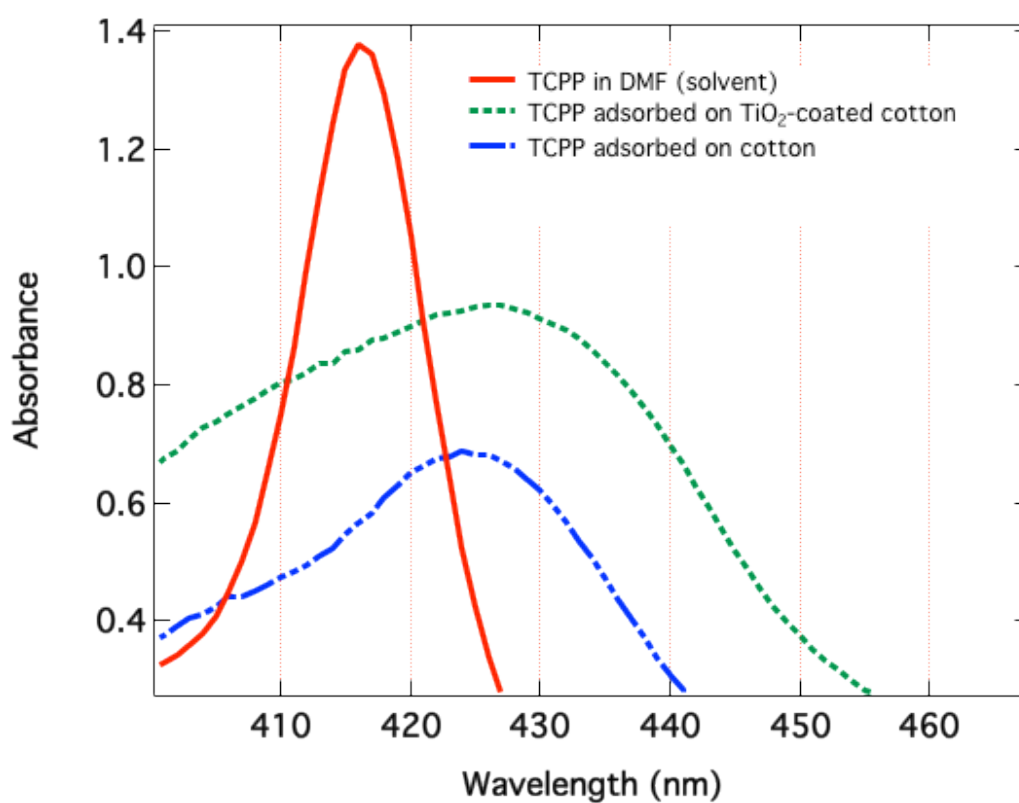


Fig. S1 UV-Vis spectra of TCPP for Soret band

2. UV-Vis Spectroscopy for evaluation of coating stability

a. Detergent washing

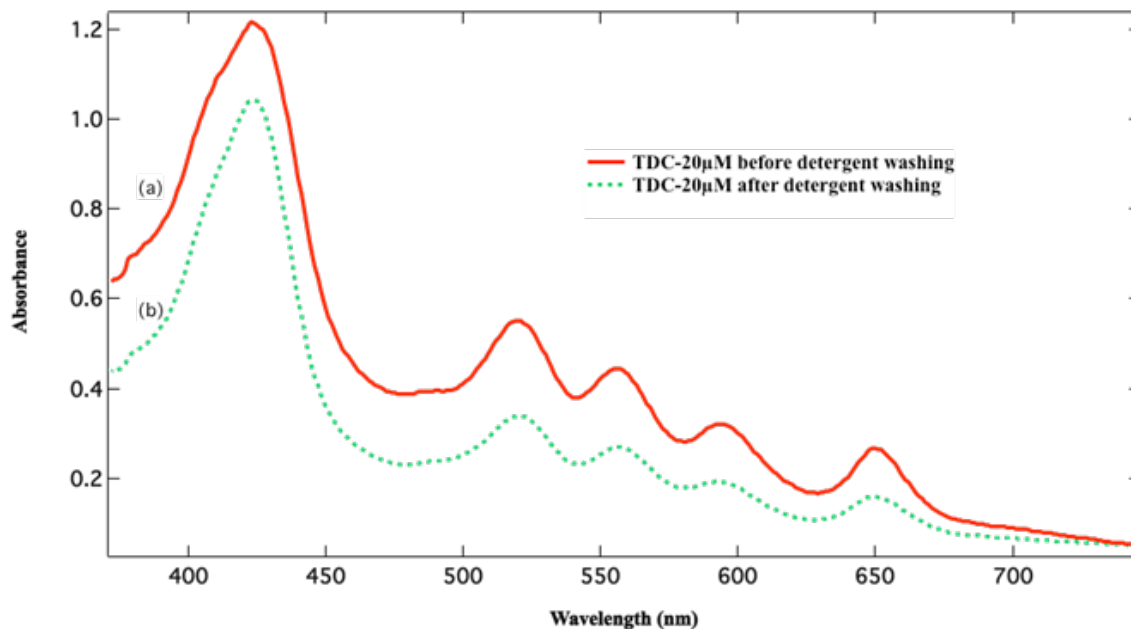


Fig. S2a UV-Vis spectra TiO₂/TCPP-coated cotton (a) before washing with detergent, (b) after washing with detergent for 45 min.

b. Petroleum ether washing

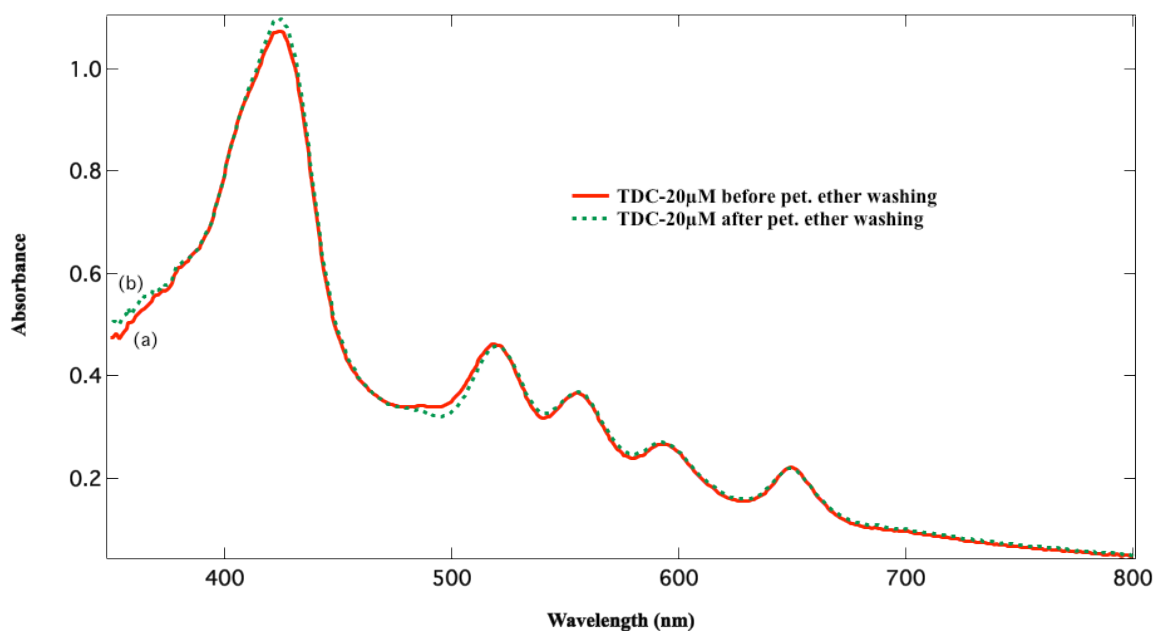


Fig. S2b UV-Vis spectra TiO₂/TCPP-coated cotton (a) before washing with petroleum ether, (b) after washing with petroleum ether for 45 min.

c. Water washing

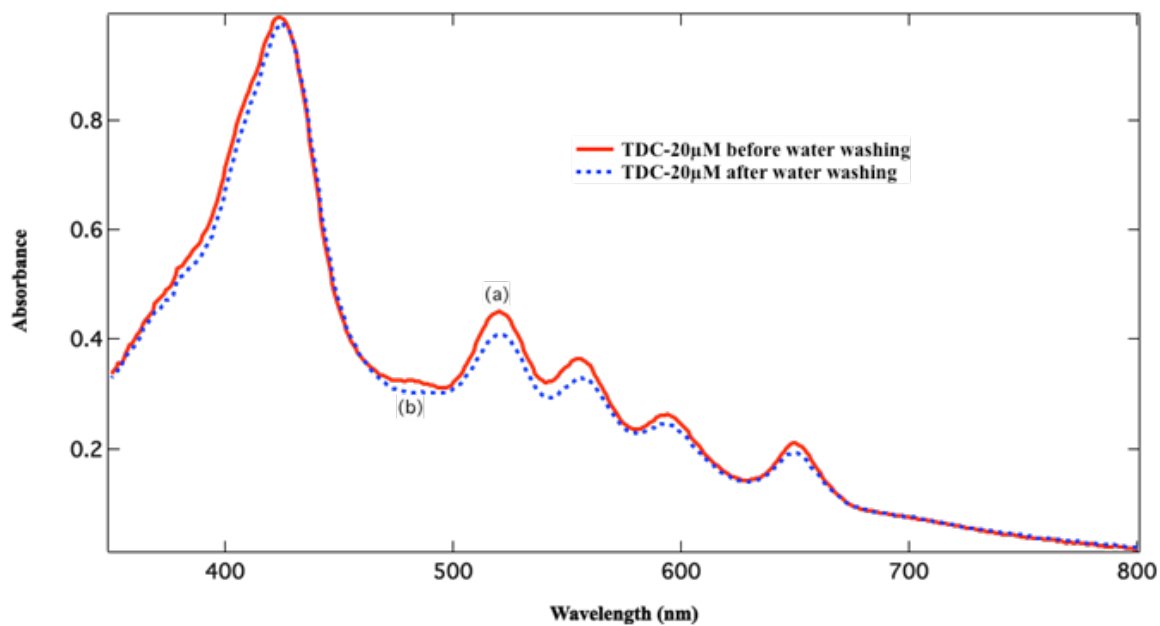


Fig. S2c UV-Vis spectra TiO₂/TCPP-coated cotton (a) before washing with water, (b) after washing with water for 45 min.

2. UV-Vis spectroscopy for evaluation of coating photostability

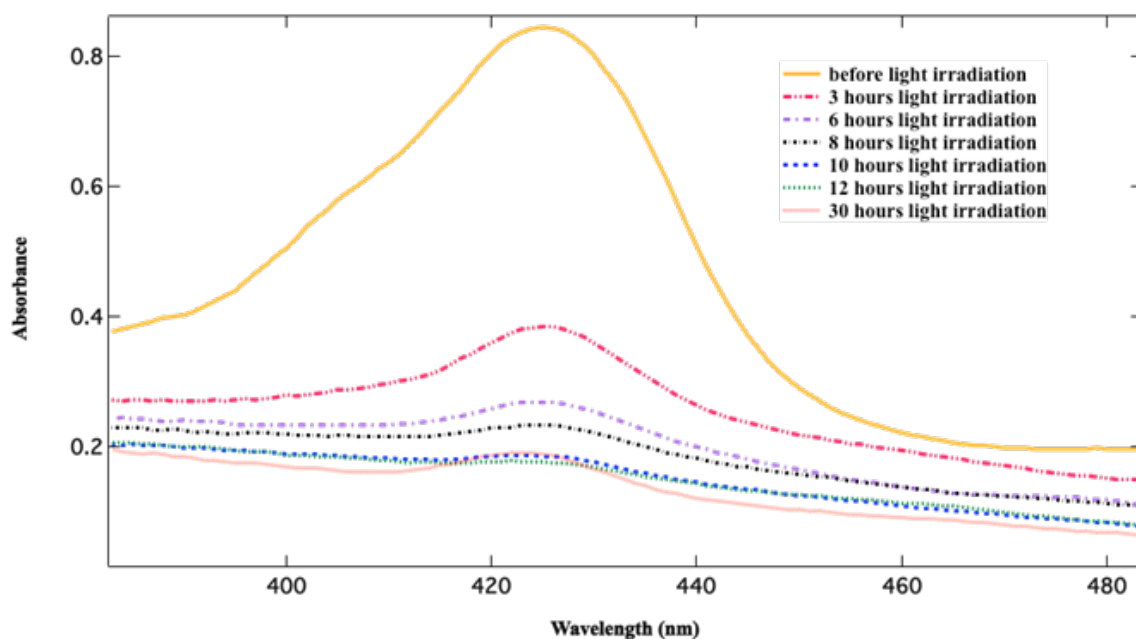


Fig. S3 UV-Vis spectra of TiO₂/TCPP-coated cotton before and after light irradiation at different time intervals.



Declaration for Thesis Chapter 3

Declaration by candidate

In the case of Chapter 3, the nature and extent of my contribution to the work was the following:

Nature of contribution	Extent of contribution
Initiation, interpretation, experiments, data analysis and writing up	65 %

The following co-authors contributed to the work. If co-authors are students at Monash University, the extent of their contribution in percentage terms must be stated:

Name	Nature of contribution	Extent of contribution (%) for student co-authors only
Walid A. Daoud	Supervision, interpretation, suggestion, discussion and revision	N/A
Steven J. Langford	Supervision, interpretation, suggestion, discussion and revision	N/A

The undersigned hereby certify that the above declaration correctly reflects the nature and extent of the candidate's and co-authors' contributions to this work.

Candidate's
Signature

	Date 4/10/2013
---	-------------------

Main
Supervisor's
Signature

	Date 4/10/2013
---	-------------------

Chapter 3:

Visible-light self-cleaning cotton by metalloporphyrin-sensitised photocatalysis



Visible-light self-cleaning cotton by metalloporphyrin-sensitized photocatalysis

Shabana Afzal^a, Walid A. Daoud^{b,*}, Steven J. Langford^c

^a School of Applied Sciences and Engineering, Monash University, Churchill 3842, Australia

^b School of Energy and Environment, City University of Hong Kong, Tat Chee Avenue, Kowloon, Hong Kong

^c School of Chemistry, Monash University, Clayton 3800, Australia

ARTICLE INFO

Article history:

Available online 26 January 2013

Keywords:

Visible-light photocatalysis
Porphyrin
Titanium dioxide
Self-cleaning

ABSTRACT

Thin films of *meso*-tetra(4-carboxyphenyl)porphyrin with different metal centres (MTCPP, M = Fe, Co and Zn) in combination with anatase TiO₂ have been formed on cotton fabric. Their self-cleaning properties have been evaluated by conducting the photocatalytic degradation of methylene blue under visible-light irradiation. All MTCPP/TiO₂-coated cotton fabrics showed superior self-cleaning performance as compared to the bare TiO₂-coated cotton. Among the three metal porphyrins, FeTCPP showed the highest photocatalytic activity with complete degradation of methylene blue in 180 min. The fabrics were characterized by FESEM, XRD, UV–vis and fluorescence spectroscopy.

© 2013 Elsevier B.V. All rights reserved.

1. Introduction

Since the discovery of the photocatalytic property of TiO₂ by Honda and Fujishima [1], the potential use of titanium dioxide in various environmental applications has been well explored. With the growing interest in photo-induced self-purification materials, self-cleaning surfaces have been developed using TiO₂ coatings on various substrates. Fujishima et al. have developed the first self-cleaning ceramic in 1990 [2]. Later on, the concept of TiO₂ photocatalysis was extended to the development of self-cleaning glasses, tents, window blinds and lamp covers [3]. Nanocrystalline TiO₂ particles immobilized on activated carbon, glass, polymeric materials and silica have been achieved [4,5], however most of these techniques required high temperature processing [6,7], thus limiting their application to substrates of low thermal resistance such as textiles. Therefore, the past decade has been witnessing extensive research to grow TiO₂ nanocrystals on organic fibres.

By using a nanotechnological approach in combination with a low-temperature sol-gel process, Daoud et al. have successfully developed an anatase TiO₂-based self-cleaning cotton that showed efficient photocatalytic properties under UV light [8–10]. A number of other UV-active textiles such as wool and polyester using various techniques of surface modification have also been developed [11,12]. TiO₂ has a wide band gap of 3.2 eV, due to which it can only be excited effectively under UV irradiation. Ultraviolet radiation reaching the earth is only 4–6% of the total solar irradiance,

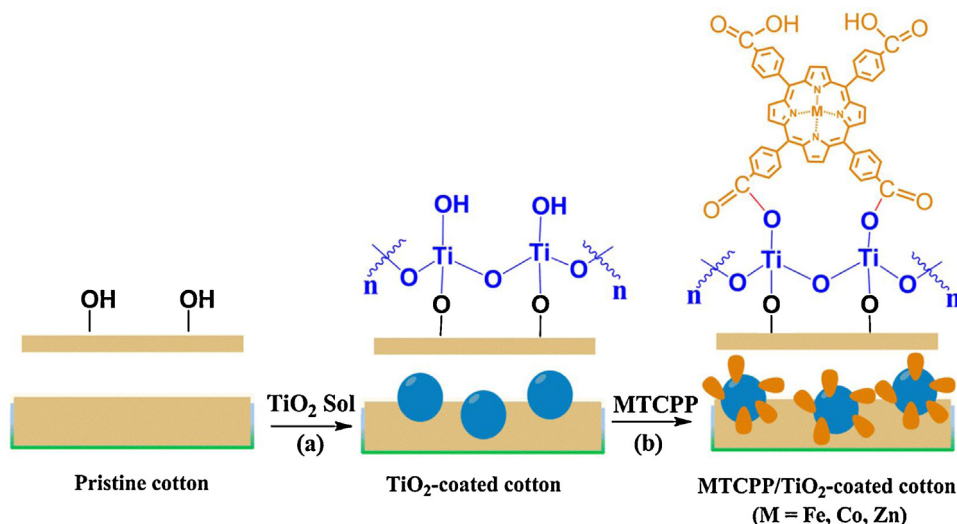
whereas 45% consists of visible-light [13]. For efficient utilization of solar light, many methods have been reported in literature to extend the light absorption of TiO₂ in the visible region; such as metal doping [14–16], non-metal doping [17], ion-implantation [18] and photosensitization [19]. Following some of these methods, very few visible-light driven self-cleaning textiles have been developed using metals [20] and non-metals [21].

Photosensitization using dyes allows efficient sensitization of TiO₂ in the visible region as compared to the other methods [22]. In photosensitization method, a photo-induced electrons transfer process takes place from excited dye to the conduction band of TiO₂ [23]. These electrons can then react with atmospheric O₂ to form superoxide radical anions (O₂^{•−}), which can cause oxidation of organic impurities present on the surface of catalyst [24,25]. Porphyrins are considered as efficient sensitizers to harvest light when adsorbed on the surface of TiO₂ [23]. Due to an extensive system of delocalized π electrons, porphyrins have very strong absorption in the visible region [26–28]. According to electrochemical measurements, electron injection from the excited state of porphyrins to the conduction band of TiO₂ is thermodynamically favoured [29]. Furthermore, the photophysical properties of porphyrins can be easily tuned by modifying the peripheral substituents and/or through metal complexation [30,31].

Recently, we have successfully developed self-cleaning cotton based on *meso*-tetra(4-carboxyphenyl)porphyrin (TCPP)-sensitized TiO₂ that showed significant photoactivity under visible-light as compared to bare TiO₂ [32]. In this manuscript, films of *meso*-tetra(4-carboxyphenyl)porphyrin with different metal centres (MTCPP, M = Fe, Co and Zn) have been formed on TiO₂-coated cotton fabric. The self-cleaning properties of fabrics have been investigated by studying the photocatalytic degradation of methylene blue (MB) under visible-light irradiation. Using a

* Corresponding author at: School of Energy and Environment, City University of Hong Kong, Tat Chee Avenue, Kowloon, Hong Kong. Tel.: +852 3442 4499; fax: +852 3442 0688.

E-mail address: daoud@cityu.edu.hk (W.A. Daoud).



Scheme 1. Formation of thin films of MTCPP on TiO₂-coated cotton. (a) Treatment of pristine cotton with TiO₂ colloid to form TiO₂ coating on cotton. (b) Treatment of TiO₂-coated cotton with MTCPP solution in DMF to form MTCPP/TiO₂-coated cotton.

simple post-adsorption method, self-assembled monolayers of MTCPP have been formed on TiO₂-coated cotton, as shown in Scheme 1.

2. Experimental

2.1. Synthesis of MTCPP/TiO₂-coated cotton

2.1.1. Synthesis of TiO₂ colloid

Colloidal TiO₂ anatase was prepared by adding a solution of titanium tetraisopropoxide and acetic acid drop wise to acidified water using 1.4% HNO₃. The mixture was stirred at 60 °C for 16 h.

2.1.2. Preparation of TiO₂-coated cotton

The TiO₂ colloid was applied to scoured cotton fabric through a dip-pad-dry-cure process. In order to remove impurities from cotton, it was scoured by the non-ionic detergent (Kieralon® F-OLB Conc.) before application of TiO₂ colloid. The scouring was carried out at 80 °C for 30 min. The scoured cotton pieces were dipped in the colloid for 1 min and then pressed in automatic horizontal press at 7.5 rpm with a nip pressure of 2.75 kg cm⁻². The pressed samples were then exposed to ammonia fumes until the surface pH 7 was reached. The neutralized samples were dried at 80 °C in a drying oven and cured at 120 °C for 3 min.

2.1.3. Synthesis of MTCPP

Fe(III), Co(II) and Zn(II) complexes of *meso*-tetra(4-carboxyphenyl)porphyrin were synthesized according to a method reported in literature [33]. Metal porphyrins (MTCPP) were synthesized by refluxing 0.33 mmol of TCP with 1.82 mmol of FeCl₃·6H₂O, Zn(Ac)₂ and CoCl₃·6H₂O in DMF for 2 h. MTCPPs were precipitated by adding in excess water. DMF and water were removed from the precipitates by repeated centrifugation. Solid dry precipitates of each metal complex were obtained by freeze drying.

2.1.4. Preparation of MTCPP/TiO₂-coated cotton

For MTCPP deposition, TiO₂-coated cotton samples were dipped in the corresponding MTCPP solution in DMF and heated at 100 °C for 5 h. The samples were then repeatedly washed with DMF to remove unreacted MTCPP molecules.

2.2. Characterization

The surface morphology of the samples was studied using field emission electron microscopy (JEOL 7001F FEGSEM). The crystallinity of TiO₂ films on cotton was determined by low angle X-ray diffraction (XRD, Philip 1140 diffractometer). The diffraction patterns of anatase TiO₂ were compared with reference to ICDD (2006) database. The UV–vis absorption spectra of MTCPP in DMF and MTCPP adsorbed on TiO₂-coated cotton were recorded on Cary 5000 spectrophotometer. The steady-state fluorescence quenching experiments were performed on Cary Eclipse fluorescence spectrophotometer.

2.3. Photocatalytic degradation

For the evaluation of self-cleaning properties, photocatalytic degradation of methylene blue (MB) was evaluated quantitatively. MTCPP/TiO₂-coated cotton pieces (0.5 g, 1.5 × 1.5 cm) were immersed in petri dish containing acidified MB (10 ml, 15.6 μM, pH = 1). The petri dishes were placed in a light-box and irradiated by visible-light for 3 h, using fluorescent lamp (30 W, 5.02 mWcm⁻² irradiance). During irradiation, the petri dishes were vigorously shaken using a bench top shaker. Prior to irradiation, the petri dishes were kept in dark for half an hour in order to attain adsorption-desorption equilibrium. The change in the concentration of MB was monitored by recording UV–vis spectra at different time intervals, during the course of photocatalytic reaction.

2.4. Stability of coating

The stability of MTCPP/TiO₂-coated cotton samples was tested against detergent, petroleum ether and water, using a modified AATCC Test Method 190-2003. The samples were washed with each solvent for 45 min at room temperature at constant stirring of 200 rpm, followed by rinsing with water and the air drying. To determine the amount of porphyrin retained on the cotton samples, UV–vis spectra of the samples were recorded before and after washing.

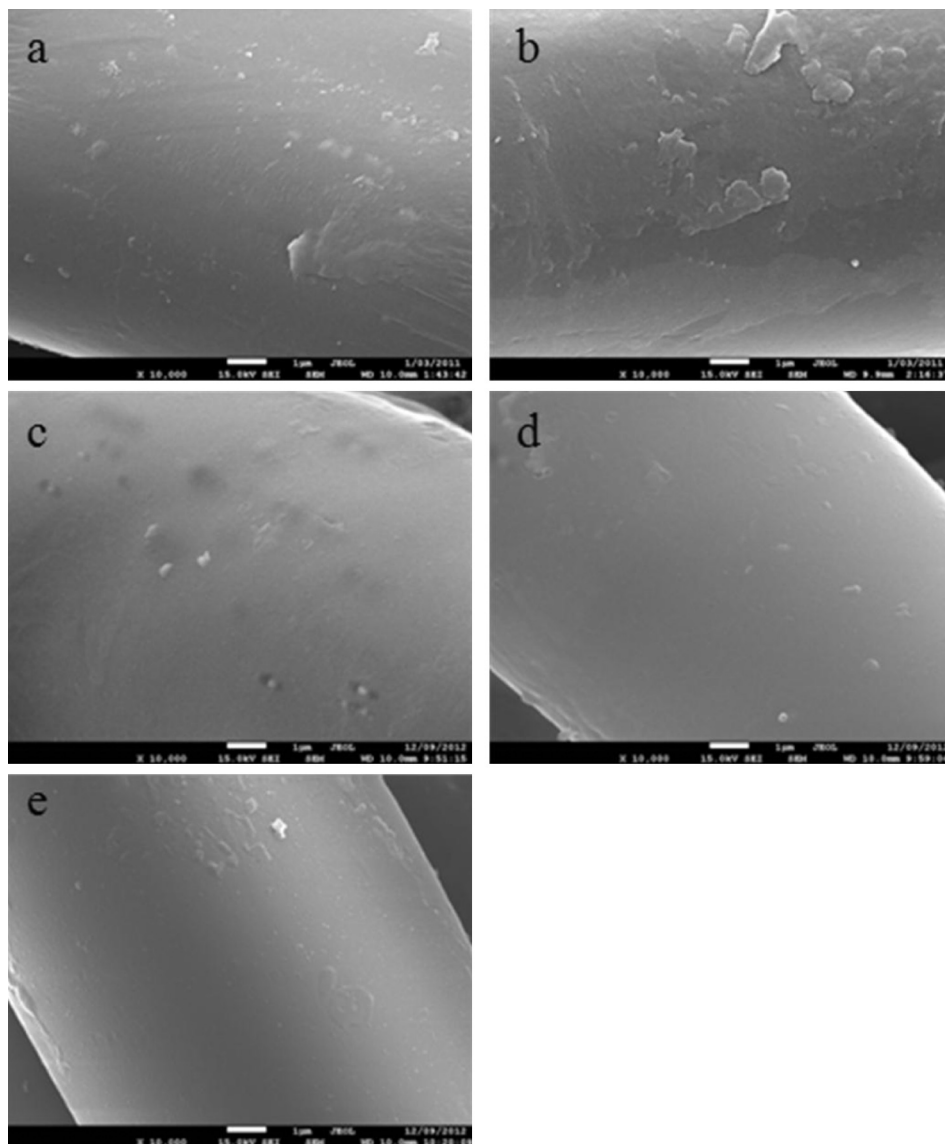


Fig. 1. FESEM images of (a) pristine cotton, (b) TiO₂-coated cotton, (c) FeTCPP/TiO₂-coated cotton, (d) CoTCPP/TiO₂-coated cotton, (e) ZnTCPP/TiO₂-coated cotton.

3. Results and discussion

3.1. SEM analysis

The surface morphology of pristine cotton and cotton samples coated with TiO₂ and MTCPP was investigated from SEM images, illustrated in Fig. 1. After TiO₂ coating, there is no major change in the surface morphology of cotton. However, aggregates of TiO₂ nanoparticles can be clearly observed in the case of TiO₂-coated cotton (Fig. 1b). Some TiO₂ aggregates formation has already been reported in the literature [34]. The formation of aggregates might be due to a decrease in the surface charge of TiO₂ when attached to cotton as compared to its large positive surface charge in the acidic colloid before deposition on cotton. The TiO₂ cotton samples coated with FeTCPP, CoTCPP and ZnTCPP (Fig. 1c, d and e, respectively) appear to have more uniform surface as compared to bare TiO₂-coated cotton sample presumably as a result of the processing.

3.2. XRD analysis

In order to study the crystallinity of titania nanoparticles deposited on the cotton samples, XRD analysis was performed.

TiO₂-coated and FeTCPP/TiO₂-coated samples exhibit characteristic diffraction peaks for anatase at $2\theta = 25.4^\circ$, 38.0° , 48.0° with miller indices (101), (104) and (200), respectively (Fig. 2b,c). The pristine sample clearly shows the absence of these peaks (Fig. 2a). The presence of anatase peaks in FeTCPP/TiO₂-coated samples indicates that TiO₂ has retained its crystallinity after adsorption of FeTCPP. For samples coated with CoTCPP and ZnTCPP, the same characteristics peaks of anatase were also observed (Supporting Information, Fig. S1).

3.3. UV-vis spectroscopy

Fig. 3 shows the UV-vis absorption spectra of different MTCPP adsorbed on TiO₂-coated samples. For comparison, UV-vis spectrum of pristine cotton was also recorded. Visible-light absorption between 400 to 700 nm can be easily observed for all the samples except pristine cotton, where no dye is present (Fig. 3d). The absorption spectra of ZnTCPP, CoTCPP and FeTCPP show strong peaks for the Soret band at 432, 435 and 425 nm, respectively (Fig. 3a, b and c). The UV-vis spectra of all MTCPP adsorbed on TiO₂-coated cotton, have a clear red shift of the Soret band as compared to their UV-vis spectra in DMF (Table 1). This red shift can be

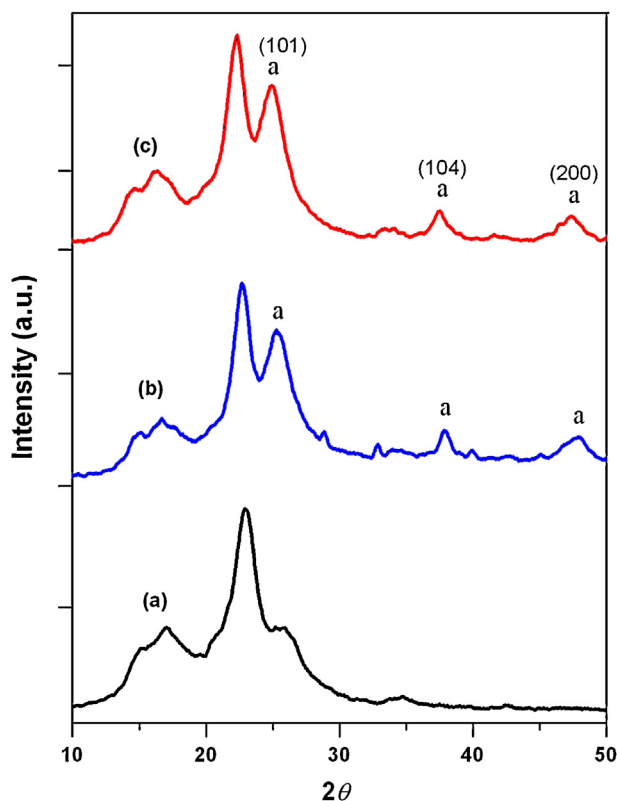


Fig. 2. XRD spectra of cotton (a) pristine, (b) TiO₂-coated, (c) FeTCPP/TiO₂-coated (a, anatase).

attributed to strong interaction between the carboxylate groups of MTCPP and TiO₂ [31,33].

3.4. Fluorescence spectroscopy

To measure the efficiency of electron injection from the dye molecules into TiO₂, steady-state fluorescence quenching experiments were conducted. The UV–vis absorption and fluorescence emission spectra of MTCPP (M= Fe, Co and Zn) adsorbed on pristine cotton in absence and presence of TiO₂ are shown in Fig. 4. Amount of dye loaded on cotton samples in presence of TiO₂ is more than that in the absence of TiO₂, as intensity of the absorption

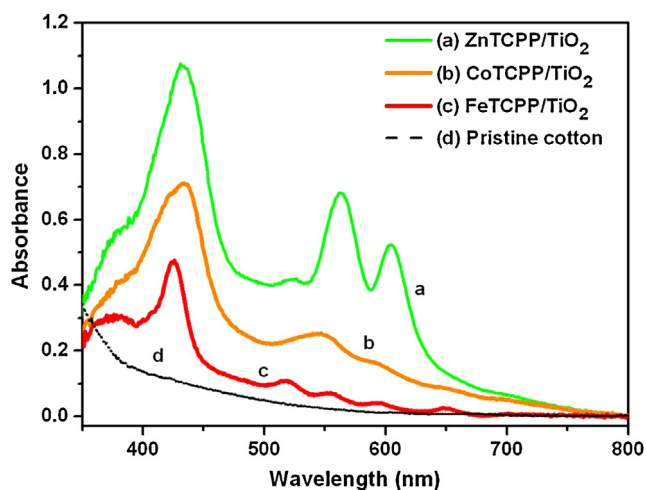


Fig. 3. UV–vis absorption spectra of pristine cotton and MTCPP adsorbed on TiO₂-coated cotton.

peaks of all dyes for TiO₂-coated samples is higher than that of pristine cotton (Fig. 4a, c and e). However, in the fluorescence spectra, the opposite trend is observed. Although the UV–vis absorption is higher for TiO₂-coated samples, the fluorescence emission is lower as compared to the pristine cotton (Fig. 4b, d and f). The decrease in emission intensity can be attributed to the quenching by TiO₂, as a result of electron injection from MTCPP to TiO₂ nanoparticles.

The fluorescence quenching behaviour of each metal complex was further studied from Stern–Volmer relation: $I_0/I = 1 + K_{sv} [Q]$, where I_0 and I correspond to fluorescence intensities of sensitizer dye in absence and presence of quencher, respectively, and K_{sv} is the Stern–Volmer rate constant. Fig. 5a shows the effect of concentration of TiO₂ on fluorescence spectrum of FeTCPP. Addition of TiO₂ colloid to a solution of FeTCPP resulted in quenching of its fluorescence emission. The K_{sv} value ($0.06 \times 10^2 \text{ M}^{-1}$) was obtained from the slope of Stern–Volmer plot for FeTCPP (Fig. 5b). The K_{sv} (M^{-1}) values for CoTCPP and ZnTCPP are 0.01×10^2 and 0.008×10^2 , respectively (Supporting Information, Fig. S2 and S3). The highest K_{sv} observed for FeTCPP as compared to CoTCPP and ZnTCPP accounts for strong association between FeTCPP molecules and TiO₂ resulting in efficient charge injection from FeTCPP into the conduction band of TiO₂.

3.5. Self-cleaning properties: photocatalytic degradation of methylene blue

For the evaluation of self-cleaning performance, MTCPP/TiO₂-coated cotton samples were subjected to quantitative analysis of photocatalytic degradation of MB under visible-light irradiation. Fig. 6 shows a plot of normalized concentration of MB (C/C_0) against time. C is the concentration of MB at different time intervals of irradiation and C_0 is the concentration of MB before irradiation. Change in concentration of MB has been monitored by recording the UV–vis spectra at different time intervals. For comparison, pristine cotton and TiO₂-coated cotton samples were also studied. The plateaued line obtained for pristine sample indicates the absence of any photocatalytic activity by cotton itself. TiO₂-coated sample showed 32% degradation of MB, whereas, all cotton samples coated with MTCPP/TiO₂ showed significant increase in photoactivity as compared to bare TiO₂. Among different metal complexes of TCPP, the results showed 86%, 89% and 99% degradation of MB for ZnTCPP, CoTCPP and FeTCPP, respectively. Thus the highest photocatalytic efficiency was observed for the sample coated with FeTCPP/TiO₂.

The degradation reaction of MB for samples coated with ZnTCPP, CoTCPP and FeTCPP follows first order kinetics. The corresponding first order rate constants [k_1 (min^{-1})], determined from the slopes of the curves in Fig. 6 are 0.011, 0.012 and 0.014 for ZnTCPP, CoTCPP and FeTCPP, respectively. Initially, within the first 60 minutes, the rate of reaction is high. Later on, it decreases with a tailing effect at the end of reaction, as the product formed gradually blocks the active sites of the catalyst.

In order to achieve efficient photocatalysis, an optimum amount of the photosensitizer dye with minimum aggregation and enhanced electron injection into TiO₂ is required [35]. Therefore,

Table 1

UV–vis absorption of MTCPP in DMF and adsorbed on TiO₂-coated cotton.

MTCPP	DMF		TiO ₂ -coated cotton	
	λ_{max} (nm)			
	Soret band	Q bands	Soret band	Q bands
FeTCPP	420	513, 583, 639	425	518, 555, 593
CoTCPP	418	531	435	546
ZnTCPP	427	564, 602	432	563, 604

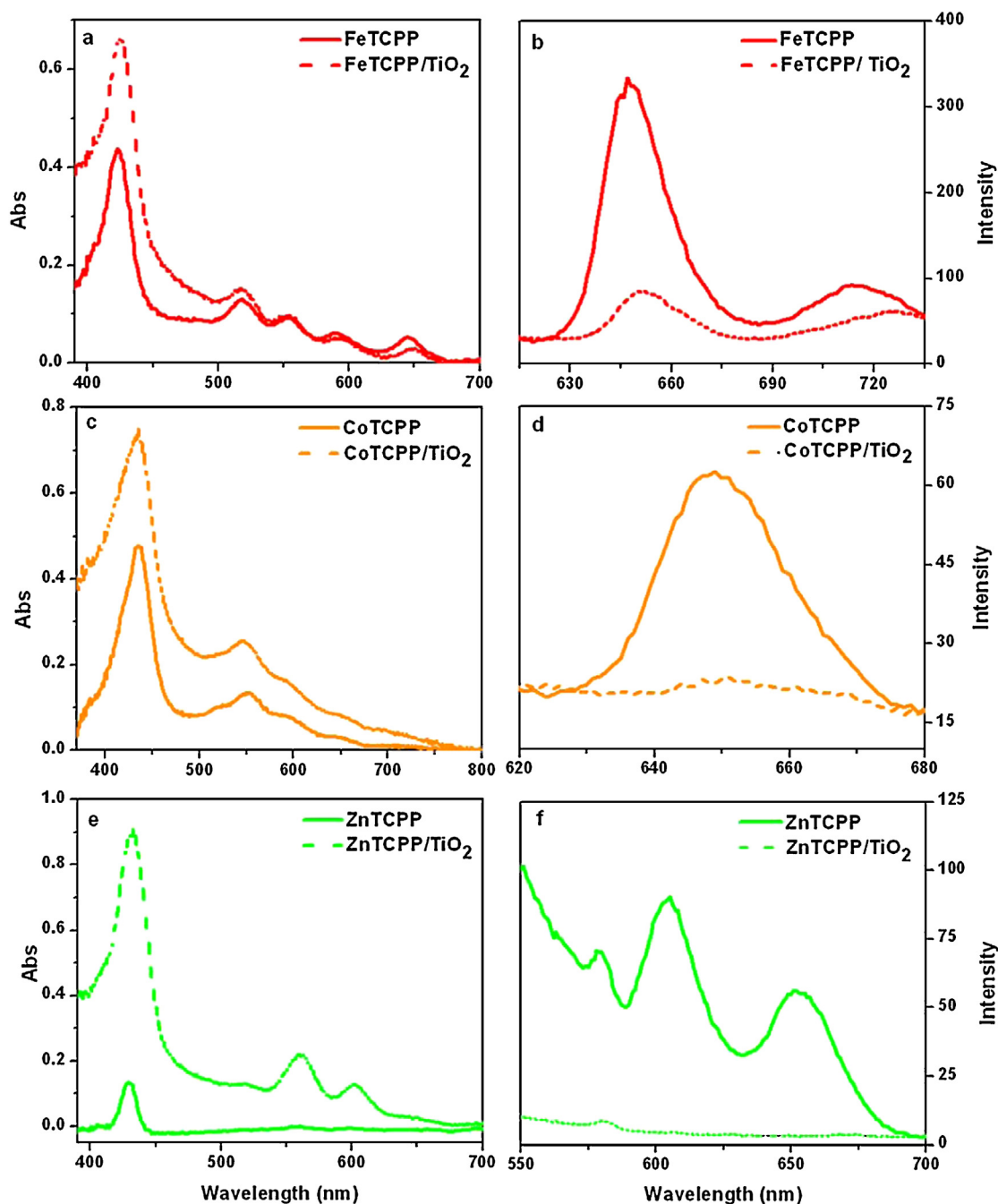


Fig. 4. UV-vis absorption (left) and fluorescence (right) spectra of MCPP adsorbed on cotton in the presence and absence of TiO_2 .

for each MTCPP, cotton samples were prepared from three different concentrations and assessed for self-cleaning performance (Supporting Information, Fig. S4). The optimized concentrations showing the highest photocatalytic efficiency for ZnTCPP, CoTCPP and FeTCPP are 20, 40 and 80 μM , respectively.

Thus, in our study, the photoactivity of MTCPP increased in the following order: ZnTCPP < CoTCPP < FeTCPP. These results indicate that the central metal of porphyrin plays an important role in determining the photocatalytic properties. In literature, several metal porphyrins in combination with TiO_2 powder have been evaluated for degradation of organic compounds [33,36,37]. The type of metal affects the photophysical properties of porphyrin by altering its π electronic structure. However, the exact role of a central metal on photocatalytic activity is still not clear. In terms of photocatalysis, FeTCPP has already been reported to show superior

activity as compared to ZnTCPP for photocatalytic degradation of atrazine [33]. Our studies show more or less similar behavior for Fe and Zn derivatives of TCPP in course of photocatalytic degradation.

3.6. Stability of MTCPP/ TiO_2 coating

Stability of the catalyst coating on textiles is an important requirement in view of its practical application. In our studies, three different catalysts have been applied: FeTCPP/ TiO_2 , CoTCPP/ TiO_2 and ZnTCPP/ TiO_2 . TiO_2 has already been reported in the literature to show strong adsorption affinity towards cotton [9]. The stability of FeTCPP, CoTCPP and ZnTCPP adsorbed on TiO_2 -coated samples was tested by washing the samples in three different media; detergent, petroleum ether and water. The change in MTCPP concentration was observed by recording UV-vis

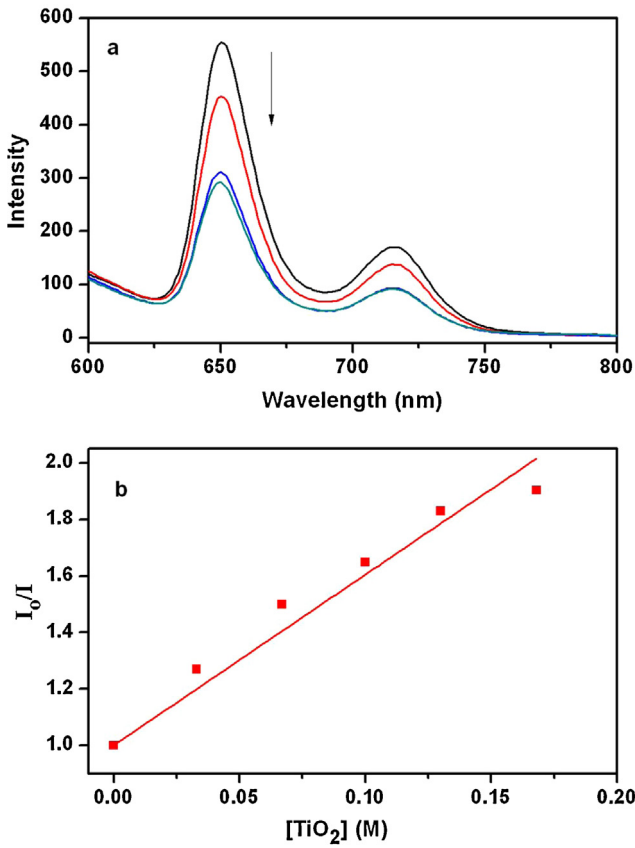


Fig. 5. (a) Steady state fluorescence quenching of FeTCPP (1×10^{-4} M) with colloidal TiO_2 in the concentration range of (0–0.16) M in water (b) Stern–Volmer plot for fluorescence quenching of FeTCPP with different concentrations of TiO_2 (0–0.16 M).

spectra before and after washing (Supporting Information, Fig. S5). Table 2 shows the retention of MTCPP on the fabric after washing. In FeTCPP, samples washed with petroleum ether showed no decrease in dye retention, whereas, samples washed with detergent and water showed 8% and 16% decrease in dye retention, respectively. Dye leaching of FeTCPP in detergent and water can be attributed to weak interactions between the dye carboxylate groups of and TiO_2 due to the change of pH and polarity of the medium.

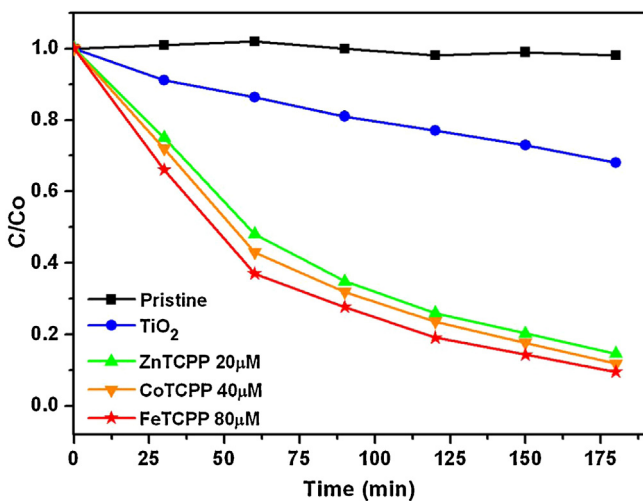


Fig. 6. Degradation of MB (10 ml, $15.6 \mu\text{M}$, pH 1) by 0.5 g of: pristine cotton, TiO_2 -coated cotton and MTCPP/ TiO_2 -coated samples with optimized concentration of $20 \mu\text{M}$ (ZnTCPP), $40 \mu\text{M}$ (CoTCPP) and $80 \mu\text{M}$ (FeTCPP) under visible-light irradiation (5.02 mW cm^{-2} irradiance) for 180 min.

Table 2
Retention of MTCPP on the fabric and the corresponding photocatalytic activity after washing with different solvents.

Washing medium	FeTCPP/ TiO_2		CoTCPP/ TiO_2		ZnTCPP/ TiO_2	
	Drop in dye retention (%)	Decrease in photoactivity (%)	Drop in dye retention (%)	Decrease in photoactivity (%)	Drop in dye retention (%)	Decrease in photoactivity (%)
Detergent	8	0	8	6	23	6
Petroleum ether	0	0	14	6	30	9
Water	16	0	2	5	29	8

Furthermore, after washing, the FeTCPP/TiO₂-coated samples were evaluated for self-cleaning performance under visible-light irradiation. Complete degradation of MB (99%) was achieved for all of the washed samples under visible-light irradiation for 180 min (Table 2). Thus the amount of FeTCPP retained on the fabric after washing was still sufficient enough to allow efficient photocatalysis. For samples coated with CoTCPP and ZnTCPP, a decrease in dye retention was observed in all of the three media with a corresponding decrease in photocatalytic activity. The highest decrease in dye retention was observed for ZnTCPP/TiO₂-coated samples. Overall, the stability of each MTCPP coating in different solvents is highly specific and depends on the nature of each metal complex.

4. Conclusions

Thin films of *meso*-tetra(4-carboxyphenyl)porphyrin with different metals ions; (MTCPP, M = Fe, Co and Zn) have successfully been formed on TiO₂-cotton fabric by a simple post-adsorption method. MTCPP/TiO₂-coated cotton fabrics have shown significant photocatalytic activity in the degradation of methylene blue under visible-light irradiation. Among the different metal complexes of TCPP, the photocatalytic activity increased in the following order: ZnTCPP < CoTCPP < FeTCPP. The highest photocatalytic efficiency has been achieved using FeTCPP/TiO₂-coated cotton. Although MTCPP leaching was observed for all coated fabrics after washing, the washed FeTCPP/TiO₂-coated fabric was able to retain its full photoactivity.

Acknowledgements

We thank the Monash Centre for Electron Microscopy (MCEM), Australia for providing assistance in FESEM measurement and Dr. S. Maniam (School of Chemistry, Monash University, Clayton Campus, Australia) for providing assistance in the synthesis of dyes. Mr. M.K. Kashif (Monash University, Clayton) is also acknowledged for providing assistance in XRD and fluorescence spectroscopy measurements.

Appendix A. Supplementary data

Supplementary data associated with this article can be found, in the online version, at <http://dx.doi.org/10.1016/j.apsusc.2013.01.141>.

References

- [1] A. Fujishima, K. Honda, *Nature* 238 (1972) 37.
- [2] T. Watanabe, K. Hashimoto, A. Fujishima, in: H. Al-Ekabi (Ed.), *Proc. 1st Int. Conf. TiO₂ Photocatalyst*, 1992.

- [3] K. Hashimoto, H. Irie, A. Fujishima, *Japanese Journal of Applied Physics Part 1: Regular Papers Brief Communications & Review Papers* 44 (2005) 8269.
- [4] A.Y. Shan, A.Y.T.I.M. Ghazi, S.A. Rashid, *Applied Catalysis A* 389 (2010) 1.
- [5] Y.J. Li, W. Chen, L.Y. Li, Y. Ma, *Science China Chemistry* 54 (2011) 9.
- [6] M.R. Dhananjeyan, E. Mielczarski, K.R. Thampi, P. Buffat, M. Bensimon, A. Kulik, J. Mielczarski, J. Kiwi, *Journal of Physical Chemistry B* 105 (2001) 12046.
- [7] L. Xiao-e, A. Green, S. Haque, A. Mills, *Journal of Photochemistry and Photobiology A* 162 (2004) 253.
- [8] W.A. Daoud, J.H. Xin, *Journal of the American Ceramic Society* 87 (2004) 953.
- [9] K. Qi, W.A. Daoud, J.H. Xin, C.L. Mak, W. Tang, W.P. Cheung, *Journal of Materials Chemistry* 16 (2006) 4567.
- [10] W.S. Tung, W.A. Daoud, *Journal of Materials Chemistry* 21 (2011) 7858.
- [11] W.A. Daoud, S.K. Leung, W.S. Tung, J.H. Xin, K. Cheuk, K. Qi, *Chemistry of Materials* 20 (2008) 1242.
- [12] K. Qi, J.H. Xin, W.A. Daoud, C.L. Mak, *International Journal of Applied Ceramic Technology* 4 (2007) 554.
- [13] M. Miyauchi, N. Akira, T. Watanabe, K. Hashimoto, *Chemistry of Materials* 14 (2002) 2812.
- [14] S. Bingham, W.A. Daoud, *Journal of Materials Chemistry* 21 (2011) 2041.
- [15] W.S. Tung, W.A. Daoud, *ACS Applied Materials & Interfaces* 1 (2009) 2453.
- [16] W.S. Tung, W.A. Daoud, *Journal of the American Ceramic Society* 19 (2012) 2330.
- [17] W. Zhao, W. Ma, C. Chen, J. Zhao, Z. Shuai, *Journal of the American Chemical Society* 126 (2004) 4782.
- [18] K. Iino, M. Kitano, M. Takeuchi, M. Matsuoka, M. Anpo, *Current Applied Physics* 6 (2006) 982.
- [19] A.F. Nogueira, L.F.O. Furtado, A.B. Formiga, M. Nakamura, K. Araki, H.E. Toma, *Inorganic Chemistry* 43 (2003) 396.
- [20] J. Kiwi, C. Pulgarin, *Catalysis Today* 151 (2010) 2.
- [21] D. Wu, M. Long, *ACS Applied Materials & Interfaces* 3 (2011) 4770.
- [22] S. Cherian, C.C. Wamser, *Journal of Physical Chemistry B* 104 (2000) 3624.
- [23] Y. Cho, W. Choi, C.H. Lee, T. Hyeon, H. Lee, *Environmental Science and Technology* 35 (2001) 966.
- [24] D.F. Watson, A. Marton, A.M. Stux, G.J. Meyer, *Journal of Physical Chemistry B* 108 (2004) 11680.
- [25] M. Gratzel, *Journal of Photochemistry and Photobiology C: Photochemistry* 4 (2003) 145.
- [26] W.M. Campbell, A.K. Burrell, D.L. Officer, K.W. Jolley, *Coordination Chemistry Reviews* 248 (2004) 1363.
- [27] H. Kurreck, M. Huber, *Angewandte Chemie (International Edition in English)* 34 (1995) 849.
- [28] D. Wöhrlé, D. Meissner, *Advanced Materials* 3 (1991) 129.
- [29] J.R. Darwent, P. Douglas, A. Harriman, G. Porter, M.C. Richoux, *Coordination Chemistry Reviews* 44 (1982) 83.
- [30] V. Balzani, A. Juris, M. Venturi, S. Campagna, S. Serroni, *Chemical Reviews* 96 (1996) 759.
- [31] T. Ma, K. Inoue, H. Noma, K. Yao, E. Abe, *Journal of Photochemistry and Photobiology A: Chemistry* 152 (2002) 207.
- [32] S. Afzal, W.A. Daoud, S.J. Langford, *Journal of Materials Chemistry* 22 (2012) 4083.
- [33] G. Granados-Oliveros, E.A. Paez-Mozo, F.M. Ortega, C. Ferronato, J.M. Chovelon, *Applied Catalysis B* 89 (2009) 448.
- [34] W.A. Daoud, J.H. Xin, Y.-H. Zhang, *Surface Science* 599 (2005) 69.
- [35] C. Wang, J. Li, G. Mele, M. Duan, X.-F. Lü, P. Leonardo, G. Vasapollo, F.-X. Zhang, *Dyes and Pigments* 84 (2010) 183.
- [36] G. Mele, D.S. Roberta, G. Vasapollo, E. García-López, L. Palmesano, M. Schiavello, *Journal of Catalysis* 217 (2003) 334.
- [37] C. Wang, J. Li, G. Mele, G.M. Yang, F.X. Zhang, L. Palmisano, G. Vasapollo, *Applied Catalysis B: Environmental* 76 (2007) 218.

Supplementary Information

Visible-light self-cleaning cotton by metalloporphyrin-sensitized photocatalysis

Shabana Afzal^a, Walid A. Daoud^{b,*}, Steven J. Langford^c

^aSchool of Applied Sciences and Engineering, Monash University, Churchill, 3842, Australia

^bSchool of Energy and Environment, City University of Hong Kong, Tat Chee Avenue, Kowloon, Hong Kong

^cSchool of Chemistry, Monash University, Clayton, 3800, Australia

*Corresponding author: School of Energy and Environment, City University of Hong Kong, Tat Chee Avenue, Kowloon, Hong Kong. Tel: + [REDACTED]; fax: + [REDACTED]

1. XRD analysis of CoTCPP/TiO₂ and ZnTCPP/TiO₂-coated cotton

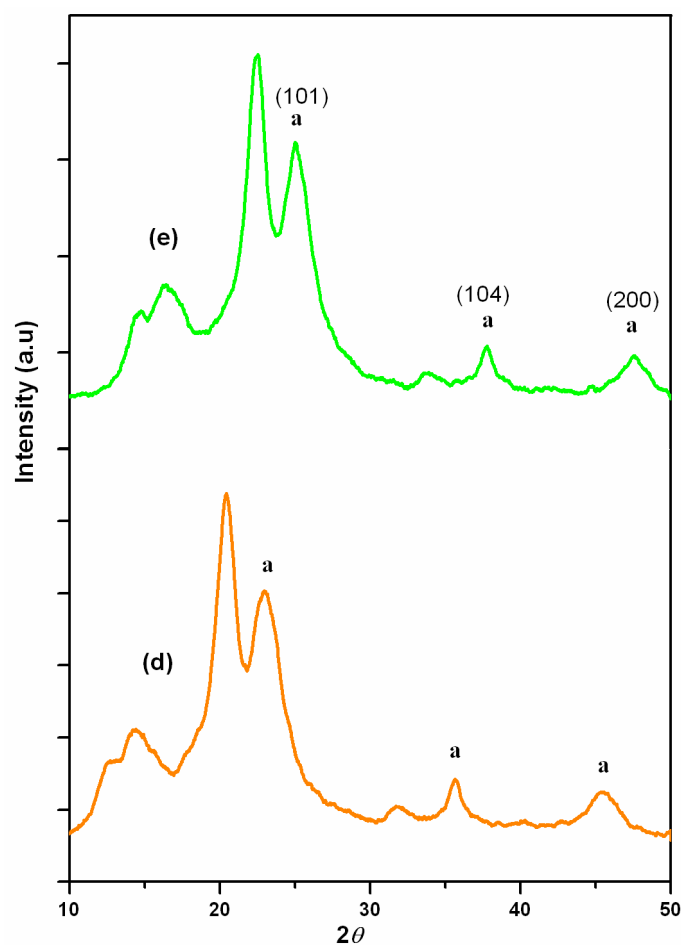


Fig. S1: XRD spectra of cotton (d) CoTCPP/TiO₂-coated, (e) ZnTCPP/TiO₂-coated (a, anatase)

2. Fluorescence quenching study of CoTCPP

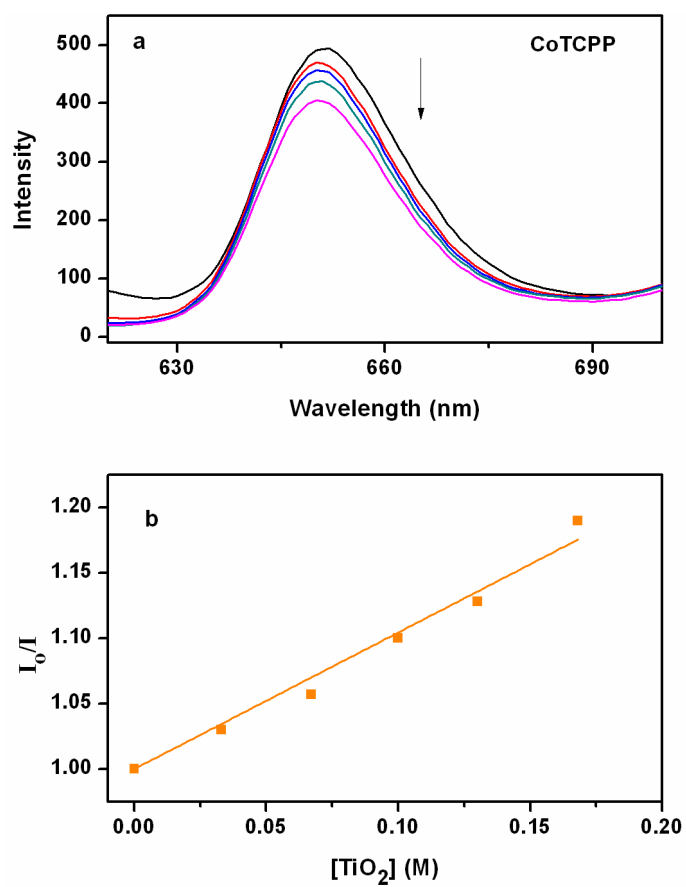


Fig. S2: (a) Steady state fluorescence quenching of CoTCPP (1×10^{-4} M) with colloidal TiO₂ in the concentration range (0-0.16 M) in water (b) Stern-Volmer plot for fluorescence quenching of FeTCPP with different concentrations (0-0.16 M) of TiO₂

3. Fluorescence quenching study of ZnTCPP

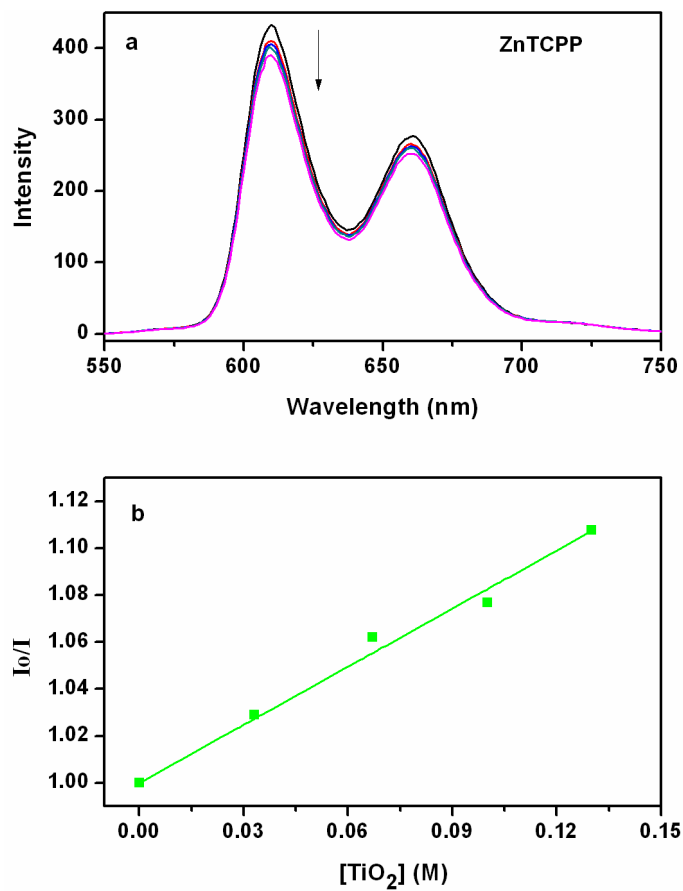


Fig. S3: (a) Steady state fluorescence quenching of ZnTCPP (1×10^{-4} M) with colloidal TiO₂ in the concentration range (0-0.16 M) in water (b) Stern-Volmer plot for fluorescence quenching of ZnTCPP with different concentrations (0-0.16 M) of TiO₂

4. Effect of concentration of MTCPP on photocatalytic degradation of MB

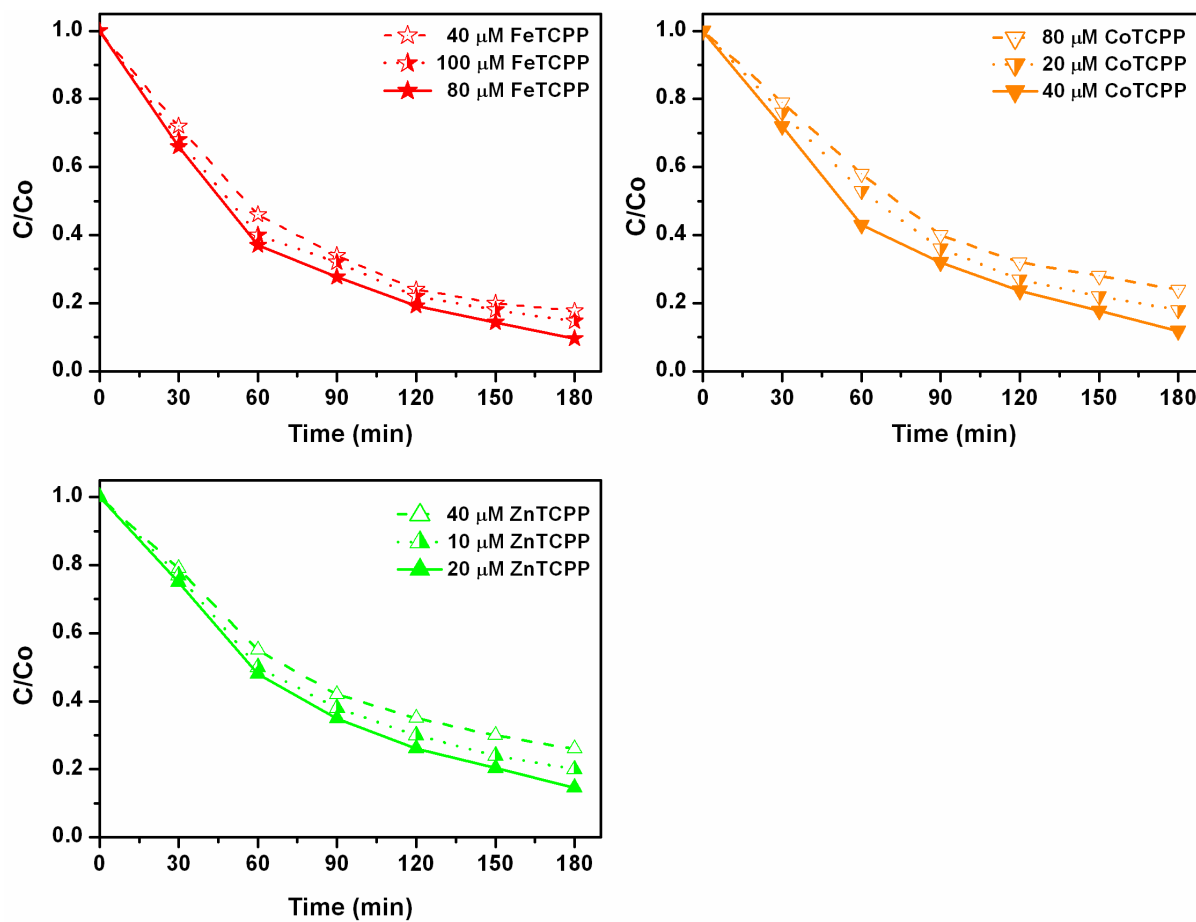


Fig. S4: Degradation of MB (10 ml, 15.6 μM , pH =1) by 0.5 g of MTCPP/TiO₂-coated cotton samples obtained from different concentrations FeTCPP, CoTCPP and ZnTCPP under visible-light irradiation (5.02 mWcm⁻² irradiance) for 180 min

5. UV-Vis data for stability evaluation of MTCPP/TiO₂ coating after:

a. Detergent washing

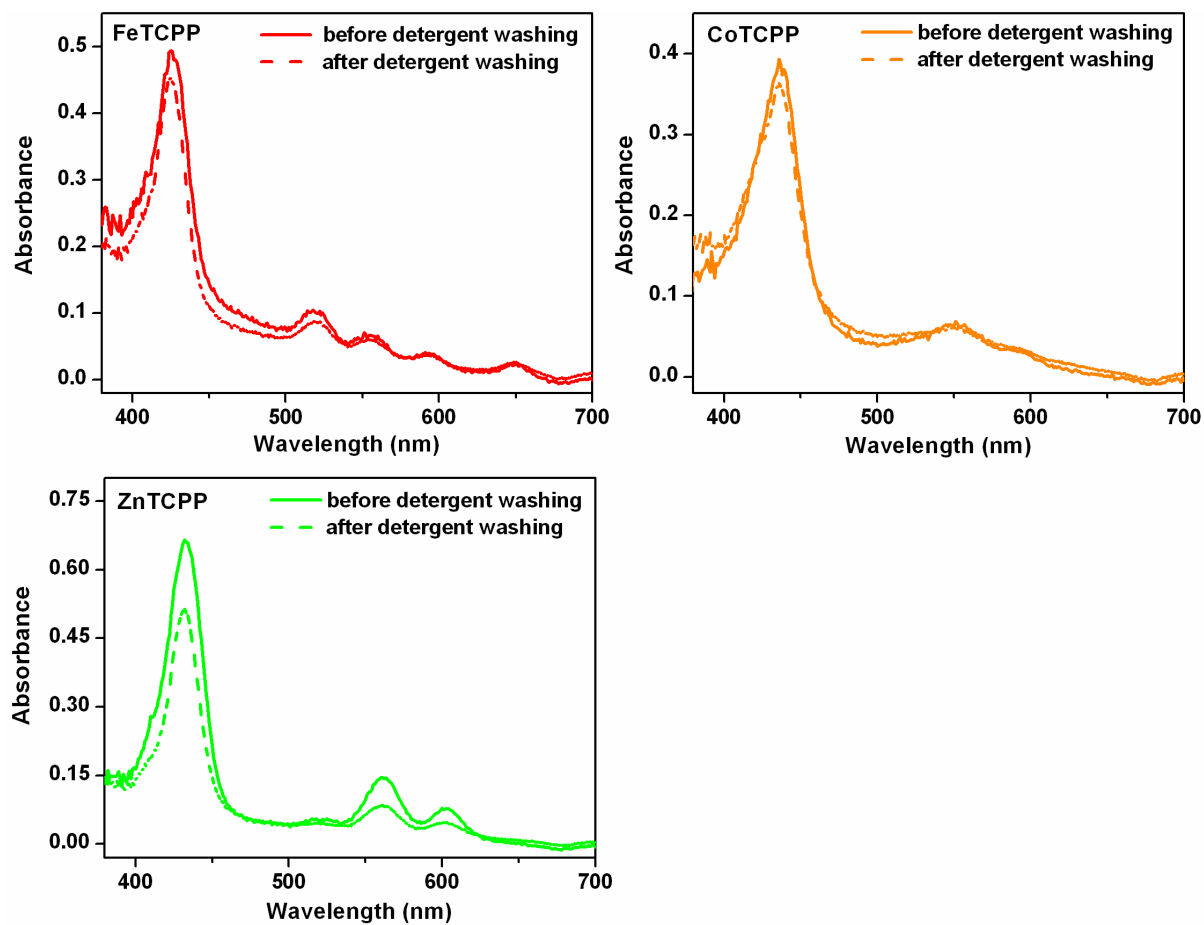


Fig. S5a: UV-Vis spectra MTCPP/TiO₂-coated cotton samples before and after washing with detergent for 45 min. M = Fe, Co, Zn

b. Petroleum ether washing

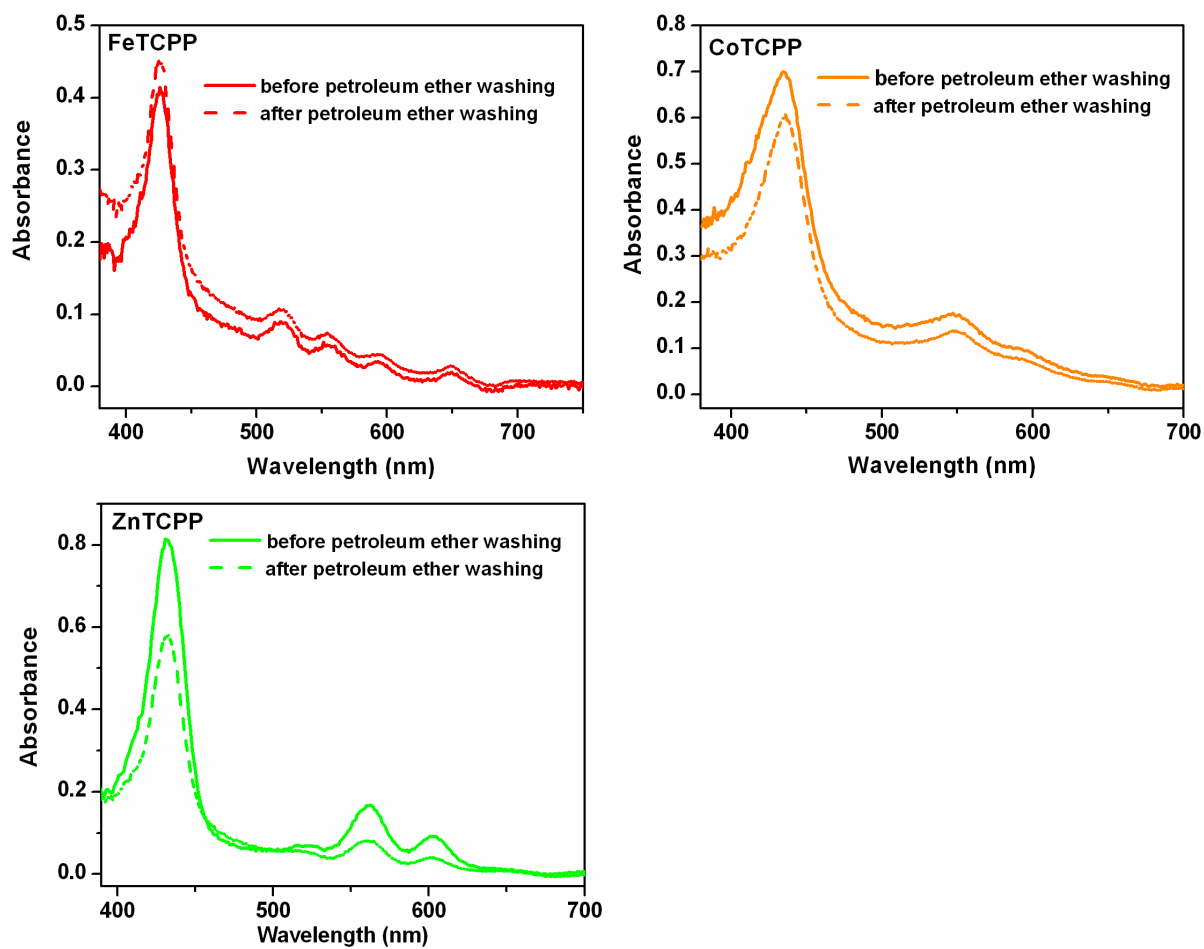


Fig. S5b: UV-Vis spectra MTCPP/TiO₂-coated cotton samples before and after washing with petroleum ether for 45 min. M = Fe, Co, Zn

c. Water washing

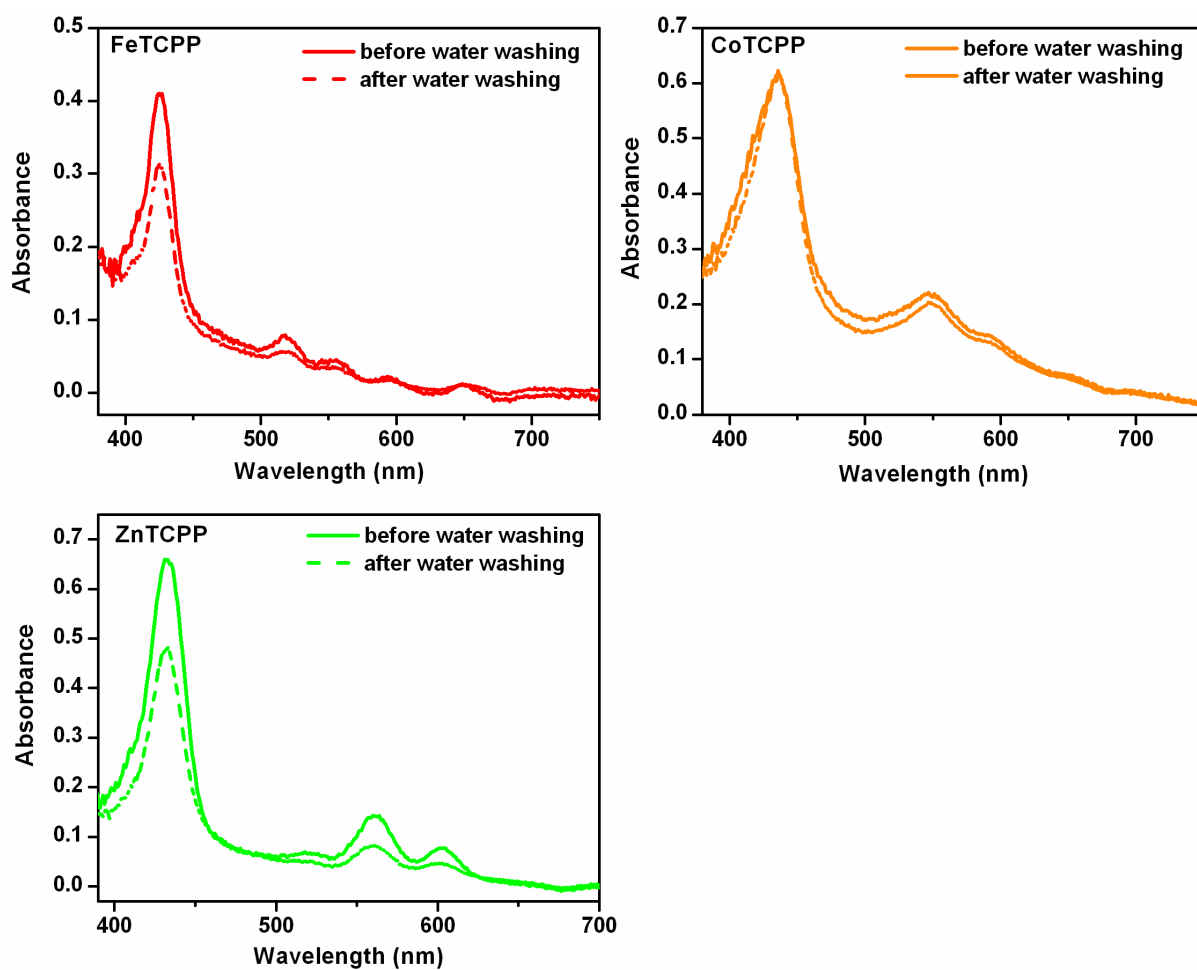


Fig. S5c: UV-Vis spectra MTCPP/TiO₂-coated cotton samples before and after washing with water for 45 min. M = Fe, Co, Zn



Declaration for Thesis Chapter 4

Declaration by candidate

In the case of Chapter 4, the nature and extent of my contribution to the work was the following:

Nature of contribution	Extent of contribution
Initiation, interpretation, experiments, data analysis and writing up	65 %

The following co-authors contributed to the work. If co-authors are students at Monash University, the extent of their contribution in percentage terms must be stated:

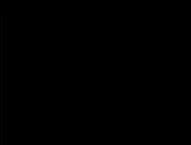
Name	Nature of contribution	Extent of contribution (%) for student co-authors only
Walid A. Daoud	Supervision, interpretation, suggestion, discussion and revision	N/A
Steven J. Langford	Supervision, interpretation, suggestion, discussion and revision	N/A

The undersigned hereby certify that the above declaration correctly reflects the nature and extent of the candidate's and co-authors' contributions to this work.

Candidate's
Signature

	Date 4/10/2013
---	-------------------

Main
Supervisor's
Signature

	Date 4/10/2013
---	-------------------

Chapter 4:

Photostable self-cleaning cotton by a copper(II) porphyrin/TiO₂ visible-light photocatalytic system

Photostable Self-Cleaning Cotton by a Copper(II) Porphyrin/TiO₂ Visible-Light Photocatalytic System

Shabana Afzal,[†] Walid A. Daoud,^{*,‡} and Steven J. Langford[§]

[†]School of Applied Sciences and Engineering, Monash University, Churchill, Victoria 3842, Australia

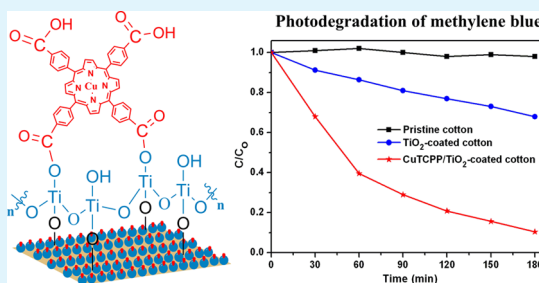
[‡]School of Energy and Environment, City University of Hong Kong, Tat Chee Avenue, Kowloon, Hong Kong

[§]School of Chemistry, Monash University, Clayton, Victoria 3800, Australia

Supporting Information

ABSTRACT: Thin films of *meso*-tetra(4-carboxyphenyl)porphyrinato copper(II) (CuTCPP) in conjunction with anatase TiO₂ have been formed on cotton fabric. Their self-cleaning properties have been investigated by conducting photocatalytic degradation of methylene blue, coffee and wine stains under visible-light irradiation. CuTCPP/TiO₂-coated cotton fabrics showed superior self-cleaning performance when compared to bare TiO₂-coated cotton. Furthermore, CuTCPP/TiO₂-coated fabrics showed significant photostability under visible-light as compared to free base TCPP/TiO₂-coated fabrics. The fabrics were characterized by FESEM, XRD and UV-vis spectroscopy. An insight into the mechanistic aspects of the CuTCPP/TiO₂ photocatalysis is also discussed. Visible-light driven self-cleaning cotton based on copper(II) porphyrin/TiO₂ catalyst exhibits significant potential in terms of stability and reproducibility for self-cleaning applications.

KEYWORDS: titania, porphyrin, visible-light, dye-sensitization, self-cleaning textiles, photocatalysis



1. INTRODUCTION

Polycrystalline semiconductor oxides exhibiting specific physiochemical and optical properties are being employed in the field of photocatalysis. In 1972, Fujishima and Honda observed the photocatalytic properties of titanium dioxide in a UV-induced water splitting experiment using TiO₂ as a photoanode.¹ Since then, TiO₂ photocatalysis has been attractive in promising applications of solar energy conversion.^{2–5} TiO₂ popularity is driven by its stability, nontoxicity, hydrophilicity, and cheap availability. Materials based on nanostructured TiO₂ have been extensively investigated in photocatalytic applications.⁶ By applying TiO₂ in the form of coatings on various substrates, the concept of self-cleaning surface has been introduced in the past decade leading to the development of self-cleaning glasses, ceramics, tents, window blinds, and lamp covers.⁷ TiO₂ can be immobilized on variety of substrates, such as glass, stainless steel, and activated carbon.⁸ As most of these immobilization techniques required high temperature processing, application of TiO₂ to substrates of low thermal resistance, such as textiles, was limited.^{9,10} However, with the development of a low-temperature sol-gol process using a nanotechnology approach, the growth of TiO₂ nanocrystals on organic fibres has been made possible in the past decade.

Anatase TiO₂-based self-cleaning textiles such as cotton, wool and polyester that show efficient photocatalytic properties under UV light have been developed.^{11–13} However, the large band gap of TiO₂ (3.2 eV for anatase) requires an excitation wavelength that falls in the UV region. Since, the solar light

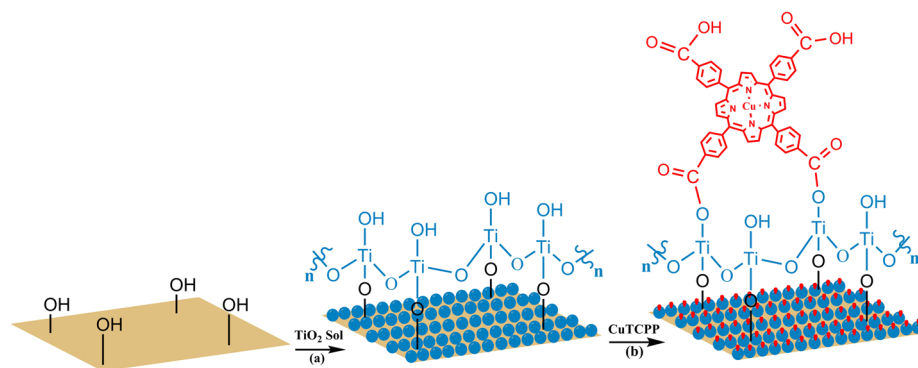
reaching the earth consists of only 5% UV and almost 43% visible light, application of UV-based TiO₂ photocatalysis is limited. To utilize the visible region of the solar spectrum for catalysis, tailoring the optical properties of titania is therefore, indispensable. In this regard, TiO₂ can be modified by many methods; such as metal doping, nonmetal doping, ion-implantation, and surface sensitization by organic dyes.^{14–18} However, very few visible-light driven self-cleaning textiles have been developed using metals and nonmetals.^{19–22}

Porphyrins are considered as efficient sensitizers to harvest light on the surface of TiO₂ because they are structural analogues of chlorophyll in plant photosynthesis.²³ Because of an extensive system of delocalized π electrons, porphyrins have very strong absorption in the visible region.^{24–26} In the photosensitization process, the sensitizer is excited over TiO₂ to appropriate singlet and triplet excited states. The excited state electrons are then injected to the conduction band of TiO₂. These electrons react with O₂ in the surrounding air to form superoxide radical anions (O₂^{•-}), which can cause oxidation of organic impurities present on the surface of the catalyst.^{27,28} Porphyrins have excellent photophysical properties such as; small singlet–triplet splitting, high quantum yield for intersystem crossing, and long triplet state lifetime.²⁹

Received: January 1, 2013

Accepted: March 6, 2013

Published: March 6, 2013

Scheme 1. Formation of Thin Films of CuTCPP on TiO₂-coated Cotton^a

^a(a) Treatment of pristine cotton with TiO₂ colloid to form TiO₂ coating on cotton. (b) Treatment of TiO₂-coated cotton with CuTCPP solution in DMF to form CuTCPP/TiO₂-coated cotton.

The photophysical properties of porphyrins can be easily tuned by metal complexation, as they can readily coordinate with metal ions in the central cavity resulting in stronger and broader photoresponse in the visible region.^{30,31} Furthermore, studies show that metal complexes of porphyrins are highly photostable, when adsorbed on the surface of TiO₂.³² Recently, we have developed self-cleaning cotton based on *meso*-tetra(4-carboxyphenyl)porphyrin (TCPP)-sensitized TiO₂ that showed superior self-cleaning properties under visible-light.³³ However, TCPP did not exhibit significant photostability for practical use. In view of self-cleaning applications envisaged, the stability of a photocatalyst is an important factor. Therefore, more photostable photocatalysts need to be explored.

Extending our research in this field, we have successfully prepared monolayers of *meso*-tetra(4-carboxyphenyl)porphyrinato copper(II) (CuTCPP) on TiO₂-coated cotton (Scheme 1) by a simple postadsorption method³³ that show excellent photocatalytic activity under visible-light irradiation as compared to bare TiO₂. Moreover, CuTCPP/TiO₂-coated cotton showed significant photostability under visible-light when compared to TCPP/TiO₂-coated cotton. We have particularly selected Cu in our study, as it has been reported to show efficient visible-light photocatalysis as compared to other metals, such as Zn, Fe, Ni and Co.^{34–39} The self-cleaning properties of our CuTCPP/TiO₂-coated system have been investigated spectrophotometrically by the photocatalytic degradation of methylene blue (MB) under visible-light irradiation as well as in more practical situations of coffee and red wine stains.

2. EXPERIMENTAL SECTION

2.1. Synthesis of CuTCPP/TiO₂-Coated Cotton. **2.1.1. Synthesis of TiO₂-Sol.** Colloidal anatase TiO₂ was prepared by adding a solution of titanium tetraisopropoxide and acetic acid dropwise to acidified water using 1.4% HNO₃. The mixture was stirred at 60 °C for 16 h.⁴⁰

2.1.2. Preparation of TiO₂-Coated Cotton. The TiO₂ sol was applied to scoured cotton fabric through a dip-pad-dry-cure process.⁴⁰ Cotton was scoured by a nonionic detergent (Kieralon F-OLB Conc) in order to remove impurities before application of TiO₂ sol. The scouring was carried at 80 °C for 30 min. The scoured cotton pieces were dipped in the TiO₂ sol for 1 min and then pressed in automatic horizontal press at 7.5 rpm with a nip pressure of 2.75 kg cm⁻². The pressed samples were then exposed to ammonia fumes until the surface pH reached 7. The neutralized samples were dried at 80 °C in a drying oven and cured at 120 °C for 3 min.

2.1.3. Synthesis of CuTCPP. Copper(II) complex of *meso*-tetra(4-carboxyphenyl)porphyrin was synthesized according to literature

methods.³⁴ CuTCPP was synthesized by refluxing 0.33 mmol of TCPP with 1.82 mmol of CuCl₂ in DMF for 2 h. CuTCPP was precipitated by adding water in excess. DMF and water were removed from the precipitates by repeated centrifugation. Solid dry samples of CuTCPP were obtained by freeze-drying.

2.1.4. Preparation of CuTCPP/TiO₂-Coated Cotton. TiO₂-coated cotton samples were dipped in a CuTCPP solution in DMF and heated at 100 °C for 5 h. The samples were then washed with DMF to remove unbound CuTCPP.

2.2. Characterization. The surface morphology of the cotton samples was studied using field emission electron microscopy (JEOL 7001F FEGSEM). The crystallinity of TiO₂ films on cotton was determined by low angle X-ray diffraction (XRD, Philip 1140 diffractometer). The UV–vis absorption spectra of TCPP and CuTCPP in DMF were recorded on Cary 5000 spectrophotometer. The UV–vis absorption spectra of pristine cotton and cotton samples coated with TCPP, CuTCPP and TiO₂ were recorded using 110 mm integrating sphere on Cary 5000 spectrophotometer. The cotton samples were masked allowing only 2 × 2 mm area to be exposed to illumination by the light source.

2.3. Photocatalytic Studies. For the assessment of self-cleaning properties, photocatalytic degradation of methylene blue (MB) was evaluated quantitatively. CuTCPP/TiO₂, TCPP/TiO₂, TiO₂ and pristine cotton pieces (0.5 g, 1.5 × 1.5 cm) were immersed in Petri dishes containing acidified MB (10 mL, 15.6 μM, pH 1). The Petri dishes were placed in a light-box and irradiated by visible-light for 3 h using a fluorescent lamp (30 W, 5.02 mW cm⁻² irradiance) containing a small UV content of 0.01 mW cm⁻² irradiance (see the Supporting Information, Figure S1). During irradiation, the Petri dishes were shaken using a benchtop shaker. Prior to irradiation, the Petri dishes were kept in the dark for 30 min in order to attain adsorption–desorption equilibrium. The change in concentration of MB was monitored by measuring UV–vis spectra at different time intervals, during the course of irradiation.

For the degradation of coffee and red wine stains, whole cotton pieces (1.5 × 1.5 cm) coated with CuTCPP/TiO₂, TCPP/TiO₂, and pristine samples were stained with coffee (0.3 g/30 mL of hot water) and red wine, followed by air drying. Each cotton piece was stained with equal volume (100 μL) of coffee and red wine. The samples, with half of the area masked, were placed in visible-light box and irradiated for 36 h using fluorescent lamp (30W, 5.02 mW cm⁻² irradiance).

2.4. Stability of Coating. The stability of CuTCPP/TiO₂-coated cotton samples was tested against detergent, petroleum ether and water, using a modified AATCC Test Method 190–2003.⁴¹ The samples were washed with each solvent for 45 min at room temperature at a constant stirring of 200 rpm, followed by rinsing with water and air drying. To determine the amount of porphyrin retained on the cotton samples, UV–vis spectra of the samples were recorded before and after washing. For the photostability tests, CuTCPP/TiO₂-coated samples were irradiated under visible-light for

30 h using a fluorescent lamp (30 W, 5.02 mW cm⁻² irradiance). UV–vis spectra of the samples were recorded before and after irradiation at different time intervals.

3. RESULTS AND DISCUSSIONS

3.1. SEM Analysis. The surface morphology of pristine cotton and cotton samples coated with TiO₂ and CuTCPP were identified from the SEM images illustrated in Figure 1.

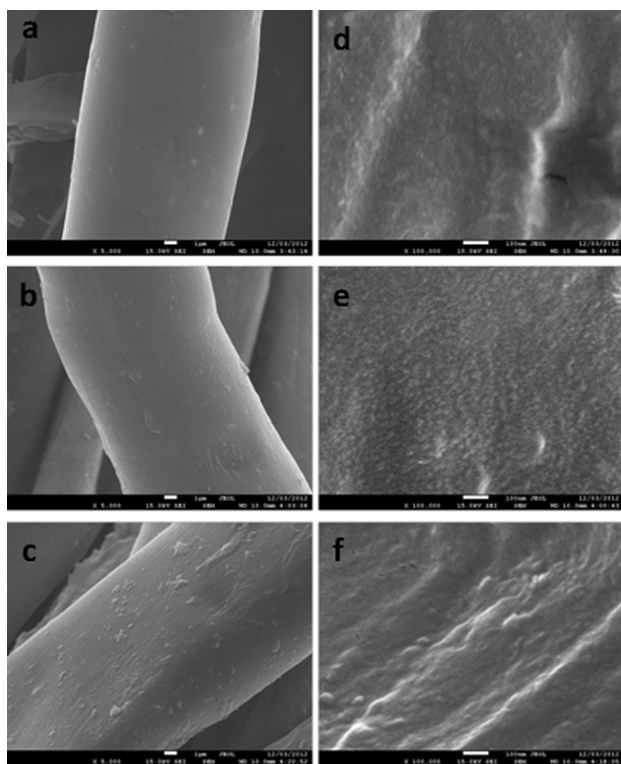


Figure 1. FESEM images of (a, d) pristine cotton, (b, e) TiO₂-coated cotton, (c, f) CuTCPP/TiO₂-coated cotton.

Low magnification images (Figure 1a, b and c) reveal no major change in surface morphology of cotton after coating with TiO₂ and CuTCPP, retaining the integrity of fibres. At higher magnification (Figure 1d–f), cotton samples coated with TiO₂ and CuTCPP appear to have rougher surface as compared to pristine cotton, presumably as a result of the coating process. Furthermore, surface aggregates can be observed in CuTCPP/TiO₂-coated sample.

3.2. XRD Analysis. To study the crystallinity of titania nanoparticles deposited on the cotton fabric, XRD analysis was performed. Anatase TiO₂ has characteristic diffraction peaks at $2\theta = 25.4, 38.0,$ and 48.0° , all of which are observed in the TiO₂-coated and CuTCPP/TiO₂-coated samples (Figure 2b and c). As expected, the pristine sample shows the absence of these peaks (Figure 2a). The presence of anatase peaks in CuTCPP/TiO₂-coated samples indicates that the TiO₂ has retained its crystallinity (and hence reactivity) after adsorption of CuTCPP.

3.3. UV–Vis Spectroscopy. Figure 3 shows the UV–vis absorption spectra of CuTCPP and TCPP adsorbed on TiO₂-coated samples. For comparison, UV–vis spectra of pristine cotton and TiO₂-coated samples were also recorded. Visible-light absorption of porphyrins between 400 to 700 nm can be easily observed for CuTCPP/TiO₂ and TCPP/TiO₂ samples

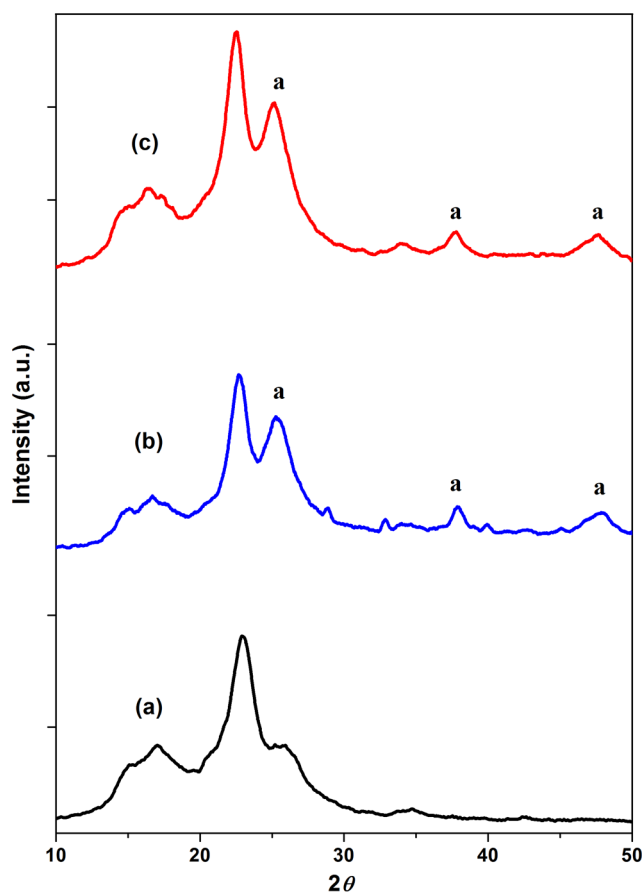


Figure 2. XRD spectra of cotton: (a) pristine, (b) TiO₂-coated, (c) CuTCPP/TiO₂-coated (a, anatase).

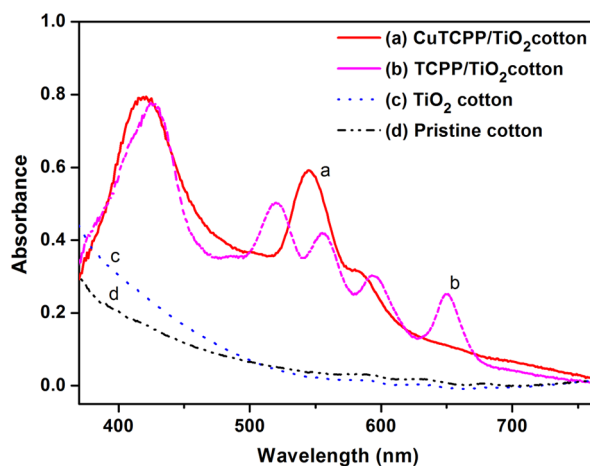


Figure 3. UV–vis spectra of (a) CuTCPP/TiO₂-coated cotton, (b) TCPP/TiO₂-coated cotton, (c) TiO₂-coated cotton, (d) pristine cotton.

(Figure 3a, b), and as expected no characteristic absorption from TiO₂-coated cotton and pristine samples was observed in this range (Figure 3c, d). The absorption spectrum of CuTCPP/TiO₂-coated cotton shows a strong peak at 419 nm identified as the porphyrin Soret band (Figure 3a). A slight red shift of 3 nm is observed for CuTCPP adsorbed on TiO₂-coated sample as compared to its absorption in DMF at 416 nm (see the Supporting Information, Figure S2). Similarly, the absorption spectrum of TCPP in DMF shows a strong peak at

418 nm for Soret band, whereas in TiO₂-coated cotton the absorption is shifted by 9 to 427 nm (see the Supporting Information, Figure S3). This red shift can be attributed to the interaction between the carboxylate groups of porphyrins and TiO₂.^{34,42}

The absorption peaks in the 500–690 nm region correspond to the Q bands of porphyrin. For TCPP, four absorption peaks of Q bands can be observed at 520, 556, 594, and 650 nm. For CuTCPP, only two Q-band absorption peaks can be observed at 545 and 583 nm. However, in the presence of DMF, some of these peaks are quenched because of interaction of porphyrins with polar solvent.⁴³ Furthermore, a significant broadening of the Soret band peaks can also be observed in the absorption spectra of CuTCPP and TCPP adsorbed on cotton as compared to the absorption spectra in DMF. The peak broadening is a usual phenomenon observed for porphyrins incorporated on solid substrates, possibly due to dye aggregation.^{44,45}

3.4. Photocatalytic Degradation of Methylene Blue (MB). Cotton samples coated with CuTCPP/TiO₂ and TCPP/TiO₂ were subjected to quantitative analysis through the photocatalytic degradation of MB under visible-light irradiation. Figure 4 shows a plot of normalized concentration of MB (C/C_0)

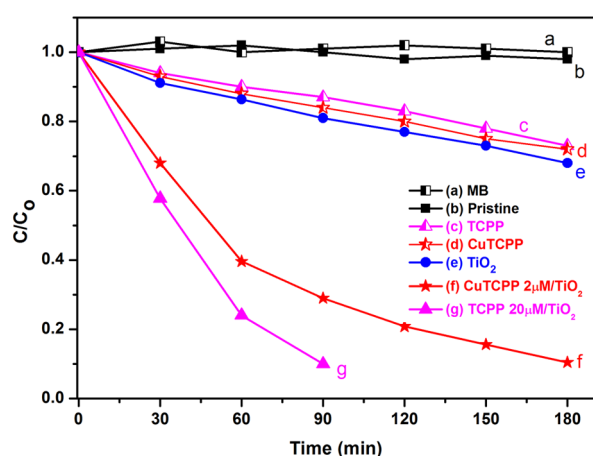


Figure 4. Degradation of MB (10 mL, 15.6 μM , pH 1) under visible-light irradiation (5.02 mW cm^{-2} irradiance) for 180 min: (a) blank MB solution, (b) pristine cotton, (c) TCPP-coated cotton, (d) CuTCPP-coated cotton, (e) TiO₂-coated cotton, (f) 2 μM CuTCPP/TiO₂-coated cotton, (g) 20 μM TCPP/TiO₂-coated cotton.

C_0) against time. The change in concentration of MB was monitored by recording the UV–vis spectra at different time intervals. For comparison, blank MB solution and pristine cotton sample were also studied. The plateaued line obtained for pristine sample and blank MB solution indicates the absence of any photocatalytic activity by cotton itself and the stability of MB at these conditions (Figure 4a, b).

TiO₂-coated sample showed a 32% degradation of MB after 180 min, whereas, the samples coated with TCPP and CuTCPP in the absence of TiO₂ also showed some photocatalytic activity with 27% and 28% degradation of MB, respectively (Figure 4c–e). Porphyrins have been reported to exhibit photocatalytic properties on their own.³¹ The samples coated with CuTCPP/TiO₂ and TCPP/TiO₂ showed a significant increase in photoactivity (Figure 4f, g). CuTCPP/TiO₂-coated samples showed almost complete degradation of MB (99%) within 180 min, whereas the TCPP/TiO₂-coated sample showed complete

degradation of MB within 90 min. Thus, the degradation rate of MB for TCPP is twice as fast as that of CuTCPP.

To achieve an efficient photocatalysis, an optimum amount of the photosensitizing dye with minimum aggregation and enhanced electron injection into TiO₂ is required.⁴⁶ Therefore, cotton samples were prepared from three different concentrations of CuTCPP (1, 2, and 3 μM) and assessed for self-cleaning performance (see the Supporting Information, Figure S4). The optimized concentration showing the highest photocatalytic efficiency for CuTCPP is 2 μM . For TCPP, the optimized concentration was 20 μM , established from our previous work illustrating a compromise between amount of material and activity.³³

3.5. Photocatalytic Degradation of Coffee and Red Wine Stains. The self-cleaning property of CuTCPP/TiO₂-coated samples was assessed qualitatively by performing the coffee and red wine stains bleaching tests. For comparison TCPP/TiO₂, TiO₂ and pristine samples were used. Figure 5 shows the degradation of coffee and wine stains on cotton samples under visible light irradiation at different time intervals. Only half the area of each cotton fabric square was irradiated,

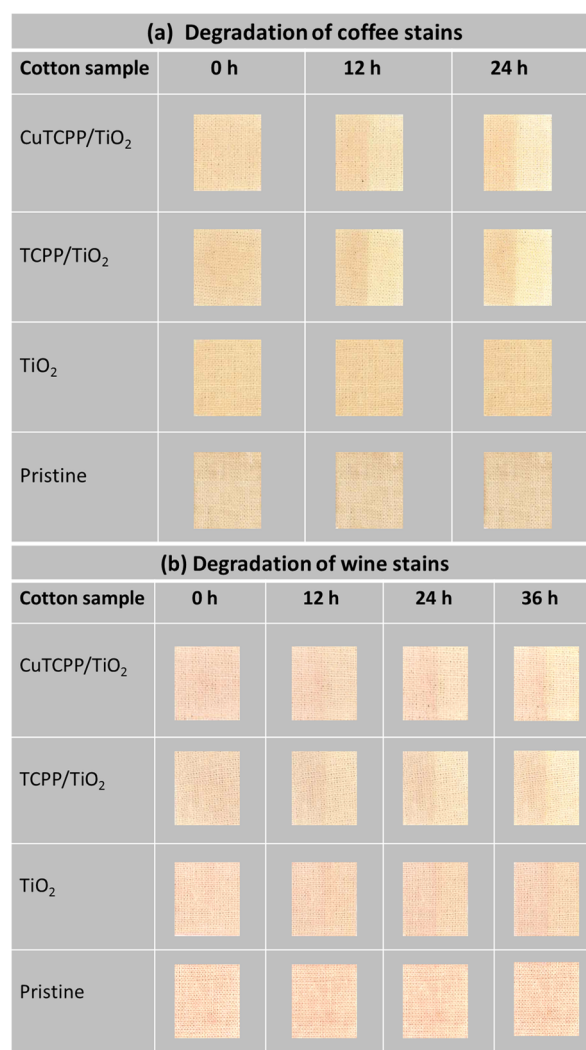


Figure 5. Photocatalytic degradation of (a) coffee stains, (b) red wine stains, by CuTCPP/TiO₂, TCPP/TiO₂, TiO₂, and pristine cotton samples at 0, 12, and 24 h of visible-light irradiation (5.02 mW cm^{-2} irradiance).

whereas the other half was masked receiving no light. Significant discolouration of coffee stains was observed for TCPP and CuTCPP samples after 24 h of irradiation (Figure 5a). However, the degradation rate of TCPP appears faster compared to that of CuTCPP. Similarly, the same trend is observed for the degradation of wine stains over 36 h of irradiation (Figure 5b).

3.6. Photostability of CuTCPP/TiO₂ Catalyst. Photostability of the catalyst under excitation is an important requirement of reusability and practical application. Therefore, a photostability study of CuTCPP/TiO₂-coated samples was conducted against the well-performing TCPP. CuTCPP/TiO₂-coated sample was irradiated in visible-light for 30 h. The change in concentration of CuTCPP was measured by recording the UV-vis spectra of cotton samples before and after irradiation (Figure 6a). A slight degradation of 5% was

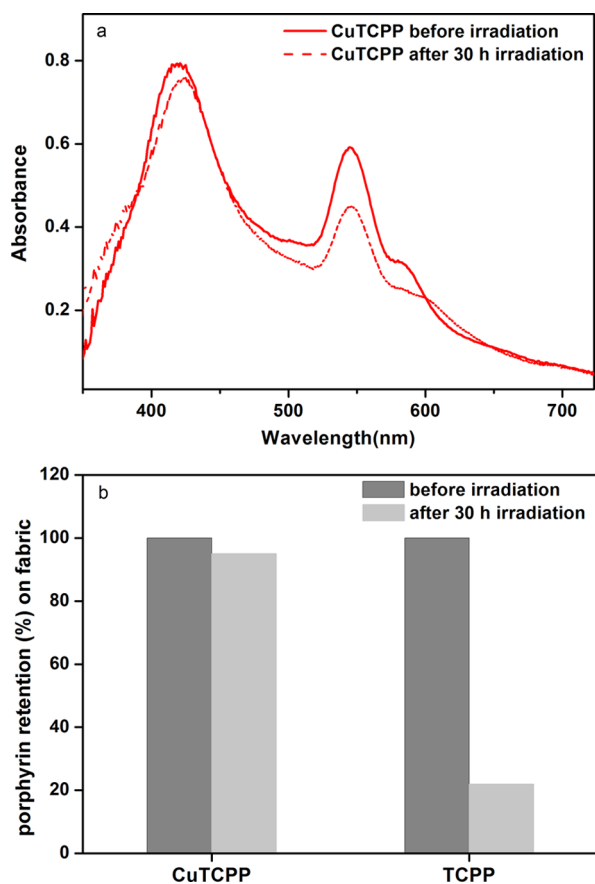


Figure 6. (a) UV-vis spectra of CuTCPP/TiO₂-coated cotton fabrics before and after 30 h irradiation. (b) Percentage retention of CuTCPP and TCPP on TiO₂-coated cotton fabrics after irradiation under visible light for 30 h.

observed for CuTCPP within the first 12 h (see the Supporting Information, Figure S5). In the following 18 h, there was no further degradation of CuTCPP, shown in the UV-vis data. The absorption peak at 419 nm (Soret band) was used as a reference to monitor the change in concentration of CuTCPP. Figure 6b shows the concentration of CuTCPP and TCPP retained on the fabric after 30 h of irradiation. Thus, CuTCPP showed significant photostability with only 5% degradation as compared to the TCPP with 78% degradation under visible-light irradiation, established from previous results.³³ Furthermore, the irradiated CuTCPP/TiO₂-coated sample was

assessed for self-cleaning performance. A reproducible degradation (99%) of MB was observed for the sample with 95% CuTCPP retention.

3.7. Stability of CuTCPP/TiO₂-Coating. TiO₂ has already been reported in literature to show strong affinity toward cotton.⁴⁰ The stability of CuTCPP adsorbed on TiO₂-coated sample was tested by washing the samples in three different media; detergent, petroleum ether and water (Figure 7). The

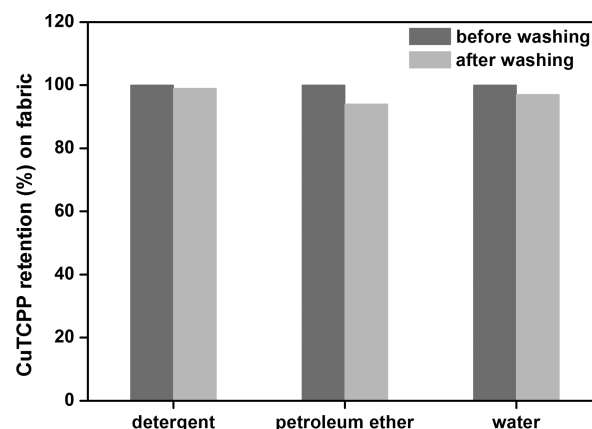


Figure 7. Percentage retention of CuTCPP on cotton fabrics after washing with detergent, petroleum ether, and water.

change in CuTCPP concentration was observed by recording the UV-vis spectra before and after washing (Supporting Information, Figure S6). All the samples washed in different solvents showed over 90% CuTCPP retention on the fabric. However, the highest dye leaching was observed for CuTCPP washed with petroleum ether, which could be due the weak interactions between carboxylate groups of dye and TiO₂, affected by the change in the polarity of medium.

CuTCPP samples washed with different solvents were also analyzed for self-cleaning performance. All the washed samples showed reproducible degradation (99%) of MB in 180 min under visible-light irradiation. Thus, no change in photocatalytic activity was observed even after washing. In spite of the slight dye leaching in petroleum ether, the dye concentration retained on the fabric was sufficient enough to allow photocatalysis at the same rate as that of prewashed original CuTCPP samples.

3.8. Mechanistic Aspects. The mechanism of TiO₂ sensitization by dyes in visible-light, generally involves the transition of electron from the ground state of porphyrin dye [Pp] to the excited singlet state ¹[Pp]*.⁴⁷ Relaxation of the singlet excited state generates the triplet excited state ³[Pp]* through a process of intersystem crossing. Electrons from ¹[Pp]* and ³[Pp]* excited states can be transferred to conduction band of TiO₂, which can be trapped further by the adsorbed O₂, resulting in formation of O₂^{•-} causing degradation of MB present on the surface of TiO₂ (Figure 8).

Free-base porphyrins such as TCPP with no unpaired electrons manifest long lifetime of excited state and are strongly fluorescent,⁴⁸ resulting in efficient electron injection in conduction band of TiO₂, confirmed by our previous findings.³³ In contrast, metal porphyrins with unpaired electrons in *d* orbital such as Cu(II)TCPP exhibit short lifetime of excited state, as no fluorescence emission has been detected for copper porphyrins in solution,⁴⁵ resulting in poor electron injection into TiO₂. This can be accounted for the slower degradation

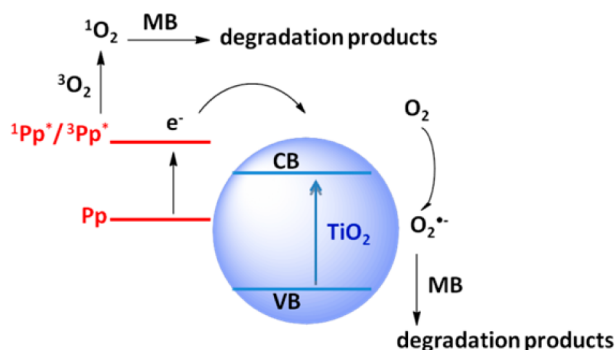


Figure 8. Proposed photocatalytic mechanism.

rate of MB in CuTCPP as compared to TCPP. Furthermore, formation of singlet oxygen ($^1\text{O}_2$) from $^3[\text{Pp}]^*$ excited state of the sensitizer dye is also reported, which can cause oxidation of MB as well.⁴⁹ This is confirmed by our findings, as some photocatalytic activity is also observed for CuTCPP and TCPP cotton samples in the absence of TiO_2 . Thus, overall, a co-operative mechanism is proposed for the degradation of MB involving both components of photocatalytic system.

The enhanced photostability of Cu(II)TCPP as compared to TCPP might be related to the paramagnetic nature of Cu in Cu(II)TCPP, which favors deactivation of its excited state, resulting in more recombination with no fluorescence emission and thus making Cu(II)TCPP less susceptible to photo-bleach.⁵⁰

4. CONCLUSIONS

Visible-light active self-cleaning cotton has successfully been developed using copper(II) porphyrin and anatase titania. CuTCPP/ TiO_2 -coated cotton has shown considerable photo-activity in the degradation of methylene blue, coffee and red wine stains. In addition, CuTCPP exhibits significant photostability as compared to TCPP. The enhanced photostability of CuTCPP shows potential in view of reproducibility and practical application of self-cleaning textiles.

■ ASSOCIATED CONTENT

Supporting Information

Results of UV-vis spectroscopy for analysis of effect of concentration of dye on photocatalysis, analysis of photostability of catalyst and stability of coating. This material is available free of charge via the Internet at <http://pubs.acs.org/>.

■ AUTHOR INFORMATION

Corresponding Author

*E-mail: [REDACTED] Phone: + [REDACTED]
Fax: + [REDACTED]

Notes

The authors declare no competing financial interest.

■ ACKNOWLEDGMENTS

We thank the Monash Centre for Electron Microscopy (MCEM), Australia for providing assistance in FESEM measurement and Dr. S. Maniam for providing assistance in the synthesis of dyes. Mr. M. K. Kashif (Monash University, Clayton) is also acknowledged for providing assistance in XRD and fluorescence spectroscopy measurements.

■ REFERENCES

- (1) Fujishima, A.; Honda, K. *Nature* **1972**, *238*, 37–38.
- (2) Yu, J. G.; Su, Y. R.; Cheng, B. *Adv. Funct. Mater.* **2007**, *17*, 1984–1990.
- (3) Friedmann, D.; Mendive, C.; Bahnemann, D. *Appl. Catal. B: Environ.* **2010**, *99*, 398–406.
- (4) Liu, G.; Wang, L.; Yang, H. G.; Cheng, H.-M.; Lu, G. Q. *J. Mater. Chem.* **2010**, *20*, 831–843.
- (5) Galindo, C.; Jacques, P.; Kalt, A. J. *Photochem. Photobiol. A: Chem.* **2000**, *130*, 35–47.
- (6) Fujishima, A.; Zhang, X.; Tryk, D. A. *Surf. Sci. Rep.* **2008**, *63*, 515–582.
- (7) Hashimoto, K.; Irie, H.; Fujishima, A. *Jpn. J. Appl. Phys.* **2005**, *44*, 8269–8285.
- (8) Shan, A. Y.; Ghazi, T. I. M.; Rashid, S. A. *Appl. Catal. A* **2010**, *389*, 1–8.
- (9) Xiao-e, L.; Green, A. N. M.; Haque, S. A.; Mills, A.; Durrant, J. R. *J. Photochem. Photobiol. A: Chem.* **2004**, *162*, 253–259.
- (10) Dhananjeyan, M. R.; Mielczarski, E.; Thampi, K. R.; Buffat, P.; Bensimon, M.; Kulik, A.; Mielczarski, J.; Kiwi, J. J. *Phys. Chem. B* **2001**, *105*, 12046–12055.
- (11) Daoud, W. A.; Xin, J. H. *J. Am. Ceram. Soc.* **2004**, *87*, 953–955.
- (12) Daoud, W. A.; Leung, S. K.; Tung, W. S.; Xin, J. H.; Cheuck, K.; Qi, K. *Chem. Mater.* **2008**, *20*, 1242–1244.
- (13) Qi, K.; Xin, J. H.; Daoud, W. A.; Mak, C. L. *Int. J. Appl. Ceram. Technol.* **2007**, *4*, 554–563.
- (14) Bingham, S.; Daoud, W. A. *J. Mater. Chem.* **2010**, *21*, 2041–2050.
- (15) Nogueira, A. F.; Furtado, L. F. O.; Formiga, A. L. B.; Nakamura, M.; Araki, K.; Toma, H. E. *Inorg. Chem.* **2003**, *43*, 396–398.
- (16) Tung, W. S.; Daoud, W. A. *ACS Appl. Mater. Interfaces* **2009**, *1*, 2453–2461.
- (17) Kumar, S. G.; Devi, L. G. *J. Phys. Chem. A* **2011**, *115*, 13211–13241.
- (18) Lino, K.; Kitano, M.; Takeuchi, M.; Matuoka, M.; Apno, M. *Curr. Appl. Phys.* **2006**, *6*, 982–986.
- (19) Kiwi, J.; Pulgarin, C. *Catal. Today* **2010**, *151*, 2–7.
- (20) Wu, D.; Long, M. *ACS Appl. Mater. Interfaces* **2011**, *3*, 4770–4774.
- (21) Wang, R.; Wang, X.; Xin, J. H. *ACS Appl. Mater. Interfaces* **2009**, *2*, 82–85.
- (22) Qi, K.; Fei, B.; Xin, J. H. *Thin Solid Films* **2011**, *519*, 2438–2444.
- (23) Cho, Y.; Choi, W.; Lee, C.-H.; Hyeon, T.; Lee, H.-I. *Environ. Sci. Technol.* **2001**, *35*, 966–970.
- (24) Campbell, W. M.; Burell, A. K.; Officer, D. L.; Jolley, K. W. *Coord. Chem. Rev.* **2004**, *248*, 1363–1379.
- (25) Kurreck, H.; Huber, M. *Angew. Chem., Int. Ed.* **1995**, *34*, 849–866.
- (26) Wöhrle, D.; Meissner, D. *Adv. Mater.* **1991**, *3*, 129–138.
- (27) Watson, D. F.; Marton, A.; Stux, A. M.; Meyer, G. J. *J. Phys. Chem. B* **2004**, *108*, 11680–11688.
- (28) Gratzel, M. J. *Photochem. Photobiol. C: Photochem. Rev.* **2003**, *4*, 145–153.
- (29) Kim, W.; Park, J.; Jo, H. J.; Kim, H.-J.; Choi, W. *J. Phys. Chem. C* **2007**, *112*, 491–499.
- (30) Balzani, V.; Juris, A.; Venturi, M.; Campagna, S.; Serroni, S. *Chem. Rev.* **1996**, *96*, 759–834.
- (31) Shiragmi, T.; Matsumoto, J.; Inuo, H.; Yasuda, M. *J. Photochem. Photobiol. C: Photochem. Rev.* **2005**, *6*, 227–248.
- (32) Mele, G.; Del-Sole, R.; Vasapollo, G.; Garcia-Lopez, E.; Palmisano, L.; Jun, L.; Slota, R.; Dyrda, G. *Res. Chem. Intermed.* **2007**, *33*, 433–448.
- (33) Afzal, S.; Daoud, W. A.; Langford, S. J. *J. Mater. Chem.* **2012**, *22*, 4083–4088.
- (34) Granados-Oliveros, G.; Paez-Mozo, E. A.; Ortega, F. M.; Ferronato, C.; Chovelon, J.-M. *Appl. Catal. B: Environ.* **2009**, *89*, 448–454.

- (35) Sun, W.-j.; Li, J.; Yao, G.-p.; Jiang, M.; Zhang, F.-x. *Catal. Commun.* **2011**, *16*, 90–93.
- (36) Luo, Y.; Li, J.; Yao, G.-p.; Zhang, F.-x. *Catal. Sci. Technol.* **2012**, *2*, 841–846.
- (37) Sun, W.-j.; Li, J.; Yao, G.-p.; Zhang, F.-x.; Wang, J.-L. *Appl. Surf. Sci.* **2011**, *258*, 940–945.
- (38) Tasseroul, L.; Pirard, S. L.; Lambert, S. D.; Paez, C. A.; Poelman, D.; Pirard, J.-P.; Heinrichs, B. *Chem. Eng. J.* **2012**, *191*, 441–450.
- (39) Granados-Oliveros, G.; Paez-Mozo, E. A.; Ortega, F. M.; Piccinato, M.; Silva, F. N.; Guedes, C. L. B.; Maruro, E. D.; Costa, M. F. D.; Ota, A. T. *J. Mol. Catal. A: Chem.* **2011**, *339*, 79–85.
- (40) Qi, K.; Daoud, W. A.; Xin, J. H.; Mak, C. L.; Tang, W.; Cheung, W. P. *J. Mater. Chem.* **2006**, *16*, 4567–4574.
- (41) AATCC *Technical Manual*; American Association of Textile Chemists and Colorists: Research Triangle Park, NC, 2006, pp 358–360.
- (42) Ma, T.; Inoue, K.; Noma, H.; Yao, K.; Abe, E. *J. Photochem. Photobiol. A: Chem.* **2002**, *152*, 207–212.
- (43) Makarska, M.; Radzki, St.; Legendziewicz, J. *J. Alloys Compd.* **2002**, *341*, 233–238.
- (44) Castellero, P.; Sanchez-Valencia, J. R.; Cano, M.; Pedrosa, J. M.; Roales, J.; Barranco, A.; Gonzalez-Elipse, A. R. *ACS Appl. Mater. Interfaces* **2010**, *2*, 712–721.
- (45) Bazzan, G.; Smith, W.; Francesconi, L. C.; Drain, C. M. *Langmuir* **2008**, *24*, 3244–3249.
- (46) Wang, C.; Li, J.; Mele, G.; Duan, M.-y.; Lu, X.-f.; Palmisano, L.; Vasapollo, G.; Zhang, F.-X. *Dyes Pigm.* **2010**, *84*, 183–189.
- (47) Wang, C.; Li, J.; Mele, G.; Yang, G.-M.; Zhang, F.-X.; Palmisano, L.; Vasapollo, G. *Appl. Catal. B: Environ.* **2007**, *76*, 218–226.
- (48) Szintay, G.; Horvath, A. *Inorg. Chim. Acta* **2001**, *324*, 278–285.
- (49) Mele, G.; Garcia-Lopez, E.; Palmisano, L.; Dyrda, G.; Slota, R. *J. Phys. Chem. C* **2007**, *111*, 6581–6588.
- (50) Gerola, A. P.; Santana, A.; Franca, P. B.; Tsubone, T. M.; Oliveira, H.; Caetano, W.; Kimura, E.; Hioka, N. *Photochem. Photobiol.* **2011**, *87*, 884–894.

Supporting Information

Photostable self-cleaning cotton by a copper (II) porphyrin /TiO₂ visible-light photocatalytic system

Shabana Afzal[†], Walid A. Daoud^{*‡} and Steven J. Langford[‡]

[†] School of Applied Sciences and Engineering, Monash University, Churchill, Victoria 3842, Australia.

[‡] School of Energy and Environment, City University of Hong Kong, Tat Chee Avenue, Kowloon, Hong Kong.

[‡] School of Chemistry, Monash University, Clayton, Victoria 3800, Australia.

1. Spectrum of fluorescent lamp used in the photodegradation experiments

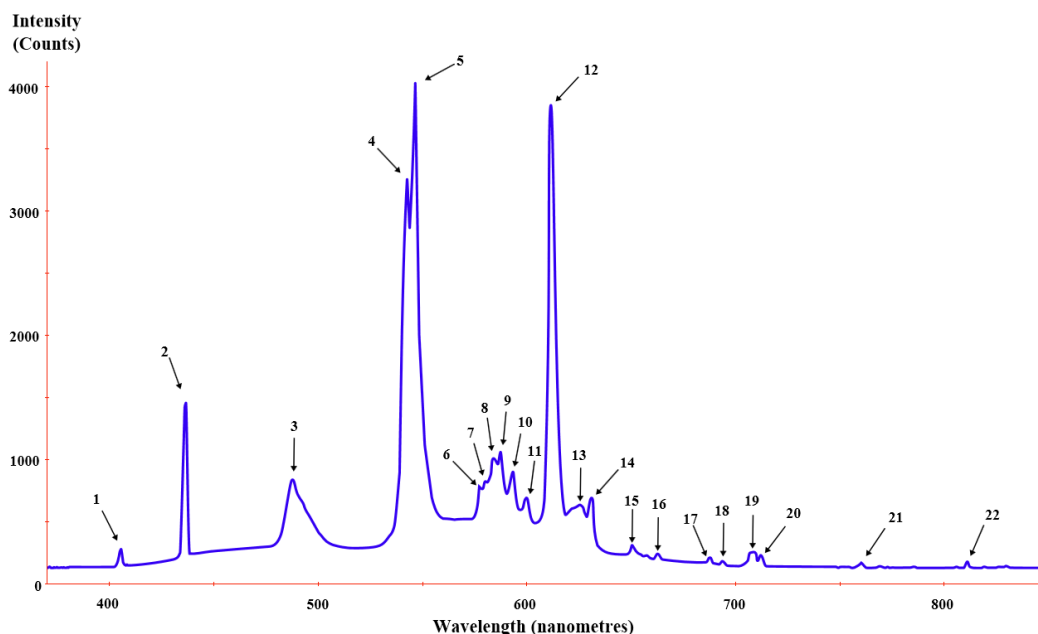


Fig. S1: Spectrum of a typical fluorescent lamp (Source:

http://en.wikipedia.org/wiki/File:Fluorescent_lighting_spectrum_peaks_labelled.svg)

2. UV-Vis absorption spectra of CuTCPP

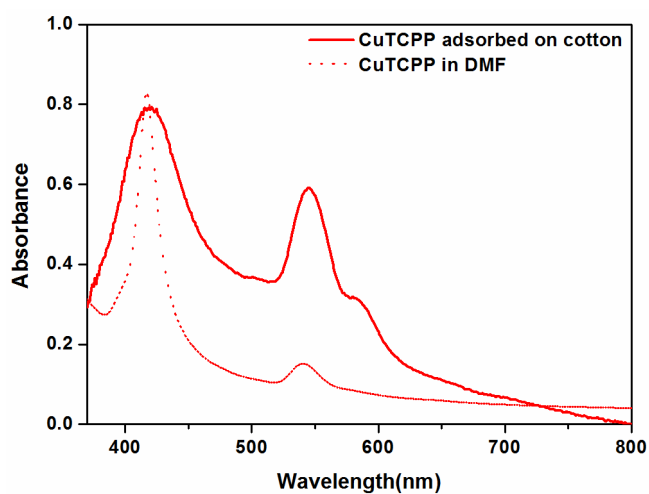


Fig. S2: UV-Vis spectra of CuTCPP in DMF and CuTCPP adsorbed on TiO₂-coated cotton

3. UV-Vis absorption spectra of TCP

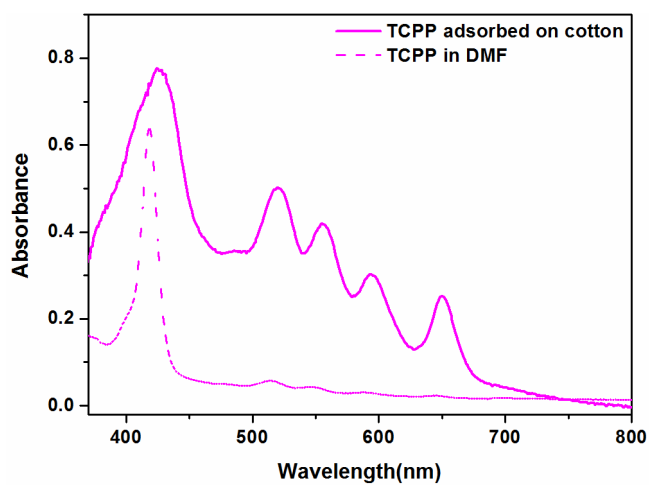


Fig. S3: UV-Vis spectra of TCP in DMF and TCP adsorbed on TiO₂-coated cotton

4. Effect of concentration of CuTCPP on photocatalytic degradation of MB

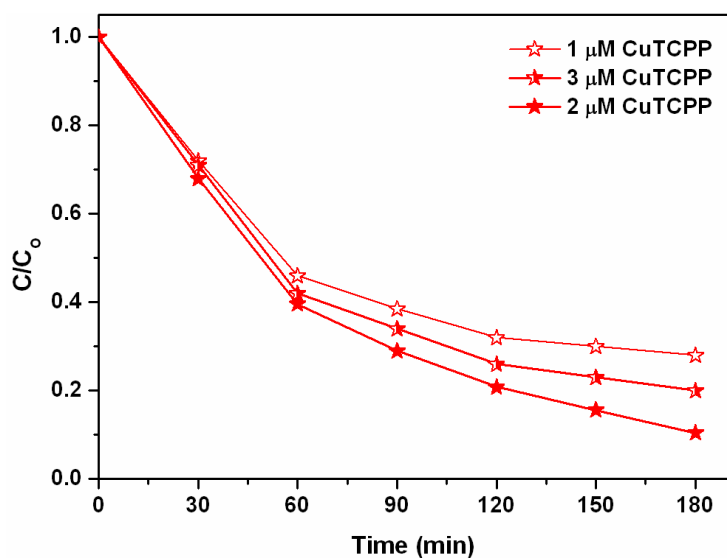


Fig. S4: Degradation of MB (10 ml, 15.6 μM , pH = 1) by 0.5 g of: CuTCPP/TiO₂-coated cotton (CuTCPP = 1, 2 and 3 μM) under visible-light irradiation (5.02 mWcm^{-2} irradiance) for 180 min

5. UV-Vis spectroscopy for photostability evaluation of CuTCPP/TiO₂ catalyst

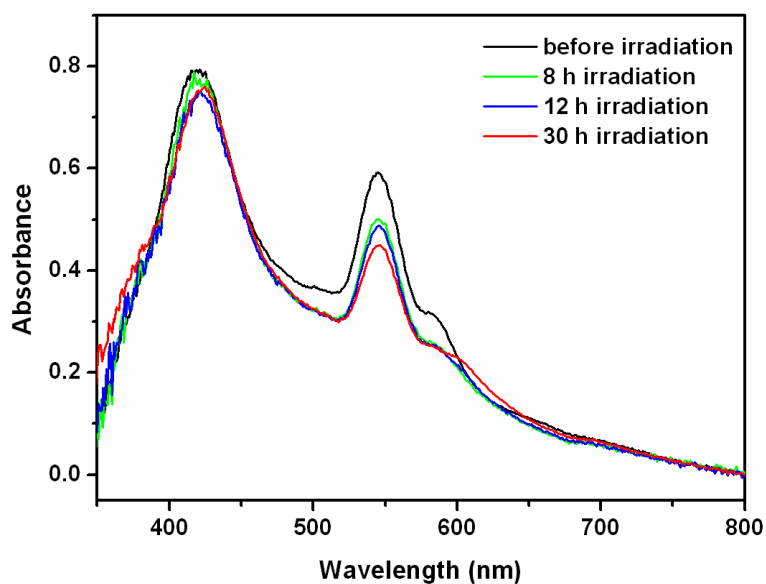


Fig. S5: UV-Vis spectra of CuTCPP/TiO₂-coated cotton before and after light irradiation at different time intervals

6. UV-Vis spectroscopy for stability evaluation of CuTCPP/TiO₂ coating after washing with different solvents

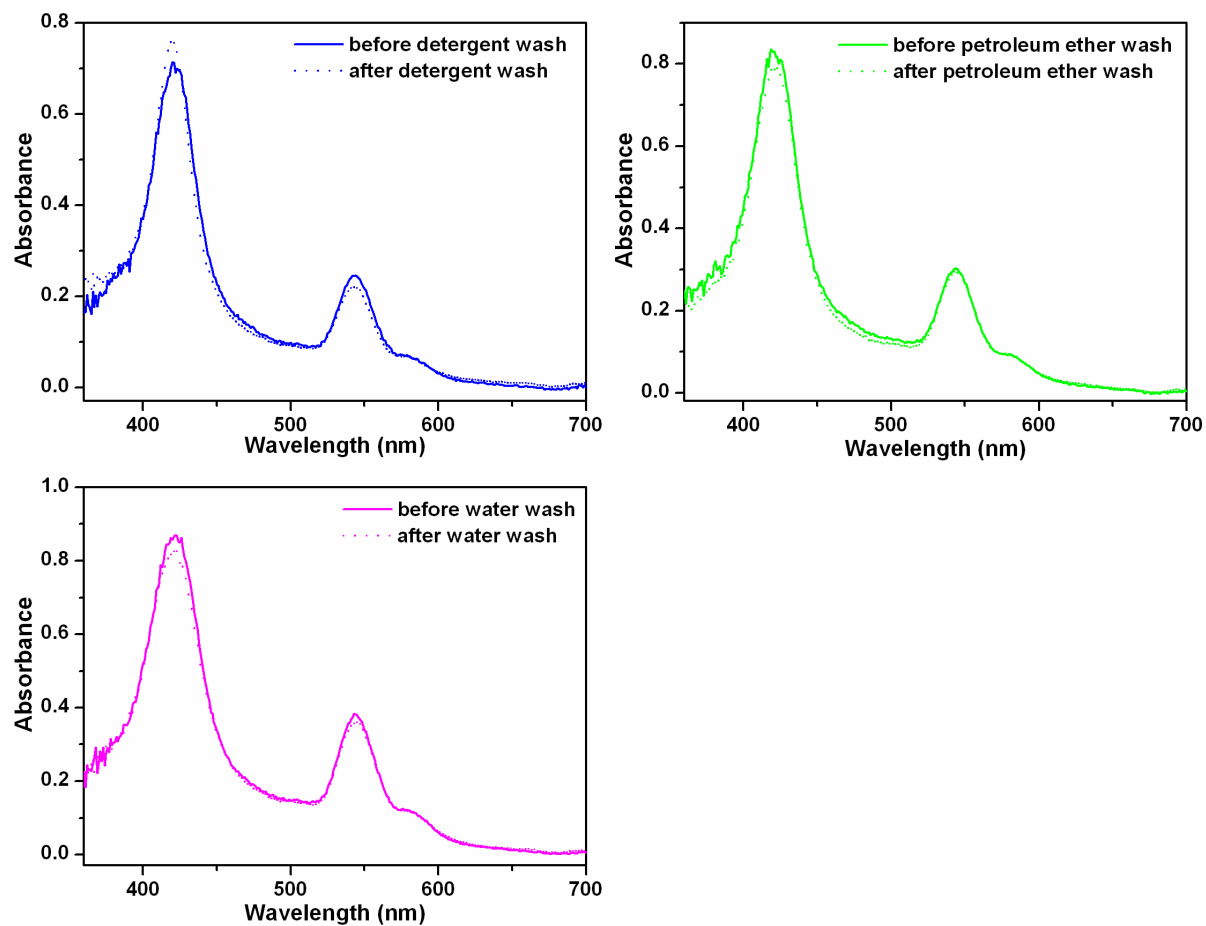


Fig. S6: UV-Vis spectra CuTCPP/TiO₂-coated cotton before and after washing with detergent, petroleum ether and water for 45 min



Declaration for Thesis Chapter 5

Declaration by candidate

In the case of Chapter 5, the nature and extent of my contribution to the work was the following:

Nature of contribution	Extent of contribution
Initiation, interpretation, experiments, data analysis and writing up	65 %

The following co-authors contributed to the work. If co-authors are students at Monash University, the extent of their contribution in percentage terms must be stated:

Name	Nature of contribution	Extent of contribution (%) for student co-authors only
Walid A. Daoud	Supervision, interpretation, suggestion, discussion and revision	N/A
Steven J. Langford	Supervision, interpretation, suggestion, discussion and revision	N/A

The undersigned hereby certify that the above declaration correctly reflects the nature and extent of the candidate's and co-authors' contributions to this work.

Candidate's Signature		Date 4/10/2013
Main Supervisor's Signature		Date 4/10/2013

Chapter 5:

Superhydrophobic and photocatalytic self-cleaning cotton

Superhydrophobic and Photocatalytic Self-Cleaning Cotton

Shabana Afzal,[†] Walid A. Daoud,^{‡,*} and Steven J. Langford[§]

[†]School of Applied Sciences and Engineering, Monash University, Churchill, Victoria 3842, Australia

[‡]School of Energy and Environment, City University of Hong Kong, Tat Chee Avenue, Kowloon, Hong Kong

[§]School of Chemistry, Monash University, Clayton, Victoria 3800, Australia

KEYWORDS: *Superhydrophobic, visible-light, photocatalysis, self-cleaning textiles, titania, porphyrin*

ABSTRACT: A superhydrophobic cotton fabric exhibiting photocatalytic self-cleaning properties under visible-light was prepared by step-wise deposition of anatase TiO₂, *meso*-tetra(4-carboxyphenyl)porphyrin (TCPP) and trimethoxy(octadecyl)silane (OTMS). The modified cotton fabrics not only exhibited excellent superhydrophobicity with a water contact angle of 156°, but also showed significant degradation of methylene blue under visible-light irradiation. The fabrics were characterized by FESEM, XRD, NMR and UV-Vis spectroscopy. Textiles with dual functionality of superhydrophobicity and visible-light TiO₂ photocatalysis are promising for a wide range of self-cleaning applications.

▪ INTRODUCTION

The research related to self-cleaning textiles has received considerable attention within the scientific community for its potential applications to industry and daily life.¹ Currently, there are two main concepts used in developing self-cleaning textiles. The first concept is based on superhydrophobic approach, also known as the lotus effect.² Superhydrophobic surfaces exhibit extreme water repellent properties with water contact angle greater than 150°. As a result, water droplets attain the spherical shape and roll off the surface carrying away the dirt particles. This effect is commonly observed in nature in plant leaves, especially lotus leaves.³ Surface energy and roughness are the two important parameters that control the wettability of a surface. Inspired by the self-cleaning properties of lotus leaves, scientists have fabricated superhydrophobic textiles by creating surface roughness in combination with low surface energy materials such as organic silanes, fluorinated silanes, alkyl amines and silicates.⁴ Popular surface modifications methods include wet chemical reactions,⁵ self-assembly and sol-gel,⁶ layer-by-layer deposition,⁷ polymerization reaction,⁸ electrochemical deposition,⁹ chemical vapour deposition,¹⁰ plasma treatment¹¹ and electrospinning.¹²

The second concept is based on hydrophilic approach, in which self-cleaning takes place by a process known as photocatalysis.¹³ As a result of photocatalysis, the dirt/stains break down to simple species, such as CO₂ and water, on exposure to light.¹³ Polycrystalline semiconductor oxides, such as TiO₂, have been applied in the form of nano-coatings, leading to the successful development of a number of UV-active self-cleaning textiles. These textiles have shown good self-cleaning properties under UV light¹⁴ and solar simulated light.¹⁵ Furthermore, visible-light active self-cleaning textiles have also been developed based on activation of TiO₂ in the visible region such as metal doping,¹⁶ non-metal doping¹⁷ and dye-sensitization.¹⁸

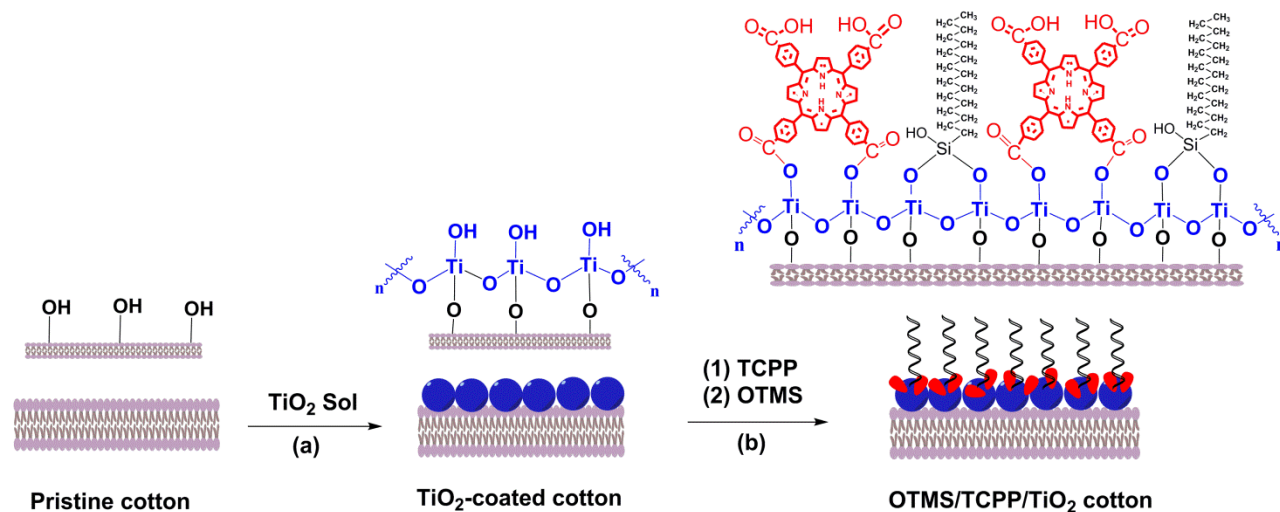
However, there are limited examples of self-cleaning materials in literature that work on both principles,¹⁹ despite the fact that dual function self-cleaning textiles can have many advantages. On one hand, extreme water repellence can keep away water soluble impurities, while on the other hand the accumulation of organic impurities can be prevented by photocatalysis. Here, we report the fabrication of a new class of self-cleaning textiles that is simultaneously superhydrophobic and photocatalytic under visible-light irradiation. Self-assembled monolayers of *meso*-tetra(4-carboxyphenyl)porphyrin (TCPP) were formed on TiO₂-coated cotton by a simple post adsorption method, followed by hydrophobization with trimethoxy(octadecyl)silane (OTMS) (Scheme 1).

We have particularly selected non-fluorinated silanes in our study, as they are considered less hazardous to skin as compared to fluorinated silanes. The as-prepared cotton fabrics exhibited excellent superhydrophobicity with water contact angle (WCA) of 156°. Moreover, the superhydrophobic fabrics showed superior photocatalytic activity under visible-light as compared to the non-hydrophobic TiO₂ and TiO₂/TCPP-coated cotton fabrics. The photocatalytic self-cleaning properties have been investigated by the degradation of methylene blue under visible-light irradiation, whereas the superhydrophobic self-cleaning properties have been evaluated by static water contact angle measurements.

▪ EXPERIMENTAL

Fabrication of TCPP/TiO₂-coated cotton. Colloidal anatase TiO₂ was synthesized by adding a solution of titanium tetraisopropoxide and acetic acid drop wise to water containing 1.4% HNO₃. The mixture was stirred at 60 °C for 16 h.^{14a} The TiO₂ sol was applied to scoured cotton fabrics through a dip-pad-dry-cure process. A non-ionic detergent (Kieralon F-OLB conc.) was used to scour the cotton samples to remove impurities. In the scouring process, the cotton pieces were immersed

Scheme 1: Formation of hydrophobized OTMS/TCPP/TiO₂-coated cotton



in detergent solution and heated at 80 °C for 30 min, followed by washing with water and then air-drying.

For coating TiO₂ on the fabric, the scoured cotton pieces were dipped in the TiO₂ sol for 1 min and then pressed in automatic horizontal press at 7.5 rpm with a nip pressure of 2.75 kg cm⁻². The pressed samples were then exposed to ammonia fumes until the surface pH reached 7. The neutralized samples were dried at 80 °C in a drying oven and cured at 120 °C for 3 min. For deposition of TCPP, TiO₂-coated fabrics were dipped in 20 μM TCPP in dimethylformamide (DMF) and heated at 100°C approximately for 5 h. Samples were then washed with DMF and water in order to remove unbound TCPP.

Hydrophobization of TCPP/TiO₂-coated cotton. Trimethoxy(octadecyl)silane (OTMS) (10 %, w/w) was added drop wise to ethanol. The solution pH was adjusted to 5 by adding acetic acid to promote hydrolysis of OTMS. The solution was then stirred at room temperature for 60 min to form a hydrolyzed alkylsilanol solution.²⁰ TCPP/TiO₂-coated fabrics were then immersed in the hydrolyzed OTMS for 30 min, followed by washing with ethanol to remove any unbound OTMS. The treated cotton samples were air dried and then heated at 110° C in drying oven for 15 min.

Characterization. The surface morphology of the cotton samples was studied using field emission electron microscopy (JEOL 7001F FEGSEM). The crystallinity of the TiO₂ films on cotton was determined by low angle X-ray diffraction (XRD, Philip 1140 diffractometer). The UV-Vis absorption spectrum of TCPP in DMF was recorded on Cary 5000 spectrophotometer. The UV-Vis absorption spectra of pristine cotton and cotton samples coated with TiO₂, TCPP/TiO₂ and OTMS/TCPP/TiO₂ were recorded using 110 mm integrating sphere on Cary 5000 spectrophotometer. The cotton samples were masked allowing only a 2 × 2 mm area to be exposed to illumination by the light source. Solid-state ²⁹Si NMR experiments were performed on a Bruker Avance 400 spectrometer operating at a static magnetic field of 9.4 T using a 4 mm multinuclear solid state probe at 300 K. The spinning rate was 10

kHz. Solid samples were packed into 4mm ZrO₂ rotors with Kel-F cap and spectra were recorded using CP-MAS techniques.

Measurement of water contact angle. For the assessment of superhydrophobic character, the water contact angles (WCA) were measured by a contact angle instrument (Data physics contact angle system, OCA20) at room temperature. Deionized water with a droplet volume of 5 μL was used. WCAs were determined after a water droplet was placed on the fabric for 60s. Average contact angle values were obtained by taking measurements at five different positions on each sample.

Photocatalytic studies. For the assessment of self-cleaning properties, photocatalytic degradation of methylene blue (MB) was conducted using previously reported conditions.¹⁸ Pristine cotton and cotton samples coated with TiO₂, TCPP/TiO₂ and OTMS/TCPP/TiO₂-coated cotton pieces (2 x 2 cm) were stained with MB solution in dichloromethane (31mM). 100 μL of MB was adsorbed on each of the sample pieces. The cotton samples were placed in a light box and irradiated by visible-light for 8 h using a fluorescent lamp (30 W, 5.02 mW cm⁻² irradiance) containing a small UV content of 0.01 mWcm⁻² irradiance. The change in concentration of MB was monitored by measuring UV-Vis spectra of cotton samples at different time intervals, during the course of irradiation.

Durability of coating. The durability of cotton samples coated with OTMS/TCPP/TiO₂ were tested against water using a modified AATCC Test Method 190-2003.²¹ The samples were washed with water for 45 min at room temperature at constant stirring of 200 rpm, followed by drying in oven. To determine the stability of OTMS coating on the cotton samples, WCA were measured after each wash cycle.

RESULTS AND DISCUSSION

FESEM analysis. SEM analysis was conducted to observe the surface morphology of pristine and treated cotton fabrics. In lower magnification images (Fig. 1-d), the overall integrity of cotton fibres is shown to be retained as there is no major

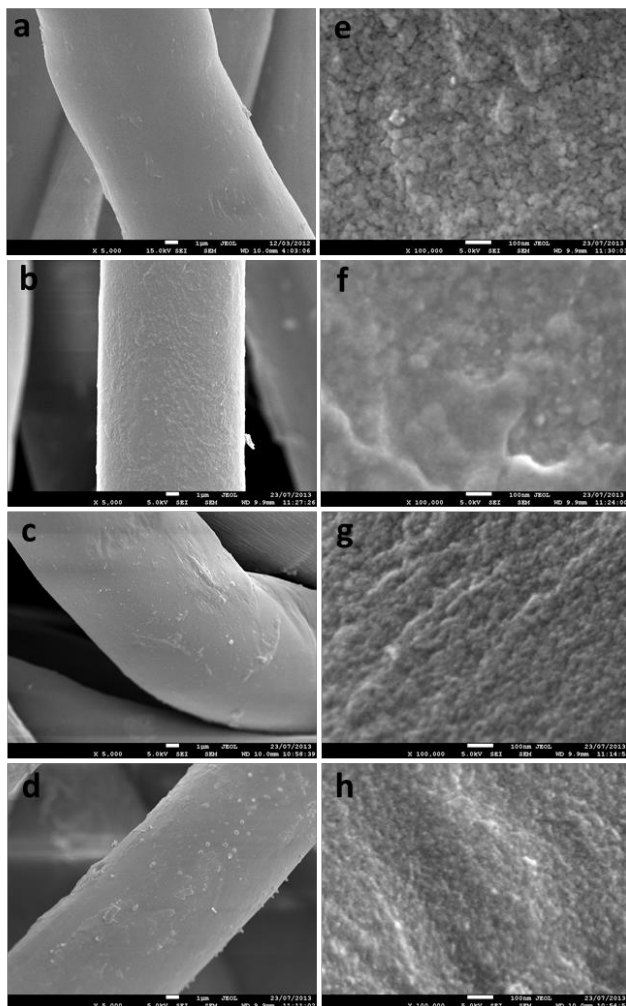


Figure 1. FESEM images of: (a, e) pristine cotton; (b, f) TiO₂-coated-cotton; (c, g) TCPP/TiO₂-coated cotton; (d, h) OTMS/TCPP/TiO₂-coated cotton.

change in the surface morphology of cotton fabrics after coating with TiO₂, TCPP/TiO₂ and OTMS/TCPP/TiO₂. At higher magnification, a change in surface roughness can be observed for the samples coated with TiO₂ and TCPP/TiO₂ (Fig. 1f-h) as compared to pristine fabric (Fig. 1e). Surface aggregates can be observed in all of the treated samples, though these appear to even out as the coating process proceed.

XRD analysis. The crystalline phase of titania nanoparticles deposited onto the cotton fabrics was determined by XRD analysis. While pristine cotton shows no anatase-associated peaks (Fig. 2a), cotton samples coated with TiO₂ show the characteristic diffraction peaks for anatase at $2\theta = 25.4^\circ$, 38.0° and 48.0° (Fig. 2b). After deposition of TCPP and OTMS, the same anatase peaks can still be observed in their XRD spectra (Fig. 2c). Hence, TiO₂ has retained its crystallinity even after modification with TCPP and OTMS.

UV-Vis spectroscopy. The UV-Vis spectra of TCPP in DMF and adsorbed on cotton in the presence of TiO₂ and OTMS are illustrated in Fig. 3. The UV-Vis spectra of TiO₂-coated and pristine cotton samples have also been recorded for comparison, which show no particular absorption peaks over 400-700 nm range (Fig. 3d and e). The absorption spectrum of TCPP in

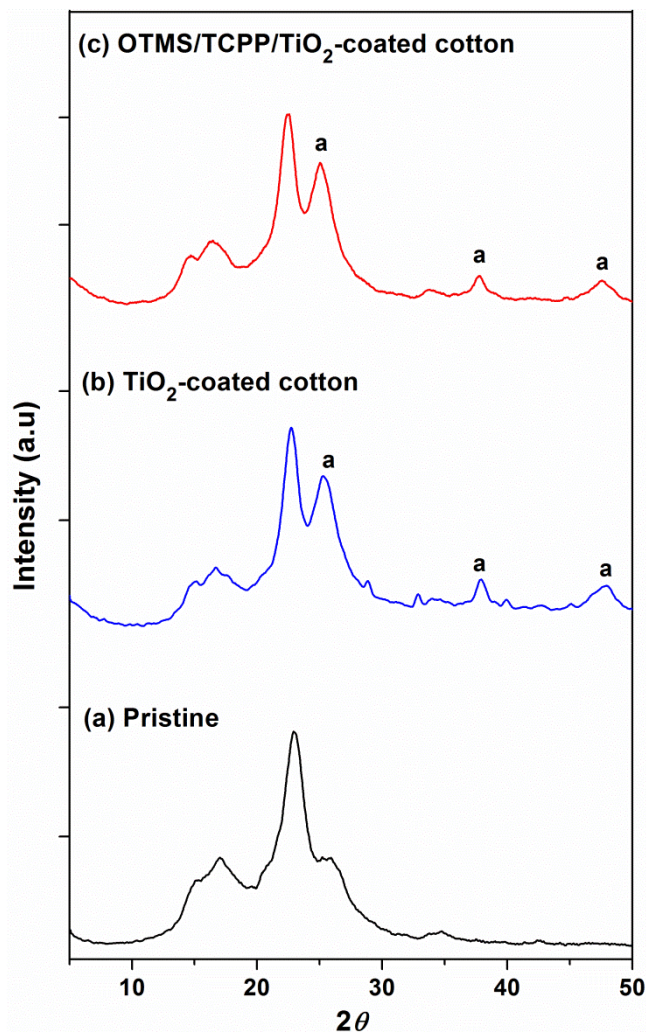


Figure 2. XRD spectra of cotton: (a) pristine, (b) TiO₂-coated, (c) OTMS/TCPP/TiO₂-coated (a = peaks associated with anatase).

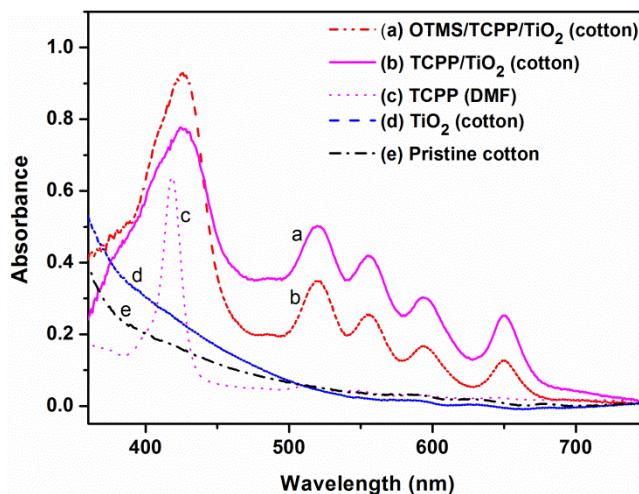


Figure 3. UV-Vis spectra of (a) OTMS/TCPP/TiO₂-coated cotton, (b) TCPP/TiO₂-coated cotton, (c) TCPP in DMF (d) TiO₂-coated cotton, (e) pristine cotton.

DMF shows a strong peak at 418 nm attributable to the porphyrin Soret band (Fig. 3c). This absorption peak is shifted by

9 nm to 427 nm in TiO₂-coated cotton (Fig. 3b). This red shift is likely to be due to the interaction between the carboxylate groups of porphyrin and TiO₂.²² After the adsorption of OTMS, no further change in porphyrin absorption peaks is observed in OTMS/TCPP/TiO₂-coated fabrics (Fig. 3a). Thus, the addition of OTMS appears to have no effect on the binding of TCPP molecules with TiO₂.

Solid state ²⁹Si NMR spectroscopy. Fig. 4 shows the ²⁹Si MAS NMR spectrum of TiO₂ nanoparticles adsorbed on TCPP and OTMS. For reference, ²⁹Si MAS NMR spectrum of TiO₂ nanoparticles adsorbed on OTMS was also recorded (Fig. 4a). In the spectrum (Fig. 4b), three peaks are observed at -47, -57 and -66 ppm, which can be associated with monodentate (T¹), bidentate (T²) and tridentate (T³) silicon environments, respectively.²³ Thus, OTMS shows different modes of binding on the surface of TCPP/TiO₂ nanoparticles. However, the dominant peak at -57 ppm indicates that the major binding mode is T², even in the absence of TCPP.

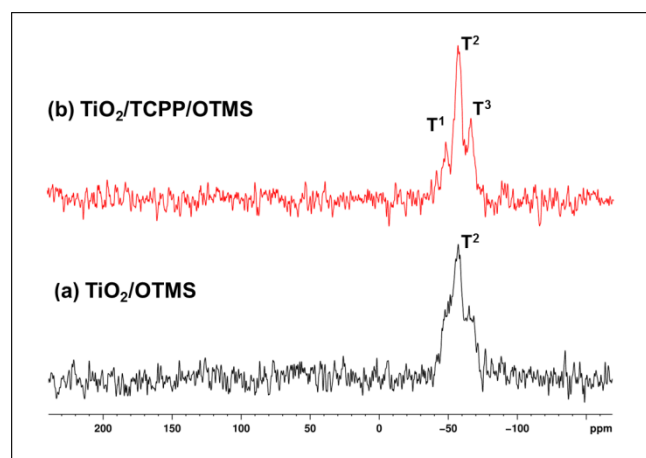


Figure 4. ²⁹Si NMR spectra of (a) TiO₂/OTMS, (b) TiO₂/TCPP/OTMS.

Superhydrophobic self-cleaning. The wettability of cotton samples was evaluated by using WCA measurements. As expected, the pristine cotton sample can be completely wetted by water (Fig. 5a), which is due to the presence of surface hydrophilic OH groups. After treatment with TiO₂, a WCA of 124° could be realized (Fig. 5b). TiO₂ particles make the fabric surface rougher, thus, introducing some hydrophobicity to the textiles. For TiO₂/TCPP-coated fabrics, a complete wettability of the surface was regained yielding no WCA. This result is consistent with the addition of the carboxylic acid groups of the TCPP molecules, which impart extreme hydrophilic character to the fabric (Fig. 5c). After further modification with OTMS, the WCA increased to 156° (Fig. 5d), showing excellent superhydrophobic properties. The superhydrophobic character was achieved due to the combined effect of surface roughness induced by TiO₂ particles and low surface energy by OTMS.

Photocatalytic self-cleaning properties. The photocatalytic activity of samples coated with TiO₂, TCPP/TiO₂ and OTMS/TCPP/TiO₂ were investigated quantitatively by exposing the cotton samples containing adsorbed MB to visible-light irradiation. The change in concentration of MB was measured by recording the UV-Vis spectra of cotton samples before and after irradiation, and at different time intervals.

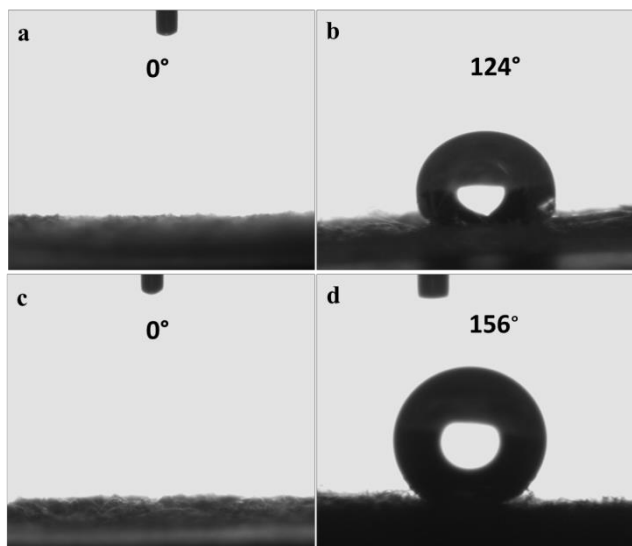


Figure 5. Images attained after 5 μ L water droplets were placed on (a) pristine cotton, (b) TiO₂-coated cotton, (c) TCPP/TiO₂-coated cotton, (d) OTMS/TCPP/TiO₂-coated cotton.

The photocatalytic efficiency of the different samples has been compared in Fig. 6. For comparison, a pristine cotton sample was also studied. The straight line obtained for the pristine sample indicates the absence of any photocatalytic activity by cotton itself. The samples coated with TiO₂, TCPP/TiO₂ and

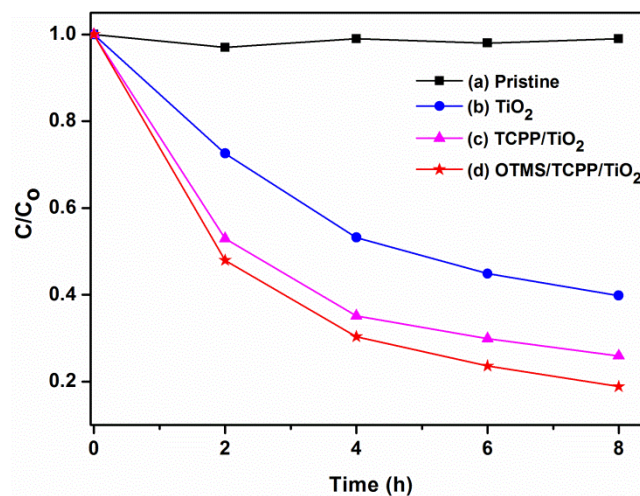


Figure 6. Degradation of methylene blue (MB) under visible-light irradiation (5.02 mW cm⁻² irradiance): (a) pristine cotton, (b) TiO₂-coated cotton, (c) TCPP/TiO₂-coated cotton (d) OTMS/TCPP/TiO₂-coated cotton.

OTMS/TCPP/TiO₂ showed 60%, 75% and 86% degradation of MB, respectively, after 8 hours of irradiation.

The enhanced photoactivity of TCPP/TiO₂-coated fabrics as compared to bare TiO₂-coated fabrics is attributable to the visible-light photosensitization of TiO₂ by the added porphyrin dye. Excitation of dye molecules upon visible-light irradiation results in electron injection into the conduction band of TiO₂ leading to formation of free radical species such as O₂^{•-} radicals in the presence of oxygen.²⁴ These radicals react with the MB adsorbed on the surface of fabric decomposing it through the bleaching processes. Interestingly, after modification of TCPP/TiO₂-coated samples by OTMS, an additional increase

of about 10 % in photocatalytic activity was observed. This can be accounted for by the reduced aggregation of MB adsorbed on the fabric in presence of OTMS.

Fig. 7 shows a region of the visible absorption spectra of MB adsorbed on cotton in presence of TiO_2 , TCPP/ TiO_2 and OTMS/TCPP/ TiO_2 . The absorption peaks at 665 nm and 614 nm correspond to monomeric and aggregated forms (mostly dimeric) of MB, respectively.^{15b, 25}

In TiO_2 and TCPP/ TiO_2 -coated samples, almost the same amount of monomeric and dimeric forms of MB is present (Fig. 7b and a), as the corresponding absorption peaks are similar in height and intensity. In contrast, in OTMS/TCPP/ TiO_2 -coated samples (Fig. 6c), the monomeric form is dominant as a result of the presence of large absorption peak at 665 nm as compared to the smaller peak (dimeric) at 614 nm. Monomeric form of MB is known to degrade faster as compared to the dimeric form.²⁵⁻²⁶ Importantly then, the presence of OTMS favours disaggregation of MB adsorbed on the surface of fabric, allowing increase in photocatalytic activity.

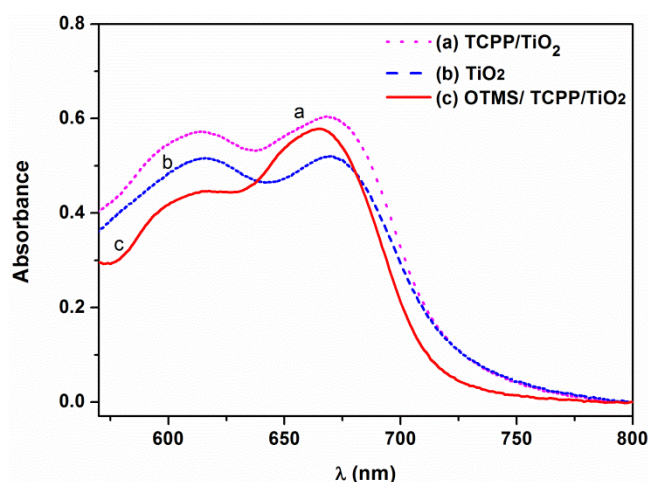


Figure 7. UV-Vis spectra of methylene blue adsorbed on: (a) TCPP/ TiO_2 -coated cotton, (b) TiO_2 -coated cotton, (c) OTMS/TCPP/ TiO_2 -coated cotton. Peaks at 665 nm and 614 nm correspond to monomeric and aggregated forms of MB, respectively.

Coating stability study. For practical application, the durability of the superhydrophobic coating on fabric is an important factor. In our case, the coating consists of TiO_2 , TCPP and OTMS. Titanium dioxide has been reported to show high affinity toward cotton,^{14a} while TCPP binds well with TiO_2 through its carboxylate groups.^{18a} For evaluating the stability of OTMS coating on the fabric, WCA's were measured after 2, 4, 6, 8 and 10 wash cycles (Supporting Information Fig. S1). After 10 wash cycles, the water contact angle of the fabric decreased slightly from 156° to 149° (Fig. 8). Hence, the modified cotton fabrics can retain their superhydrophobic character after prolonged washing.

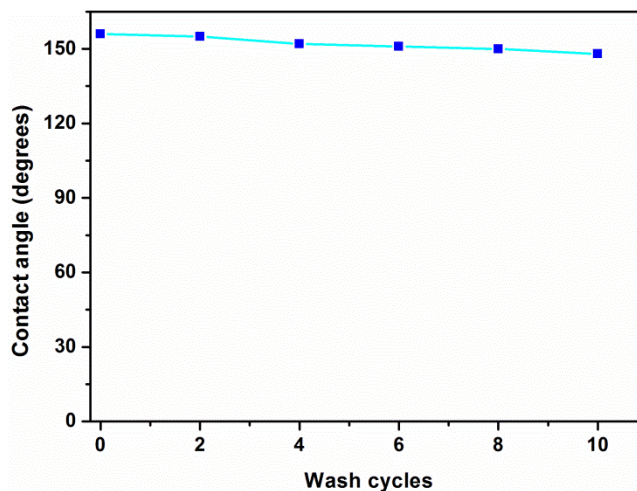


Figure 8. WCA of OTMS/TCPP/ TiO_2 -coated cotton fabrics as a function of the number of wash cycles.

CONCLUSIONS

We have successfully prepared cotton fabrics exhibiting both superhydrophobic and visible-light photocatalytic activity. This has been achieved by introducing anatase TiO_2 coating in conjunction with TCPP on the fabric, followed by modification with OTMS. OTMS/TCPP/ TiO_2 -coated cotton fabrics exhibited a WCA of 156° . The cotton fabrics also showed considerable photodegradation of methylene blue under visible-light irradiation. Development of dual function self-cleaning textiles offers great potential in view of practical applications of self-cleaning.

ASSOCIATED CONTENT

Supporting Information. Measurement of water contact angles for OTMS/TCPP/ TiO_2 -coated cotton samples after repeated wash cycles. This material is available free of charge via the Internet at <http://pubs.acs.org>.

AUTHOR INFORMATION

Corresponding Author

* E-mail: [REDACTED] Phone: + [REDACTED]
Fax: + [REDACTED]

Author Contributions

The manuscript was written through contributions of all authors. All authors have given approval to the final version of the manuscript.

Notes

The authors declare no competing financial interest.

ACKNOWLEDGMENT

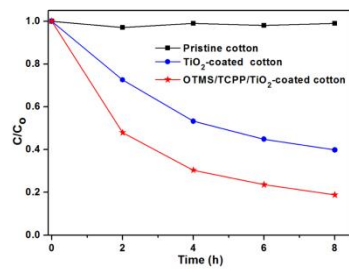
We thank the Monash Centre for Electron Microscopy (MCEM), Australia for providing assistance in FESE measurement and Mr. M. K. Kashif (Monash University, Clayton) is also acknowledged for providing assistance in XRD measurements.

REFERENCES

- (1) Tung, W. S.; Daoud, W. A. *J. Mater. Chem.* **2011**, *21*, 7858-7869.
- (2) Bhushan, B., *Langmuir* **2012**, *28*, 1698-1714.
- (3) Barthlott, W.; Neinhuis, C. *Planta* **1997**, *202*, 1-8.

- (4) (a) Daoud, W. A.; Xin, J. H.; Zhang, Y. H.; Mak, C. L. *Thin Solid Films* **2006**, *515*, 835-837. (b) Daoud, W. A.; Xin, J. H.; Tao, X. M. *J. Am. Ceram. Soc.* **2004**, *87*, 1782-1784.
- (5) (a) Wang, S.; Feng, L.; Jiang, L. *Adv. Mater.* **2006**, *18*, 767-770. (b) Zimmermann, J.; Reifler, F. A.; Fortunato, G.; Gerhardt, L.-C.; Seeger, S. *Adv. Funct. Mater.* **2008**, *18*, 3662-3669.
- (6) (a) Yin, S.; Wu, D.; Yang, J.; Lei, S.; Kuang, T.; Zhu, B. *Appl. Surf. Sci.* **2011**, *257*, 8481-8485. (b) Nakajima, A.; Fujishima, A.; Hashimoto, K.; Watanabe, T. *Adv. Mater.* **1999**, *11*, 1365-1368.
- (7) (a) Zhang, L.; Chen, H.; Sun, J.; Shen, J. *Chem. Mater.* **2007**, *19*, 948-953. (b) Zhao, Y.; Xu, Z.; Wang, X.; Lin, T. *Langmuir* **2012**, *28*, 6328-6335.
- (8) Ramirez, S. M.; Diaz, Y. J.; Sahagun, C. M.; Duff, M. W.; Lawal, O. B.; Iacono, S. T.; Mabry, J. M. *Polym. Chem.* **2013**, *4*, 2230-2234.
- (9) Zhang, J.; France, P.; Radomyselskiy, A.; Datta, S.; Zhao, J.; van Ooij, W. *J. Appl. Polym. Sci.* **2003**, *88*, 1473-1481.
- (10) Huang, L.; Lau, S. P.; Yang, H. Y.; Leong, E. S. P.; Yu, S. F.; Praver, S. *J. Phys. Chem. B* **2005**, *109*, 7746-7748.
- (11) Takke, V.; Behary, N.; Perwuelz, A.; Campagne, C. *J. Appl. Polym. Sci.* **2011**, *122*, 2621-2629.
- (12) Acatay, K.; Simsek, E.; Ow-Yang, C.; Menciloglu, Y. Z. *Angew. Chem. Int. Ed.* **2004**, *43*, 5210-5213.
- (13) Fujishima, A.; Zhang, X.; Tryk, D. A. *Surf. Sci. Rep.* **2008**, *63*, 515-582.
- (14) (a) Qi, K.; Daoud, W. A.; Xin, J. H.; Mak, C. L.; Tang, W.; Cheung, W. P. *J. Mater. Chem.* **2006**, *16*, 4567-4574. (b) Daoud, W. A.; Leung, S. K.; Tung, W. S.; Xin, J. H.; Cheuk, K.; Qi, K. *Chem. Mater.* **2008**, *20*, 1242-1244.
- (15) (a) Bozzi, A.; Yuranova, T.; Kiwi, J. *J. Photochem. Photobiol. A: Chem.* **2005**, *172*, 27-34. (b) Uddin, M. J.; Cesano, F.; Scarano, D.; Bonino, F.; Agostini, G.; Spoto, G.; Bordiga, S.; Zecchina, A. *J. Photochem. Photobiol. A: Chem.* **2008**, *199*, 64-72. (c) Kiwi, J.; Pulgarin, C. *Catal. Today* **2010**, *151*, 2-7.
- (16) (a) Wang, R.; Wang, X.; Xin, J. H. *ACS Appl. Mater. Interfaces* **2009**, *2*, 82-85. (b) Qi, K.; Fei, B.; Xin, J. H. *Thin Solid Films* **2011**, *519*, 2438-2444.
- (17) Wu, D.; Long, M. *ACS Appl. Mater. Interfaces* **2011**, *3*, 4770-4774.
- (18) (a) Afzal, S.; Daoud, W. A.; Langford, S. J. *J. Mater. Chem.* **2012**, *22*, 4083-4088. (b) Afzal, S.; Daoud, W. A.; Langford, S. J. *ACS Appl. Mater. Interfaces* **2013**, *5*, 5753-4759. (c) Afzal, S.; Daoud, W. A.; Langford, S. J. *Appl. Surf. Sci.* **2013**, *275*, 36-42.
- (19) (a) Macias-Montero, M.; Borrás, A.; Saghi, Z.; Romero-Gomez, P.; Sanchez-Valencia, J. R.; Gonzalez, J. C.; Barranco, A.; Midgley, P.; Cotrino, J.; Gonzalez-Eliphe, A. R. *J. Mater. Chem.* **2012**, *22*, 1341-1346. (b) Cao, H.; Zheng, H.; Liu, K.; Fu, R. *Cryst. Growth Des.* **2009**, *10*, 597-601. (c) Nakajima, A.; Hashimoto, K.; Watanabe, T.; Takai, K.; Yamauchi, G.; Fujishima, A. *Langmuir* **2000**, *16*, 7044-7047. (d) Crick, C. R.; Bear, J. C.; Kafizas, A.; Parkin, I. P. *Adv. Mater.* **2012**, *24*, 3505-3508. (e) Zhang, Y.; Li, S.; Huang, F.; Wang, F.; Duan, W.; Li, J.; Shen, Y.; Xie, A. *Russ. J. Phys. Chem. A* **2012**, *86*, 413-417.
- (20) Witucki, G. L. *J. Coatings Technol.* **1993**, *65*, 57-60.
- (21) *AATCC Technical Manual*; American Association of Textile Chemists and Colorists: Research Triangle Park, NC, **2006**, pp 358-360.
- (22) (a) Granados-Oliveros, G.; Páez-Mozo, E. A.; Ortega, F. M.; Ferronato, C.; Chovelon, J.-M. *Appl. Catal. B: Environ.* **2009**, *89*, 448-454. (b) Ma, T.; Inoue, K.; Noma, H.; Yao, K.; Abe, E. *J. Photochem. Photobiol. A: Chem.* **2002**, *152*, 207-212.
- (23) (a) Kailasam, K.; Natile, M. M.; Glisenti, A.; Müller, K. J. *Chromatogr. A* **2009**, *1216*, 2345-2354. (b) Pereira, C.; Alves, C.; Monteiro, A.; Magén, C.; Pereira, A. M.; Ibarra, A.; Ibarra, M. R.; Tavares, P. B.; Araújo, J. P.; Blanco, G.; Pintado, J. M.; Carvalho, A. P.; Pires, J.; Pereira, M. F. R.; Freire, C. *ACS Appl. Mater. Interfaces* **2011**, *3*, 2289-2299.
- (24) Huang, H.; Gu, X.; Zhou, J.; Ji, K.; Liu, H.; Feng, Y. *Catal. Comm.* **2009**, *11*, 58-61.
- (25) Murugan, K.; Rao, T. N.; Gandhi, A. S.; Murty, B. S. *Catal. Comm.* **2010**, *11*, 518-521.
- (26) Strataki, N.; Bekiari, V.; Stathatos, E.; Lianos, P. *J. Photochem. Photobiol. A: Chem.* **2007**, *191*, 13-18.

Photodegradation of methylene blue by superhydrophobic cotton



Supporting Information

Superhydrophobic and photocatalytic self-cleaning cotton

Shabana Afzal,[†] Walid A. Daoud,^{‡,*} and Steven J. Langford[§]

[†]School of Applied Sciences and Engineering, Monash University, Churchill, Victoria 3842, Australia

[‡]School of Energy and Environment, City University of Hong Kong, Tat Chee Avenue, Kowloon, Hong Kong

[§]School of Chemistry, Monash University, Clayton, Victoria 3800, Australia

Measurement of water contact angles for 10 wash cycles

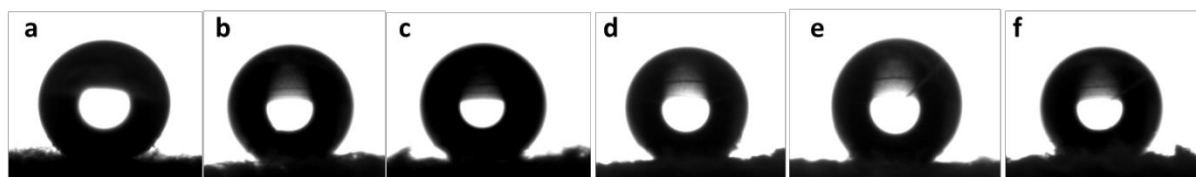


Fig. S1: Water contact angles of OTMS/TCPP/TiO₂-coated cotton samples; (a) 156° before washing, (b) 155° after 2 wash cycles, (c) 152° after 4 wash cycles, (d) 151° after 6 wash cycles, (e) 150° after 8 wash cycles, (f) 149° after 10 wash cycles

Chapter 6:

Conclusion and Perspectives

CHAPTER 6: CONCLUSION AND PERSPECTIVES

6.1 Summary

In the field of renewable resources, the unique photocatalytic properties of titania offer a great potential in the exploration of environment-friendly methods for the degradation of organic contaminants.¹ This encompasses the creation of self-cleaning surfaces.² From the fabrication of titania-based coatings immobilized on hard materials, such as glasses and ceramics involving high-temperature methods,³ the research has now been extended to investigating coating substrates of low thermal resistance, such as organic fibres.⁴ By using a nanotechnological approach, in conjunction with low-temperature sol-gel process, anatase-based self-cleaning textiles have successfully been established and utilised.⁵ However, the requirement for titania excitation only in the ultraviolet region of the solar spectrum confines the efficient utilisation of solar light. Hence, the self-cleaning capability of these textiles is limited to a low percentage of the electromagnetic spectrum only.

At the onset of this project, this intrinsic limitation of titania was identified as one of the major drawbacks in the field of self-cleaning textiles. Outside of dye-sensitised solar cells (DSSCs), few research efforts were underway that aimed at finding suitable methods to sensitise TiO₂ in the visible-region, let alone followed by application to textiles. Of these efforts, notable advances included the fabrication of visible-light driven textiles based on metal doping such as Fe and Au,⁶ and non-metal doping using triethylamine as a source of nitrogen to modify the electronics of TiO₂.⁷

The research elaborated in this thesis represents a significant step forward in establishing efficient visible-light active self-cleaning textiles. Following the dye-sensitisation approach, the concept of “dye-sensitised textiles” has been introduced for the first time as published in a series of advances in four articles shown as Chapters 2-5.⁸ Amongst the various dyes on offer, porphyrins were particularly

selected in our work because of their strong absorption bands in the visible spectrum, relatively good chemical photostability (though this was evaluated through this thesis), low cost of production and lower toxicity as compared to the conventional ruthenium bipyridyl complexes which have been employed in DSSC technologies. The ease of peripheral modification of porphyrins according to the requirements (such as attachment, solubility, spectral properties) was yet another incentive to use them in our experiments. Being a π -conjugated macrocycle with extensive delocalization, porphyrins also exhibit long triplet state lifetimes and high quantum yields capable of intersystem crossing, leading to an efficient electron injection into the conduction band of TiO_2 upon excitation under visible-light.⁹

Self-assembled monolayers of *meso*-tetra(4-carboxyphenyl)porphyrin (TCPP) and various metalloporphyrins (Fe, Co, Zn and Cu) were formed on anatase coated-cotton fabric by a post-adsorption method with industrial applicability. The cotton prepared by this method, coated by the porphyrin-sensitised photocatalyst exhibited excellent self-cleaning properties as evinced by the degradation of methylene blue, coffee and red wine stains under visible-light irradiation.

The ability of the carboxylate groups on TCPP to bind with TiO_2 facilitated its coating on the fabric by a simple one-step thermal process. The binding of TCPP with TiO_2 was ultimately confirmed by a red shift of 9 nm for Soret band in the UV-Vis absorption spectrum of TCPP/ TiO_2 -coated cotton. The observed peaks characteristic of anatase found in the XRD spectrum of fabrics coated with TCPP and TiO_2 supported the fact that TiO_2 had retained its crystallinity, in spite of the presence of TCPP. Furthermore, fluorescence studies established strong evidence for an efficient electron injection from porphyrin molecules into the conduction band of TiO_2 .

Despite possessing outstanding photosensitising properties, TCPP also exhibited significant photobleaching, when exposed to extended periods of strong visible-light. This major shortcoming was another source of motivation that directed our research efforts towards exploration of the more stable derivatives which retain the photocatalytic properties. Our results indicated that *meso*-tetra(4-carboxyphenyl)porphyrinato copper(II) proved to be the most stable photocatalyst. Unlike TCPP, Cu(II)TCPP displayed significant stability under visible-light irradiation. The enhanced photostability of Cu(II)TCPP as compared to TCPP might be related

to the paramagnetic nature of Cu in Cu(II)TCPP, leading to the deactivation of its excited state resulting in more recombination with no fluorescence emission and thus making Cu(II)TCPP less susceptible to photobleaching.¹⁰

In addition to the photocatalytic self-cleaning mechanism, we also attempted to explore the addition of another surface phenomenon; the lotus/superhydrophobic effect, combining the two remarkable self-cleaning approaches in textiles.¹¹ In nature, lotus plants provide a perfect example of self-cleaning materials. Inspired by the self-cleaning properties of lotus leaves, extensive research efforts have been dedicated to the fabrication of superhydrophobic textiles.¹² Surface modification of the textiles was accomplished by optimising the surface roughness in conjunction with incorporation of low surface energy materials.

Our research emphasis was to develop dual functional self-cleaning textiles capable of exhibiting a complete set of self-cleaning properties. The extreme water repellence attained by a superhydrophobic surface could repel the water soluble impurities, whereas the accumulation of organic contaminants could be prevented by TiO₂ photocatalysis. Hence, in the final phase of this research project, fabrication of a new class of self-cleaning textiles is reported, that utilised these two effects simultaneously.

Monolayers of *meso*-tetra(4-carboxyphenyl)porphyrin (TCPP) were formed on TiO₂-coated cotton by a simple post adsorption method, followed by hydrophobisation with trimethoxy(octadecyl)silane (OTMS). The superhydrophobic cotton fabrics not only exhibited excellent superhydrophobicity with water contact angle (WCA) of 156° but also retained their significant photocatalytic activity under visible-light irradiation by degrading methylene blue. Furthermore, only slight variation in WCA was observed after 10 wash cycles indicating considerable durability of OTMS coating on the fabric. Textiles with dual functionality of superhydrophobicity and visible-light TiO₂ photocatalysis are promising for a wide range of self-cleaning applications.

6.2 Limitations of visible-light driven self-cleaning textiles

Whilst porphyrin-sensitised textiles may provide an efficient means of visible-light photocatalysis, their application in the practical scenario is much more of a challenge. Porphyrins were particularly selected in our study, as they are less hazardous in the

case of skin contact as compared to the conventional highly efficient photosensitising dyes. Evaluation of self-cleaning performance obtained from porphyrin/titania-coated fabrics showed promising results, however the poor photostability of TCPP limited their practical utilisation. This problem was resolved to some extent, when photostable Cu(II) complex of porphyrin was applied on the fabric. However, the application of CuTCPP could result in inducing harmful effects on skin, as CuTCPP is considered more toxic as compared to metal-free TCPP. Therefore, alternative dyes need to be explored, which would be photostable and at the same time, suitable to skin without any detrimental effects.

Another limitation associated with porphyrin-based self-cleaning textiles is the incomplete utilisation of solar spectrum for harvesting light with subsequent sensitisation of TiO₂. The photocatalytic performance of TiO₂ could be maximised by adding other dyes such as phthalocyanines. Phthalocyanines are also macrocyclic organic compounds that are structurally related to porphyrins. They exhibit high absorption molar coefficients around 300 nm (Soret band) and 620-700 nm (Q bands).¹³ In order to utilise a wider range of the solar spectrum, phthalocyanines could be used to sensitise TiO₂ in fabricating self-cleaning textiles. However, absorption is only one component of criteria for useful photocatalysis.

Although, the present method of coating dye on textiles, used in this research work is simple, cost-effective and provided a proof-of-principle, aggregation of dye molecules on the fabric surface, might have decreased the photocatalytic efficiency. Alternative methods of coatings could be used such as atomic layer deposition. By adopting this method, dye aggregation could be prevented, as the single layer of dye molecules of uniform thickness is deposited on the surface of fabric in atomic layer deposition.

The superhydrophobic/photocatalytic textiles present an interesting example of blend of hydrophobic and hydrophilic approaches, encompassing the primary phenomena of self-cleaning. However, the methodology of coating comprised layer-by-layer deposition of TiO₂, TCPP and OTMS which is a tedious process. This complex method of coating could be simplified by using hydrophobic analogues of dyes such as fluoroalkyl-substituted porphyrins. Hydrophobic porphyrins would probably

sensitise TiO₂ in the visible region of spectrum and at the same time impart superhydrophobicity to the fabrics.

6.3 Future of self-cleaning textiles

Recent developments in the technology of self-cleaning coatings lead to commercialisation of many products, suitable for a wide range of applications. Utilising the photocatalytic properties of titania, Pilkington Glass announced the development of the first self-cleaning windows, Pilkington Activ™ in 2001. It comprised of a 20–30 nm layer of nanocrystalline anatase TiO₂ deposited by an atmospheric pressure CVD technique onto soda-lime silicate float glass.¹ Later on, several other glass companies released similar products including Sunclean™, SGG Aquaclean (first generation) and Bioclean (2nd generation). TOTO Ltd. manufactured Hydrotect™ outdoor tiles and paint to be applied on buildings.¹ However the development of commercially viable nanocrystalline TiO₂ based coatings on organic substrates such as textiles is still at infancy stage.

Limitation of TiO₂ photoactivity to UV radiation is only one of the aspects addressed in this thesis. There are many other factors need to be considered in future to bring them to market. These include the removal of degraded products from the surface of fabrics, low resistance of nanoparticles against washing, negative effect on mechanical properties such as tensile strength, tearing strength, softness and abrasion resistance and harmful effects of TiO₂ nanoparticles on environment during their release in the recycling stage of fabrics.¹⁴

Superhydrophobic textiles have also been commercialised. Nano-Tex LLC has marketed a cotton-blended fabric, named Nano-Care.¹⁵ It has whisker-shaped 10 nm molecules of a fluorinated monomer copolymerised with a carboxylic acid oligomer which are converted to the anhydride to react with the fibre. The brand Nao-Pel is similar to Nano-care, designed for wool fabrics.¹⁵ Schoeller Textiles AG has introduced its NanoSphere technology which imparts water repellency, soil-repellent, anti-adhesive and self-cleaning properties.¹⁵ It involves formation of micro-rough three-dimensional surface structures from which water, dirt and oil simply roll off. However, durability of these coatings is the main barrier, limiting their application for long-term usage.

Overall, in this research work, successful outcomes have been acquired by introducing porphyrins in the form of coatings on textiles. Whilst still far from being a marketable product, the results obtained provide compelling evidence as a 'proof of concept' for developing porphyrin-sensitised textiles coupled with the lotus effect. Future of these dual functional (photocatalytic /superhydrophobic) textiles seems to be quite promising, offering huge potential in commercialisation of innovative textiles with high value added functional performance levels.

6.4 References

1. Parkin, I. P.; Palgrave, R. G. *J. Mater. Chem.* **2005**, *15*, 1689-1695.
2. (a) Reisch, M. "Cleaning Glass: A Thing Of The Past?" *Chem. Eng. News Archive* **2001**, *79* (27), p8. (b) Reisch, M. S., "Essential Minerals" *Chem. Eng. News Archive* **2003**, *81* (13), p13.
3. (a) Dhananjeyan, M. R.; Mielczarski, E.; Thampi, K. R.; Buffat, P.; Bensimon, M.; Kulik, A.; Mielczarski, J.; Kiwi, J. *J. Phys. Chem. B* **2001**, *105*, 12046-12055. (b) Xiao-e, L.; Green, A. N. M.; Haque, S. A.; Mills, A.; Durrant, J. R. *J. Photochem. Photobiol. A: Chem.* **2004**, *162*, 253-259.
4. Tung, W. S.; Daoud, W. A. "Self-Cleaning Fibers and Fabrics" *Self-Cleaning Materials and Surfaces: A Nanotechnology Approach*, John Wiley & Sons Ltd. **2013**, p 129-152.
5. (a) Daoud, W. A.; Xin, J. H. *J. Am. Ceram. Soc.* **2004**, *87*, 953-955. (b) Qi, K.; Daoud, W. A.; Xin, J. H.; Mak, C. L.; Tang, W.; Cheung, W. P. *J. Mater. Chem.* **2006**, *16*, 4567-4574. (c) Tung, W. S.; Daoud, W. A. *J. Mater. Chem.* **2011**, *21*, 7858-7869.
6. (a) Qi, K.; Fei, B.; Xin, J. H., *Thin Solid Films* **2011**, *519*, 2438-2444. (b) Wang, R.; Wang, X.; Xin, J. H. *ACS Appl. Mater. Interfaces* **2009**, *2*, 82-85.
7. Wu, D.; Long, M. *ACS Appl. Mater. Interfaces* **2011**, *3*, 4770-4774.
8. Afzal, S.; Daoud, W. A.; Langford, S. J. *J. Mater. Chem.* **2012**, *22*, 4083-4088.
9. Kim, W.; Park, J.; Jo, H. J.; Kim, H-J.; Choi, W. *J. Phys. Chem. C* **2007**, *112*, 491-499.
10. Gerola, A. P.; Santana, A.; França, P. B.; Tsubone, T. M.; de Oliveira, H. P. M.; Caetano, W.; Kimura, E.; Hioka, N. *Photochem Photobiol.* **2011**, *87*, 884-894.
11. Barthlott, W.; Neinhuis, C. *Planta* **1997**, *202*, 1-8.
12. Xue, C.-H.; Ma, J.-Z. *J. Mater. Chem. A* **2013**, *1*, 4146-4161.
13. de la Torre, G.; Claessens, C. G.; Torres, T. *Chem. Comm.* **2007**, 2000-2015.
14. Reijnders, L. "The Environmental Impact of a Nanoparticle-Based Reduced Need of Cleaning Product and the Limitation Thereof" *Self-Cleaning Materials and Surfaces: A Nanotechnology Approach*, John Wiley & Sons Ltd. **2013**, p 313-346.
15. Holme, I. *Color. Technol.* **2007**, *123*, 59-73.